THE ROLE OF CD3 DELTA AND RAG1AP1 PROTEINS IN T CELL RECEPTOR EXPRESSION

by
NAZLI KESKİN

Submitted to the Graduate School of Engineering and Natural Sciences
in partial fulfillment of
the requirements for the degree of
Master of Science

Sabancı University
August 2010

THE ROLE OF CD3 DELTA AND RAG1AP1 PROTEINS
IN T CELL RECEPTOR EXPRESSION

APPROVED BY:

Assoc. Prof. Dr. Batu Erman .....
(Thesis Supervisor)

Assist. Prof. Dr. Alpay Taralp .....

Assist. Prof. Dr. Devrim Gözüaçık .....

Assoc. Prof. Dr. Hikmet Budak .....

Assoc. Prof. Dr. Levent .....

DATE OF APPROVAL: 05.08.2010

ABSTRACT

THE ROLE OF CD3 DELTA AND RAG1AP1 PROTEINS
IN T CELL RECEPTOR EXPRESSION

Nazlı Keskin
Biological Sciences and Bioengineering, MSc. Thesis, 2010
Thesis supervisor: Batu Erman

Keywords: CD3 delta, TCR, Rag1Ap1, Venus, Flow cytometry

CD3 subunits of the of T cell receptor (TCR) are essential for the assembly and signal transduction initiated from this receptor complex in T lymphocytes. The first part of this study aims to generate a CD3 delta conditional knockout construct by recombineering bacterial artificial chromosomes. We generated multiple plasmids that were designed to target the CD3 delta gene locus in mouse embryonic stem cells. In the second part of the study, we focused on a CD3 delta interacting protein called Rag1Ap1, which was identified in a yeast two hybrid screen. We confirmed the interaction of CD3 delta and Rag1Ap1 by co-immunoprecipitation in HEK 293T cells. To study the subcellular localization of the CD3 – Rag1Ap1 interaction, we generated a plasmid expressing a Rag1Ap1 – Venus (YFP) fusion protein. We analyzed the subcellular localization of the Rag1Ap1-Venus protein by fluorescent and confocal microscopy in transfected HeLa cell lines. Furthermore, we tested the effect of the overexpression and shRNA mediated knockdown of Rag1Ap1 on TCR expression levels in T lymphocyte cell lines, by flow cytometry. These experiments indicate that Rag1Ap1 interacts with CD3 delta in the endoplasmic reticulum and may play a role in TCR assembly and surface expression.

ÖZET

CD3 DELTA VE RAG1AP1 PROTEİNLERİNİN T HÜCRESİ RESEPTÖRÜ İFADESİNDEKİ ROLÜ

Nazlı Keskin

Biyoloji Bilimleri ve Biyomühendislik, Master Tezi, 2010

Tez Danışmanı: Batu Erman

Anahtar Kelimeler: CD3 delta, TCR, Rag1Ap1, Venus, Akım Sitometresi

T hücresi reseptörünün (TCR) CD3 zincirleri, T lenfositlerdeki bu reseptör komplesinin oluşumu ve sinyal iletişimi için gereklidir. Bu çalışmanın ilk bölümünde yapay bakteri kromozomlarında rekombinasyon teknikleri kullanılarak CD3 delta zincirini koşullu olarak silmeyi amaçladık. Fare embriyonik kök hücrelerinde CD3 delta gen bölgesini hedefleyen plazmidler oluşturduk. Çalışmanın ikinci bölümünde, maya ikili hibrit taramasında CD3 delta ile etkileşimi olduğu belirlenen Rag1Ap1 isimli bir proteine odaklandık. CD3 delta ve Rag1Ap1 etkileşimini HEK293T hücrelerinde immün çökeltme yaparak doğruladık. CD3 delta – Rag1Ap1 etkileşiminin hücre içindeki lokasyonunu incelemek icin Rag1Ap1 – Venus (YFP) füzyon proteinini ifade eden bir plazmid oluşturduk. Rag1Ap1 – Venus füzyon proteininin hücre içindeki lokasyonunu transfeksiyon yapılmış HeLa hücre hatlarında floresan ve konfokal mikroskop ile analiz ettik. Ayrıca, T lenfosit hücre hatlarında Rag1Ap1 ifadesinin arttırımının ve shRNA yoluyla Rag1Ap1 baskılamasının TCR ifadesi üzerindeki etkilerini akım sitometresinde belirledik. Bu deneyler Rag1Ap1'ın CD3 delta ile etkileşiminin endoplazmik retikulumda olduğunu ve bu etkileşimin TCR oluşumu ve hücre yüzeyindeki ifadesinde rol oynayabileceğini göstermektedir.

To my mother…

ACKNOWLEDGEMENT

First and foremost I would like to thank my supervisor Assoc. Prof. Dr. Batu Erman for his guidiance, advice, support and patience during my master's project. His comments and ideas for every single experiment throughout the whole project gave me the enthusiasm for science.

I would like to convey my heartfelt thanks to my comitee members, Assist. Prof.Dr. Alpay Taralp, Assist. Prof. Dr. Devrim Gözüaçık, Assoc. Prof. Dr. Hikmet Budak and Assoc. Prof. Dr. Levent Öztürk for their support and ideas for thesis dissertation.

Thanks to my supervisor, my lab collagues, Dr. Jitka Eryılmaz, Manolya Ün, İzzet Mehmet Akçay, Emre Deniz, Dr. Ceren Tuncer and Dr. Belkıs Atasever and previous lab members Dr. Şafak Işıl Çevik, Serkan Belkaya, Gamze Günal and İlçim Özlü, I have felt the honur of being a member of Erman lab for two years.

My dearest friends Nurten Ükelgi, Elif Levent, Mine Bakar, Duygu Kuzuoğlu, Ayşegül Altıntaş, Sedef Dinçer, Fatma Uzbaş, Gökçen Gokçe and Aslı Çalık deserve a really big thanks for their presence in my all not only good but also hard times.

I owe special thanks to my parents, Zülal and Ali Rıza Keskin, my brothers Zafer and Tanfer Keskin and my aunt Gül Hıdıroğlu for their continuous and unconditional love. In addition, I am so lucky to have such an understanding and supportive mother. Without her support, help, advice and love it was impossible for me to overcome everyting. Her existance as a co-pilot in my life is a gift for me.

Finally, I would like to thank to Scientific and Technological Research Council of Turkey, TÜBİTAK BİDEP for the support during my thesis.

TABLE OF CONTENTS

LIST OF FIGURES

LIST OF TABLES

LIST OF ABBREVIATIONS

α	Alpha
β	Beta
δ	Delta
γ	Gamma
ε	Epsilon
Amp	Ampicillin
APC	Antigen Presenting Cell
bp	Base pair
CD	Cluster of Differentiation
Chl	Chloramphenicol
CIAP	Calf Intestine Alkaline Phosphatase
CMV	Cytomegalovirus
Da	Dalton
DMEM	Dulbecco's Modified Eagle Medium
DMSO	Dimethylsulfoxide
DN	Double Negative
DNA	Deoxyribonucleic Acid
DP	Double Positive
EDTA	Ethylene diamine tetra acetic acid
FACS	Flourescence Activated Cell Sorting
FBS	Fetal Bovine Serum
GFP	Green Flourescent Protein
HEK	Human Embryonic Kidney
IP	Immunoprecipitation
ITAM	Immunoreceptor Tyrosine-based Activation Motif
Kan	Kanamycin
LB	Luria Broth
Lck	Lymphocyte Specific Protein Tyrosine Kinase

MHC	Major Histocompatibility Complex
min	Minute
Neo	Neomycin
OD	Optical Density
PBS	Phosphate Buffered Saline
PCR	Polymerase Chain Reaction
rpm	Revolution per minute
RNA	Ribonucleic Acid
SDS-PAGE	Sodium Dodecyl Sulfate Polyacrilamide Gel Electrophoresis
SP	Single Positive
SV40	Simian Virus 40
TBE	Tris Borate EDTA
TCR	T Cell Receptor
Tc	Cytotoxic T Cell
Th	T Helper Cell

1. INTRODUCTION

1.1 Overview of the Immune System

The immune system evolved to defend multicellular organisms from foreign invaders. The main role of the immune system is to produce an enormous variety of cells which can specifically recognize and eliminate pathogens.[1-3]

Innate and adaptive immunity are the two types of immunity that collaborate for the protection of the body. Innate immunity is a first line of defense, which has the capability of eliminating foreign invaders within hours of encounter. Most of the molecular and cellular components of the innate immune system are ready to eliminate before infection. However, the recognition system of innate immunity is limited to differentiation of only self and non-self. This system is not specialized to recognize pathogens specificity and to protect the organism from reinfection. On the other hand, adaptive immunity starts in response to infection and requires some time for innate immunity to provide the first line of defense. However, its slowness is compensated by the production of a large repertoire of lymphocytes with different antigen specificities. Therefore, the adaptive immune system can potentially recognize any foreign antigen. In addition to this, adaptive immunity has an immunologic memory that enables the system to induce a heightened state of reaction in case of reinfection.[1-6]

1.2 T-Cell Mediated Immunity

The cellular arm of the mammalian immune system depends on the direct interactions of T lymphocytes and foreign peptides presented on antigen presenting cells (APC).[7] T lymphocytes can only recognize antigenic peptides bound to cell membrane proteins called major histocompatibility complex (MHC) molecules.[8] There are two classes of MHC molecules: MHC class I molecules, expressed on nearly all nucleated cells and MHC class II molecules only expressed on professional APCs, such as macrophages, dentritic cells and B lymphocytes. There are two types of mature T lymphocytes: T helper (Th) and T cytotoxic (Tc) cells.

Th cells express the CD4 co-receptor on the cell surface and can recognize peptide bound to MHC class II molecules. The main role of Th cells is to release cytokines and chemokines to activate macrophages and attract them to the site of infection. Also, Th cells play a role in activating the humoral arm of immunity by stimulating the proliferation and differentiation of B lymphocytes into plasma cells that can secrete antibodies. On the other hand, cytotoxic Tc cells express the CD8 co-receptor on their cell surface and use their TCR to recognize peptides bound to MHC class I molecules. The main function of cytotoxic T cells is to secrete enzymes such as perforin to directly kill virus infected cells.[9-12]

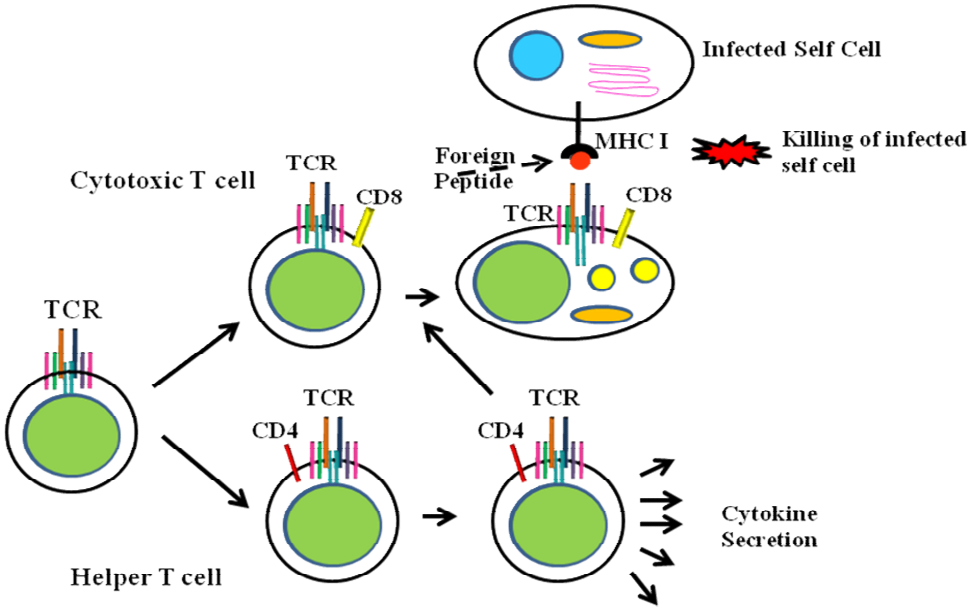

Figure 1.1 Activation of T cells. T cell development in the thymus results in the differentiation of either CD4 or CD8 co-receptor expressing cells from a CD4+ CD8+ bi-potential precursor (shown on the left). Th cells can secrete cytokines that provide help for the function of B and Tc lymphocytes (shown on the bottom right). Tc cells can kill infected cells after recognition of foreign peptides presented on MHC I molecules by the TCR+CD8 co-receptor complex.

1.3 T Cell Receptor (TCR): CD3 Receptor Complex

All T-cell activation events such as proliferation, cytotoxic killing, cytokine secretion and induction of programmed cell death are initiated by the TCR – CD3 complex on the surface of T lymphocytes.[13] The commonly accepted structure of the T cell receptor is composed of the TCRα and TCRβ chains, which are responsible for binding to MHC:peptide complexes and the CD3δ, CD3γ, CD3ε and TCRζ chains, which are responsible for signal transduction.[14-16]

The stochiometry of the TCR:CD3 complex expressed on the surface of T lymphocytes is such that it has one copy of the TCRα, TCRβ, CD3δ, CD3γ and two copies of the CD3ε and TCRζ subunits. These subunits assemble to neutralize the charged residues in the transmembrane domains of each of these subunits.[17]

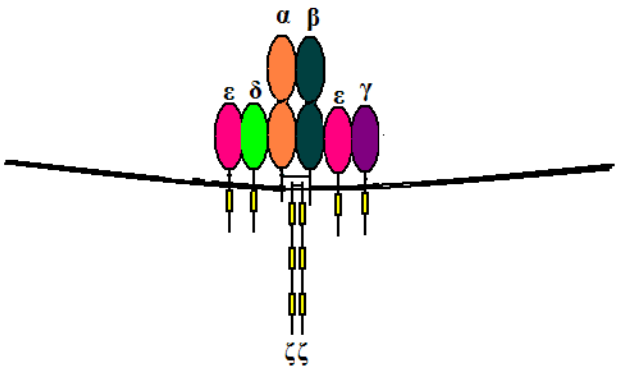

Figure 1.2 TCR:CD3 receptor complex

ITAMs (Immunoreceptor Tyrosine-Based Activation Motif) are the domains in the cytoplasmic tails of CD3 subunits. CD3ε, CD3δ and CD3γ subunits have one and TCRζ subunits have three ITAMs. After signal transduction is initiated by the TCR:CD3 complex, tyrosine amino acids in the ITAMs are phosphorylated by the Lck tyrosine kinase, which is bound to the cytoplasmic tail of either the CD4 or CD8 co-receptor. This phosphorylation recruits the ZAP-70 tyrosine kinase to the ITAMs. Signal transduction continues with the phosphorylation and activation of ZAP-70, which results in the phosphorylation of adaptor proteins and eventually the activation of transcription factors such as NFAT, NFkB and AP1.[18-21]

1.4 The Mechanism of TCR Assembly

All subunits of the TCR:CD3 complex have essential roles in TCR assembly. The assembly of a functional multi-subunit receptor starts in the endoplasmic reticulum and not in the cell surface.[22] The first step of this assembly is the formation of CD3ε:CD3δ and CD3ε:CD3γ dimers.

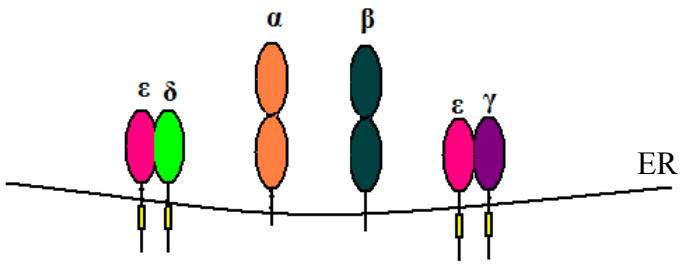

Figure 1.3 Formation of CD3ε:CD3δ and CD3ε:CD3γ dimers

Later, TCRα and TCRβ subunits are bound to the CD3ε:CD3δ and CD3ε:CD3γ dimers, respectively. This binding results in the formation of two trimers: TCRα:CDε:CD3δ and TCRβ:CD3ε:CD3γ.

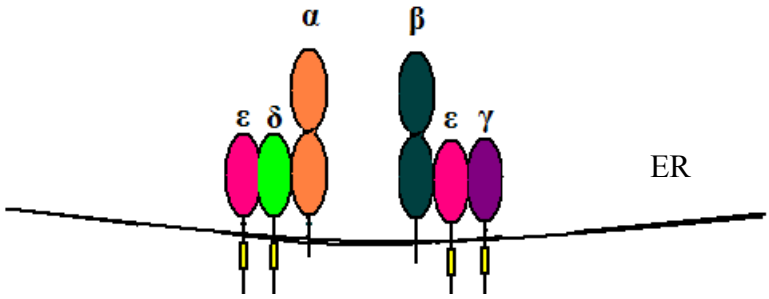

Figure 1.4 Formation of TCRα:CDε:CD3δ and TCRβ:CD3ε:CD3γ trimers

The two trimers come together to form a six chain complex which is then associated with a disulphide linked dimer of TCRζ chains. Only after the assembly of such a full TCR:CD3 complex in the endoplasmic reticulum, can it be exported to the cell membrane.[22-24]

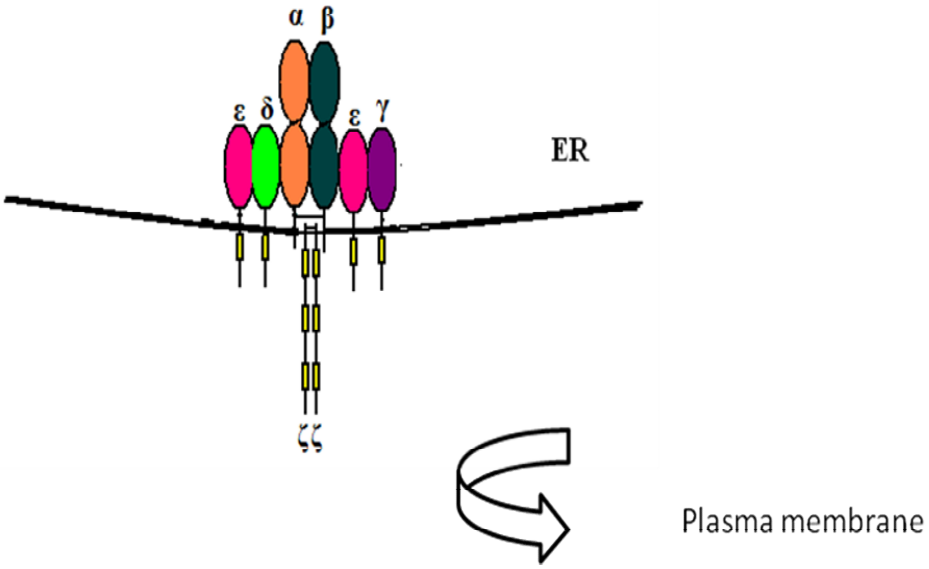

Figure 1.5 Transport from the endoplasmic reticulum to the plasma membrane after full assembly

1.5 TCR Signaling in T Cell Development

Pluripotent hematopoitic stem cells (HSCs) differentiate into common lymphoid progenitors (CLP) which are the precursors of T lymphocytes. These precursors enter the thymus after being formed in bone marrow. These cells express neither TCR nor co-receptors on the cell surface and are called double negative (DN) cells because of the absence of CD4 and CD8 proteins on their surface.[25-27]

DN thymocytes rearrange their TCRβ gene locus and as a result express the TCRβ protein. The new expressed TCRβ protein assembles with the non-rearranged preTα and other CD3 subunits to form the preTCR complex on the cell surface. The only difference between the preTCR and TCR protein complexes is the substitution of the preTα chain with the TCRα chain. The signals coming from preTCR initiates the survival, proliferation and differentiation of DN thymocytes into double positive (DP) thymocytes which express both CD4 and CD8 co-receptors on the cell surface.[28,29] DP cells undergo TCRα gene rearrangement and express TCRα proteins. From this point onwards, the thymocytes express surface TCR. Therefore, the DP stage is the first stage for thymocytes to express TCR on the cell surface. Thymocytes are trained to recognize MHC:peptide complexes expressed on the surface of the cells of the thymic epithelium. Depending on the affinity of recognition between the TCR and MHC:peptide complex, thymocytes can be positively selected.[30] Cells with receptors that do not have enough affinity undergo programmed cell death and apoptosis. On the other hand, thymocytes that recognize the MHC:peptide complex with too high affinity (presumably because of self-peptide recognition) also cannot mature and undergo apoptosis.[31] This process, negative selection is thought to eliminate the risk of T lymphoctyes recognizing self molecules. Positively and negatively selected thymocytes continue their maturation by turning off either the CD4 or the CD8 co-receptors.[32,33] These selected thymocytes that express only a CD4 or CD8 co-receptor are called single positive (SP). SP cells can migrate from the thymus to the periphery as mature T lymphocytes.[34-37]

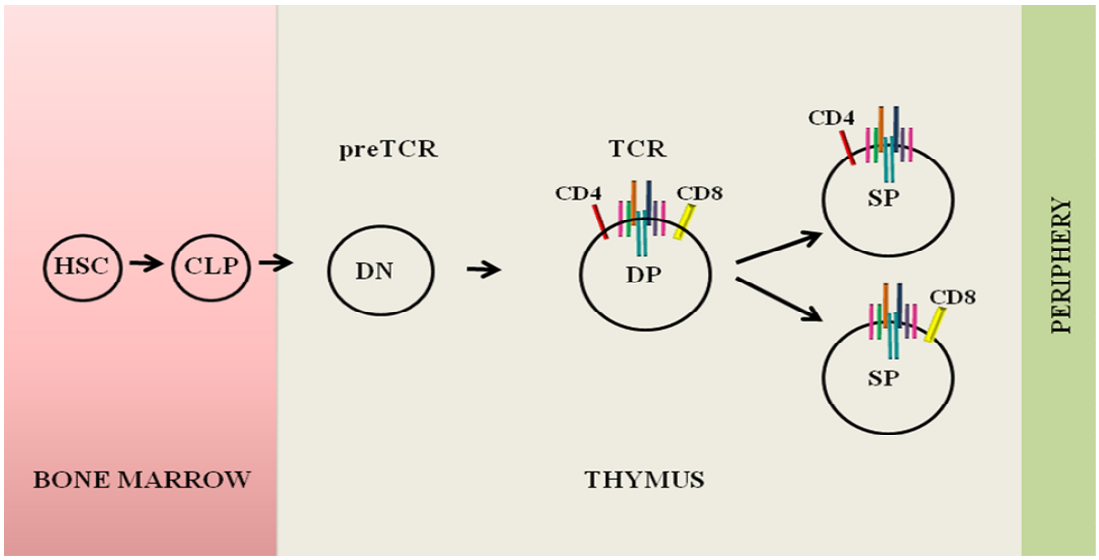

Figure 1.6 Schematic diagram of T cell development

1.6 The Importance Of CD3delta For TCR Signaling In T Cell Development

The significance of the role of the TCR:CD3 subunits has been studied by knockout experiments. It has been published that except for CD3δ, the absence of any CD3 subunit results in a block of preTCR signaling and the DN to DP transition.[38-40]

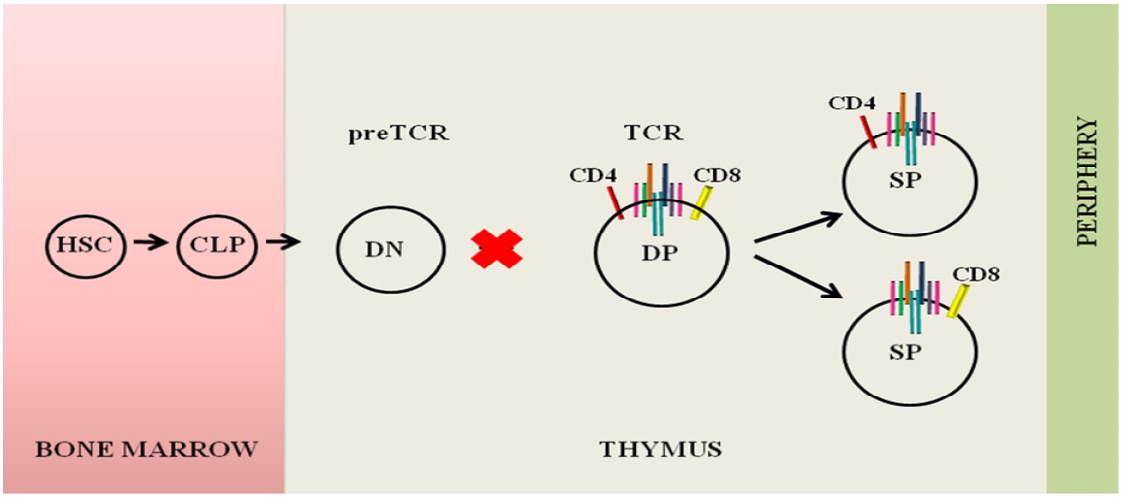

Figure 1.7 T cell development is blocked in absence of any subunits of TCR:CD3 receptor complex except for CD3δ

The absence of CD3δ does not affect the transition of thymocytes from DN to DP stage. Therefore, CD3δ deficient DP T lymphocytes can express TCR on their cell surface. Although, CD3δ deficiency does not affect DN to DP transition, further steps of T cell development are blocked.[41,42] Unlike TCR signaling, preTCR signaling requires neither CD4 nor CD8 co-receptors. Therefore CD3δ may play a critical role in co-receptor dependent signaling of TCR.

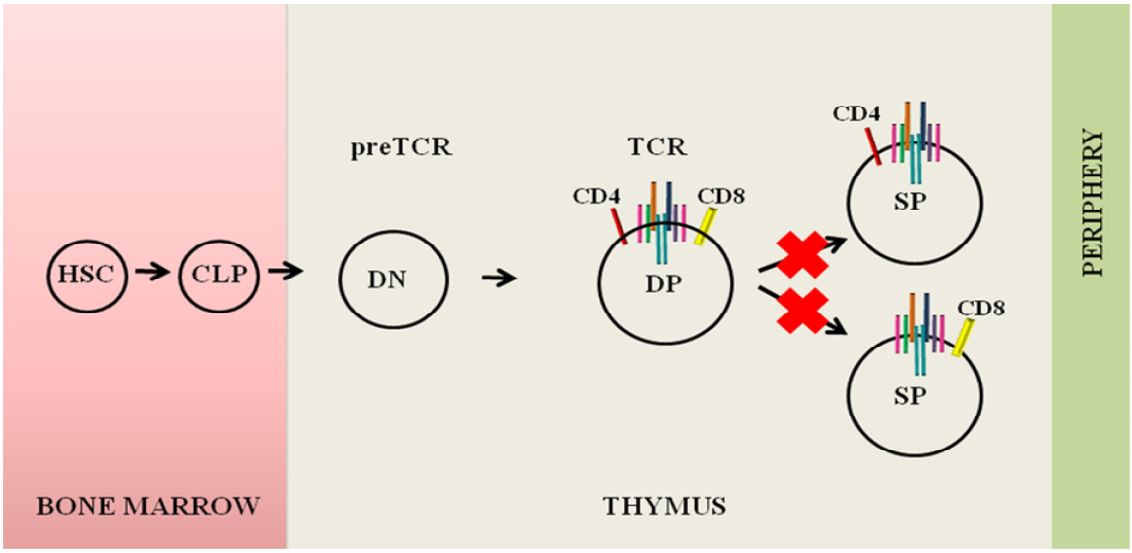

Figure 1.8 T cell development in absence of CD3delta

2. AIM OF THE STUDY

The cellular arm of the immune response starts with the recognition of foreign peptidic antigens presented on MHC molecules on antigen presenting cells by the TCR and CD4 or CD8 co-receptors on T lymphocytes. All T-cell activation events such as proliferation, cytotoxic killing, cytokine secretion and induction of programmed cell death are initiated by TCR – CD3 complex on the surface of T lymphocytes. The TCRα and TCRβ subunits of the TCR:CD3 complex are responsible for ligand binding and the CD3δ, CD3γ, CD3ε and TCRζ subunits are responsible for signal transduction. Among these subunits, CD3δ is unique because inactivation of CD3δ does not block the transition of immature T thymocytes from DN stage to DP stage in the thymus. DN cells express the preTCR receptor that is composed of preTα, TCRβ and the CD3 subunits. This receptor is responsible for signaling the transition of DN immature cells to DP stage. DN cells express neither the CD4 nor the CD8 co-receptors as these co-receptors are not required for preTCR signaling. On the other hand co-receptors are necessary for signaling by most TCR receptors at the DP and SP stages. Therefore, CD3δ might be a critical subunit for co-receptor dependent signaling of T-cell receptors.

In the first part of the project, our aim was to prepare a conditional knockout construct to analyze the effect of CD3δ deficiency on T cell development. In the second part of the project, we focused on a protein called Rag1Ap1 which is known to interact with CD3δ. The Rag1Ap1 protein is not thoroughly studied so that not much is known about this protein. Therefore, we performed localization, overexpression and shRNA mediated silencing experiments to discover the effect of this protein on TCR assembly and expression.

3. MATERIALS AND METHODS

3.1 Materials

3.1.1 Chemicals

All the chemicals used in this project are listed in the Appendix A.

3.1.2 Equipment

All the equipments used in this project are listed in the Appendix B.

3.1.3 Buffers and Solutions

Standard buffers and solutions used in the project were prepared according to the protocols in Sambrook et al ., 2001.

3.1.3.1 Bacterial Transformation Buffers and Solutions

Calcium Chloride ($CaCl_2$) Solution: 60mM $CaCl_2$ (diluted from 1M stock), 15% Glycerol, 10mM PIPES at pH 7.00 were mixed and the solution prepared was autoclaved at 121 °C for 15 min and stored at 4 °C.

3.1.3.2 Mammalian Cell Culture Buffers and Solutions

Phosphate-buffered saline (PBS): 9.88g of DPBS powder (Cellgro, Mediatech #55- 031-PB) was dissolved in1 L ddH_2O.

2X HEPES-buffered saline (2XHBS): 0.8g NaCl, 0.027g $Na_2HPO_4.2H_2O$ and 1.2g HEPES were dissolved in 90mL of ddH_2O. pH was adjusted to 7.05 with 5 M NaOH and the solution was completed to 100mL with ddH_2O. The buffer was filter-sterilized and stored at -20 °C.

Trypan blue dye (0.4% w/v): 40µg of trypan blue was dissolved in 10mL PBS

TX100 Lysis Buffer: For 10mL lysis buffer; 0.5mL 20% TX100, 0.5mL 1 M tris at pH 7.4, 0.3mL 5M NaCl, 0.04mL 0.5M EDTA at pH 8.00, 8.7mL ddH_2O, and 1 tablet protease inhibitor (complete mini EDTA free) were mixed.

1X PBS-Tween20 (PBST) Solution: 0.5mL of Tween20 was dissolved in 1L of 1X PBS.

Blocking Buffer: 0.5g Milk powder was dissolved 10mL 1XPBST.

3.1.3.3 Gel Electrophoresis Buffers and Solutions

Agarose gel: For 1% w/v agarose gel preparation, 1 g of agarose was dissolved in 100 mL 0.5X TBE buffer by heating. 0.01% (v/v) ethidium bromide was added to the solution.

10X Tris-Borate-EDTA (TBE) Buffer: 104g Tris base, 55g Boric acid and 40mL 0.5M EDTA at pH 8.0 were dissolved in 1L of ddH_2O.

10X SDS Running Buffer: 30.3g Tris base, 144g Glycine, 10g SDS were dissolved in 1L ddH_2O.

10X Transfer Buffer: 14.5g Tris and 72g Glycine were dissolved in 1L ddH_2O. pH of the solution was adjusted to 8.3

1X Transfer Buffer: 80mL 10X Transfer Buffer, 160mL methanol, and 560mL ddH_2O.

5X Protein Loading Buffer Pack: Fermentas pack (#R0891) that includes 5X loading dye (0.313 M Tris HCl (pH 6.8 at 25°C), 10% SDS, 0.05% bromophenol blue, 50% glycerol) and 20X Reducing agent (2M DTT) was used.

SDS Separating Gel (13%): For 10mL gel; 2.5mL Tris 1.5M at pH 8.8, 3mL ddH_2O, 4.34mL Acryl: Bisacryl (30%), 100µL 10% SDS, 100µL 10% APS, and 10µL TEMED were mixed.

SDS Stacking Gel (4%): For 5mL gel; 1.25mL Tris 0.5 M at pH 6.8, 2.70mL H_2O, 1mL Acryl: Bisacryl (30%), 50µL 10% SDS, 15µL 10% APS, and 7.5µL TEMED were mixed.

3.1.4 Growth Media

3.1.4.1 Bacterial Growth Media

Luria Broth from BD was used for liquid culture of bacteria. 20 g of LB Broth was dissolved in 1 L of distilled water and autoclaved at 121^{o}C for 15 min. For selection, ampicillin with a final concentration of 100µg/mL, kanamycin with a final concentration of 50µg/mL and chloramphenicol with a final concentration of 12.5µg/mL were added to the liquid medium after autoclave.

LB agar from BD was used for preparation of solid medium for the growth of bacteria. 40g of LB agar was dissolved in 1L distilled water and autoclaved at 121^{o}C for 15 min. For selection, ampicillin with a final concentration of 100µg/mL, kanamycin with a final concentration of 50µg/mL and chloramphenicol with a final concentration of 12.5µg/mL were added to the medium after cooling down to 50^{o}C. Antibiotic added medium was poured onto sterile Petri dishes (~ 20 mL/plate). Sterile solid agar plates were kept at 4^{o}C.

3.1.4.2 Tissue Culture Growth Media

Growth Media For Adherent cell lines: HEK 293T and HeLa cell lines were grown in filter-sterilized DMEM that is supplemented with 10% heat-inactivated fetal bovine serum, 2mM L-Glutamine, 100 unit/mL penicillin and 100 unit/mL streptomycin.

Growth Media For Suspension cell lines: VL3-3M2, AKR1 and RLM11 cell lines were grown in filter-sterilized RPMI1640 that is supplemented with 10% heat-inactivated fetal bovine serum, 2mM L-Glutamine, 100unit/mL penicillin, 100unit/mL streptomycin and 50µM beta mercaptoethanol.

Freezing Medium: All the cell lines were frozen in medium containing DMSO added into fetal bovine serum (FBS) at a final concentration of 10% (v/v) and stored at $4^{o}C$.

3.1.5 Commercial Molecular Biology Kits

- QIAGEN Plasmid Midi Kit, 12145, QIAGEN, Germany
- QIAGEN Plasmid Maxi Kit, 12163, QIAGEN, Germany
- Qiaprep Spin Miniprep Kit, QIAGEN, Germany
- Qiaquick Gel Extraction Kit,28706, QIAGEN, Germany
- Qiaquick PCR Purification Kit,28106, QIAGEN, Germany
- Anti-HA Immunoprecipitation Kit, SIGMA. Germany

3.1.6 Enzymes

All the restriction enzymes and their corresponding 10X reaction buffers, DNA modifying enzymes and polymerases used in this study were from Fermentas.

3.1.7 Cell Types

3.1.7.1 Bacterial Cells

E. coli DH-5α (F- endA1 glnV44 thi-1 relA1 gyrA96 deoR nupG lacZdeltaM15 hsdR17) competent cells were used for bacterial transformation of plasmids. HB101 strain was used transformation of LMP plasmids. SW102, SW105 and SW106 were used for electroporation of BAC DNA.

3.1.7.2 Tissue Culture Cell Lines

HEK293T (derivative of human embryonic kidney 293 cell line that stably Express large T antigen of SV40 and plasmids containing the SV40 origin are replicated to a copy number of between 400 - 1000 plasmids per cell within 293T, and therefore express at a higher level) was used for the transfection and immunoprecipitation experiments (ATCC: CRL-Zch5n). VL3-3M2 is a double positive thymic lymphoma cell line and used for transfection and analysis of TCR expression level with FACS. HeLa is a human epithelial carcinoma cell line. This cell line with its large cell size is used for the subcellular localization studies. (ATCC: CCL-2)

3.1.8 **Vectors and Primers**

Vectors and primers used in this project are listed in Table 3.1 and Table 3.2

Vector Name	Use	E.coli Resistance Marker	Mammalian Resistance Marker
pcDNA-GFP	Transfection Control Vector	Amp	N/A
pHA-Mex	Mammalian Expression Vector with N Terminal HA Tag	Kan	Neo
pcDNA3.1 Myc	Mammalian Expression Vector with C Terminal Myc Tag	Amp/Kan	Neo
LMP	MSCV Based Retroviral Vector with GFP	Amp	Puro
pVenus-N1	Mammalian Expression Vector Containing Venus	Kan	Neo
pLTM332	Bacterial Expression Vector Containing loxP Sites	Amp/Kan	Neo
pLTM260	Bacterial Expression Vector Containing loxP and frt sites	Amp/Kan	Neo
pKO917TK	Bacterial Expression Vector Containing TK	Amp	N/A
RP23-432G9	BAC Containing CD3δ	Chl.	N/A
pMIGII-AND-TCR	MSCV Based Retroviral Vector Containing TCR α and β	Amp.	N/A
pMIGII-CD3DGEZ	MSCV Based Retroviral Vector Containing CD3δ, γ, ε and ζ	Amp.	N/A

Table 3.1 Vectors used in this project

Primer Name	Sequence	Use
miR30-Forward	CAGAAGGCTCGAGAAGGTATATTGCTGTTGACAGTGAGCG	Primers to amplify shRNAs from template 97 nucleotide DNA oligo and clone into LMP.
miR30-Reverse	CTAAAGTAGCCCCTTGAATTC CGAGGCAGTAGGCA	Primers to amplify shRNAs from template 97 nucleotide DNA oligo and clone into LMP
Rag1Ap1For	ATCTCGAGACCATG GAGGCGGGCGGCTTTC	Forward primer to clone Rag1Ap1 without a stop codon into pVenus-N1 vector
Rag1Ap1Rev	ATAAGATCTGAGGTTT GCAGGAGCCAGTAG	Reverse primer to clone Rag1Ap1 without a stop codon into pVenus-N1 vector
97mer oligo Rag1Ap1-1	TGCTGTTGACAGTGAGCG AACTCTTTATATCCTGGCA TATTAGTGAAGCCACAGA TGTAATATGCCAGGATAT AAAGAGTCTGCCTACTGC CTCGGA	97mer oligo for constructing shRNAmir against RagAp1
97mer oligo Rag1Ap1-2	TGCTGTTGACAGTGAGCG AGCTGTCCTTCTCCTGGGT TATTAGTGAAGCCACAGA TGTAATAACCCAGGAGAA GGACAGCCTGCCTACTGC CTCGGA	97mer oligo for constructing shRNAmir against RagAp1
97mer oligo Rag1Ap1-3	TGCTGTTGACAGTGAGCG ACGTGGCAGACTCTTTCC TTTCTAGTGAAGCCACAG ATGTAGAAAGGAAAGAGT CTGCCACGCTGCCTACTG CCTCGGA	97mer oligo for constructing shRNAmir against RagAp1

Table 3.2 Primers used in this project

3.1.9 DNA and Protein Molecular Weight Markers

DNA and protein molecular weight markers used in this project are listed in Appendix C.

3.1.10 DNA Sequencing

Sequencing service was commercially provided by McLab, CA, USA. (http://www.mclab.com/home.php)

3.1.11 Software and Computer Based Programs

The software and computer based programs used in this project are listed in Table 3.3

Program Name	Website/Company	Use
Vector NTI 9.1.0	Invitrogen	Vector maps, primer design, restriction analysis, alignments
FlowJo 7.6.1	http://www.flowjo.com	View and analyze FACS data
Finch TV 1.4.0	Geospiza Inc.	View and analyze sequencing results
ZEN 2009 Light Edition	Carl Zeiss Inc.	View and analyze confocal microscope data
Quantity One	Bio-Rad	Analyze gel images
Uniprot	http://www.uniprot.org/	Secondary structure prediction of membrane proteins
Sosui	http://bp.nuap.nagoya- u.ac.jp/sosui/	
Tmpred	http://www.ch.embnet.org/software/TMPRED_form.html	
Tmhmm	http://www.cbs.dtu.dk/services/TMHMM/	

Table 3.3 Software and computer based programs used in this project

3.2 Methods

3.2.1 General Molecular Cloning Methods

3.2.1.1 Bacterial Cell Culture

Bacterial Culture Growth: *E.coli* DH5α and HB101 strains were grown overnight (12-16h) at 37^{o}C shaking at 250 rpm in Luria Broth (LB) and 2XLB (low salt), respectively. Temperature sensitive SW102, SW105 and SW106 strains were grown overnight in LB with moderate shaking in a 32^{o}C water-bath. For the glycerol stock preparation of bacterial cells, glycerol was added to the overnight grown bacterial cultures to a final concentration of 10%. Cells were frozen first in liquid nitrogen and stored at -80^{o}C. Bacterial strains either streaked or spreaded were grown on LB agar petri dishes overnight. Growth temperature on LB agar medium was 37^{o}C for DH5α and HB101 and 32^{o}C for SW102, SW105 and SW106 strains. All growth medium were prepared with or without selective antibiotic prior to any application.

Preparation of Chemically Competent Bacterial Cells: *E.coli* DH5α and HB101 competent cells were prepared starting from a single colony of previously streaked on LB agar without any selective antibiotics. A single colony from that plate was inoculated in 50mL LB without any selective antibiotics in a 200mL flask overnight at 37^{o}C, 250 rpm. Next day, 4mL from the overnight culture was diluted within 400mL LB medium in a 2L flask and incubated at 37^{o}C, 250 rpm until the optical density at 590nm reaches 0.375. The culture was then transferred into 50mL falcon tubes (8 tubes totally) and incubated on ice for 10 minutes prior to centrifugation at 1600g for 10min at 4^{o}C. After centrifugation, cell pellets were resuspended in 10mL (for each falcon tube) ice-cold $CaCl_2$ solution and centrifuged at 1100g for 5 min at 4^{o}C. The cell pellets were resuspended in 10mL (for each falcon tube) ice-cold $CaCl_2$ solution again and incubated on ice for 30min. Following the final centrifuge at 1100g for 10 min at 4^{o}C,

the pellet was resuspended in 2mL (for each falcon tube) ice-cold $CaCl_2$ solution and dispensed into 200µL aliquots into pre-chilled 1.5mL eppendorf tubes. Aliquotted competent cells were frozen immediately in liquid nitrogen and then stored at -80^oC. Transformation efficiency of the competent cells was tested by pUC19 plasmid transformation.

Chemical Transformation of Bacterial Cells: Chemically competent cell which was previously treated with $CaCl_2$, was taken from -80^oC and 100pg of DNA was added before the cells were completely thawed. The cells were then incubated on ice for 30 min. After the incubation on ice, the cells were heat shocked for 90 seconds at 42^oC and transferred back onto ice for 60 seconds. 800µL of sterile LB without any antibiotics was added on the cells and this culture was incubated for 45 min at 37^oC for the recovery of the cells. After 45 min, the cells were spread with 4mm glass beads on the LB agar plate containing appropriate antibiotic for selection. The plate was incubated overnight at 37^oC.

Plasmid and BAC DNA Isolation: Plasmid DNA isolation was performed with either alkaline lysis protocols in Smabrook et al or Qiagen Mini-Midiprep Kits. For BAC DNA isolation, small and large scale DNA isolation was performed with alkaline lysis protocols in Smabrook et al, and Qiagen Midiprep Kits containing revised protocols for BAC, respectively. The concentration and purity of the DNA isolated were determined by using UV-spectrophotometer. Measurements for DNA concentration and purity were done at an optical density of 260nm by using quartz cuvettes.

3.2.1.2 Vector Construction

Polymerase Chain Reaction (PCR) Amplification:

Optimized PCR conditions are shown in Table 3.4

PCR Reaction	Volume Used	Final Concentration
Template DNA	1-10µL	4pg/µL – 4ng/µL
10X Pfu Polymerase Buffer with $MgCl_2$	2.5µL	1X
dNTP mix (10mM)	0.5µL	0.2mM
Forward Primer (10µM)	2µL	0.8µM
Reverse Primer (10µM)	2µL	0.8µM
Pfu Polymerase (2.5U/µL)	0.5µL	0.025U/µL
ddH_2O	Up to 25µL	
Total	25µL	

Table 3.4 Optimized PCR conditions

Optimized PCR thermal cycle conditions are shown in Table 3.5

Step	Temperature (^oC)	Time (min)	
Initial Denaturation	95	4	
Denaturation	95	1	30 cycles
Annealing	56	1	
Extension	72	2	
Final Extension	72	10	
Hold	4	∞	

Table 3.5 Optimized PCR thermal cycle conditions

Restriction Enzyme Digestion:

Components and amounts for restriction enzyme digestion are shown in Table 3.6

Components	Used Amount
Plasmid DNA	1µg-10µg
Restriction enzyme (10U/µL)	1.5µL
Compatible Buffer (10X)	1.5µL
ddH_2O	Up to 15µL
Total	15µL

Table 3.6 Components and amounts for restriction enzyme digestion

Restriction enzyme digestion reactions were set by the mixture of ddH_2O, DNA, the enzyme and the compatible buffer in a 1.5mL eppendorf tube and incubated at the optimum temperature for 2 – 2.5 hours. For diagnostic digestions 1µg of DNA was used. 10µg or more DNA was digested for gel extraction and cloning purposes. If the DNA was a digested vector that would be used in the ligation, 5' overhang of the linear plasmid was dephosphorylated by calf intestinal alkaline phosphatase, CIAP (Fermentas).

Agarose Gel Electrophoresis: PCR products, digestion products and DNA samples were observed with 1% agarose gels. Gel was prepared by dissolving 1g of agarose in 100mL 0.5X TBE. The mixture was heated in a microwave until the agarose was completely dissolved. The solution was then cooled down and ethidium bromide with a final concentration of 0.001v/v was added. After mixing properly, the gel was poured onto the gel apparatus and let to cool down and solidify. When the gel was in solid form, the DNA samples which were previously mixed with 6X DNA loading dye reaching to a final concentration of 1X were loaded to the gel. 0.5X TBE was used as a running buffer. The gel was run at 100V for 75 min and the bands were observed under UV.

DNA Extraction: DNA samples were extracted with Qiagen Gel Extraction Kit.

Ligation: The ligation reaction mixtures were composed of insert either digested or amplified by PCR and digested thereafter, digested vector, T4 ligation buffer (Fermentas), T4 DNA ligase (Fermentas) and ddH_2O. Ligations were done according to 1:3, 1:5 and 1:10 vector:insert molar ratio using 100ng of vector. For ligations, vectors which were dephosphorylated by using calf intestine alkaline phosphatase, CIAP (Fermentas) after digestion, in order to avoid self ligation. Also for each ligation, a ligation reaction mixture without insert was used as negative control. Ligation reactions were done at 16^{o}C for 16 hours. The mixture was then transformed into chemically competent bacterial cells.

3.2.2 Preparation of Electrocompetent Cells and BAC Electroporation

BAC electroporation experiments were done according to Warming et al. A single colony of SW106 cells was inoculated in 5mL LB without any antibiotics overnight with moderate shaking in a 32^{o}C water bath. Next day, 500µL of the overnight culture was inoculated in 25mL LB without antibiotics in a 50mL baffled flask and incubated with moderate shaking in the 32^{o}C water bath until optical density at 600nm reached 0.6. The culture was then cooled down in ice/water slurry and transferred into pre-cooled 15mL falcon tubes. The cells were then centrifuged at 5000 rpm for 5 minutes at 4^{o}C. After removing the supernatant, the cells pellets were resuspended in 1mL ice-cold sterile ddH_2O by moving the 15mL falcon tubes in circles gently in the ice/water slurry. When the cells were resuspended, the suspension was filled up to 10mL with sterile ddH_2O and centrifuged thereafter. This washing step was repeated two times more. After final centrifugation, the cells were resuspended in 50µL sterile ddH_2O and 25µL of the freshly prepared electrocompetent cell was transferred to a pre-cooled 1.5mL eppendorf tube. The 5µg freshly isolated BAC DNA to be transfected was mixed with the cell suspension in the eppendorf and transferred to a pre-cooled 1mm-gap electroporation cuvette. Electroporations were done with Bio-RadECM630 electroporator. The optimum condition for BAC electroporation was 1.7kV, 25µF and 200Ω. After electroporation cells were recovered with 1mL LB without antibiotics in a

shaking water bath at 32°C. RP23-432G9, BAC containing CD3δ was resistant to chloramphenicol. 100µL from the cell suspension and dilutions like 1:10 and 1:100 and 100µL resuspension of rest of cells after a full spin were spread on LB agar plates with a chloramphenicol concentration of 12.5µg/mL. The plates were incubated at 32°C for 16-24 hours.

3.2.3 BAC Recombination

BAC recombination experiments were done according to Warming et al. A single colony of SW106 cells containing CD3δ BAC was inoculated in 5mL LB with a chloramphenicol concentration of 12.5µg/mL with moderate shaking in a 32°C water bath. Next day, 500µL of the overnight culture was inoculated in 25mL LB with a chloramphenicol concentration of 12.5µg/mL in a 50mL baffled flask and incubated with moderate shaking in the 32°C water bath until optical density at 600nm reached 0.6. 10mL of the culture was transferred to a 50mL baffled flask and heat shocked at 42°C for exactly 15 minutes. Rest of the culture was continued to be incubated at 32°C as the negative control of the experiment. After the heat shock at 42°C, the cells were cooled on ice and then transferred to 15mL falcon tubes and made electrocompetent according to the protocol explained in 3.2.2. Before electroporation the freshly made electrocompetent cells were mixed with 10ng linearized DNA. Then, the mixture was transferred to a pre-cooled 1mm-gap electroporation cuvette and electroporated as explained in 3.2.2. After recovery, the cells from the cell suspension and dilutions like 1:10 and 1:100 and 100µL resuspension of rest of cells after a full spin werespread on LB- agar plates had a ampicillin concentration of 100µg/mL. The plates were incubated at 32°C for 2-3 days.

3.2.4 Mammalian Cell Culture

3.2.4.1 Preparation and Maintenance of Mammalian Cells

Maintenance of Suspension Cells: Suspension cells used in this project were VL3-3M2, AKR1 and RLM11 cells. These cell lines were grown in filter-sterilized RPMI that was supplemented with 10% heat-inactivated fetal bovine serum, 2mM L-Glutamine, 100unit/mL penicillin, 100unit/mL streptomycin and 50μM beta mercaptoethanol in tissue culture flasks in a 37^{o}C, 5%CO_2 incubator. Cells were splitted into a pre-warmed, fresh medium with a ratio of 1:20 once in two days.

Maintenance of Adherent Cells: Adherent cells used in this project were HEK 293T and Hela cells. These cell lines were grown in filter-sterilized DMEM that was supplemented with 10% heat-inactivated fetal bovine serum, 2mM L-Glutamine, 100unit/mL penicillin and 100unit/mL streptomycin in 10mm tissue culture plates in a 37^{o}C, 5%CO_2 incubator. When the plate reached to 70-80% confluency, cells were splitted into a pre-warmed, fresh medium with a ratio of 1:10. Adherent cells were trypsinized before splitting.

Trypsinization: Adherent cells were trypsinized to detach the cells both from the plate and from each other. After removing the old medium, plate was washed with serum free DMEM to remove the serum which would lead to deactivate trypsin, form the surface. 2mL of trypsin was added on the plate and incubated until the cells were detached from the plate (approximately 2 minutes) at 37^{o}C. 8 mL of fresh medium containing serum was then added to the trypsin on the plate surface and cells were harvested to a 15 mL falcon tube. After centrifugation at 1000 rpm for 5 minutes, the medium was removed and cells were resuspended in pre-warmed fresh DMEM that was supplemented with 10% heat-inactivated fetal bovine serum, 2mM L-Glutamine, 100unit/mL penicillin and 100unit/mL streptomycin for further incubation.

Cell Freezing: 10^6 cells were centrifuged at 1000 rpm for 5 minutes and the medium was removed. The cells were then resuspended in 1 mL ice-cold freezing medium containing DMSO added into fetal bovine serum (FBS) at a final concentration of 10% (v/v) and were put in cryovials. They were stored at -80^{o}C in cryobox for 24-48 hours and were then transferred to liquid nitrogen tank.

Cell Thawing: Frozen cells in the cryovials were resuspended in 10mL complete growth medium in a 15mL falcon tube. The cells were then centrifuged at 1000 rpm for 5 minutes. After removing the supernatant, the cells were resuspended in 10mL pre-warmed fresh complete medium and transferred to either plates or flasks.

3.2.4.2 Transient Transfection of Suspension Cells

Suspension cell used in this project was VL3-3M2. Transient transfection of this cell line was done by using Neon Device. One day before transfection cells were splitted 1:10 ratio in order to obtain healthy and growing cells for the experiment. On the transfection day, the cells were first counted and medium containing 10^7 cells for each sample was centrifuged in 15mL falcon tubes at 1000 rpm for 5 minutes. After removing the supernatant, the cells were resuspended in filter sterilized 1XPBS and centrifuged at 1000 rpm for 5 minutes. Supernatant was then removed and cells were resuspended in 100µL HBS. 10µg of DNA was added to the suspension of cells in 100µL HBS. This mixture was taken into 100µL golden tips of Neon Device and inserted into the machine. Optimum condition for transfection of suspension cells was 1500V, 20ms and 1 pulse. After transfection, the cells were transferred into pre-warmed 10mL RPMI that was supplemented with 10% heat-inactivated fetal bovine serum, 2mM L-Glutamine and 50µM beta mercaptoethanol. 48 hours after transfection, cells were analyzed with FACS.

3.2.4.3 Transient Transfection of Adherent Cells with Calcium Phosphate

Adherent cells used in this project were HEK293T and Hela cells. Transient transfection of these cell lines were done by using calcium phosphate method. One day before transfection 10^7 cells were splitted onto 10-cm plates. On the transfection day, 2 hours before the experiment the medium was removed and 10mL fresh complete medium was added to the plate. In a 15mL falcon tube, 10µg DNA and 120µL 1M filter-sterilized $CaCl_2$ were mixed and the volume was completed to 500µL with sterile ddH_2O. 500µL sterile 2XHBS with a pH of 7.05 was added to the mixture drop by drop with bubbling and the mixture was vortexed immediately. The mixture was incubated at room temperature for 15 minutes. After the incubation, the mixture was added on the cells. 16 hours after transfection, medium of the cells was changed with fresh 10mL complete DMEM. 48 hours after transfection the cells were analyzed with FACS.

3.2.4.4 Cell Lysis and Immunoprecipitation

48 hours after transfection of expression plasmids to HEK293T cells, cells were trypsinized and harvested in a 15mL falcon tube. After centrifugation at 1000 rpm for 5 minutes, the cells were washed with 1XPBS and transferred to a 1.5mL eppendorf tube. Another centrifugation at 1000 rpm for 5 minutes was done to remove the PBS and the cells were then resuspended in 500µL Triton-X Lysis buffer. The cells were incubated with the lysis buffer suspension on ice for 30 minutes and then centrifuged at 13.200 rpm for 10 minutes. Lysate (the supernatant after centrifugation) was transferred to a clean 1.5mL eppendorf tube. Lysates were stored at -80^oC for western-blot experiments, however if there was an immunoprecipitation experiment going on, then the lysates were freshly used.

Immunoprecipitations in this project were done by using anti-HA immunoprecipitation kit (Sigma). 450µL of lysate, 10µL anti-HA agarose suspension and 140µL 1X IP buffer coming with the kit (Sigma) were mixed and transferred to the columns of the kit. The mixture in the columns was incubated by mixing head over tail

at 4°C overnight. The next day, beads in the column were washed 7-10 ten times with 1X IP buffer coming with the kit. Finally, beads in the column were boiled at 95°C in 1X SDS loading buffer (Fermentas) and 1X reducing agent (Fermentas) for 5 minutes leading the protein samples transfer from beads to the buffer. After centrifugation, the samples were ready to be loaded to SDS gel.

3.2.4.5 SDS Gel, Transfer and Western-Blot

The SDS gels used in this project had a 13% separating part and a 4% stacking part and their contents were explained in 3.1.3.1. After the samples were loaded, the SDS gels were run with 1X running buffer at constant 100V for 1.5-2 hours using BIORAD MiniProtean Tetra Cell. After running, the gels were transferred to 0.45µm PVDF membranes (Thermo Scientific) in 1X transfer buffer at constant 100V for 1 hour at 4°C using BIORAD Mini Trans-blot wet electrophoretic transfer cells. Membranes were then blocked in 10mL PBST-milk at room temperature for 1 hour with constant shaking. Primary antibody incubations were done overnight at 4°C and secondary antibody incubations were done for 1 hour at room temperature. Membranes were washed with PBST 3 times for ten minutes after blockings, primary antibody incubations and secondary antibody incubations. After final washing step, the membranes were incubated with an enhanced chemiluminescent substrate (Supersignal west pico chemiluminescent substrate, Thermo Scientific lot number JL126474) for 4 minutes at room temperature in dark room for HRP to be detected. Membranes were then transferred to cassettes. Films (Roche) were exposed to the membranes, development and fixation were done in dark room.

3.2.5 shRNAmir Expression

MSCV-LTRmiR30-PIG (LMP) is a MSCV based retroviral vector that can be used to clone shRNA of interest and use for shRNA mediated gene silencing. In order to get shRNAs against the gene used in this project, three different mir30-based shRNA template oligonucleotides were designed. There different inserts coming from three different oligos were amplified by PCR.

PCR conditions for preparing shRNAmir-LMP constructs are shown in Table 3.7

PCR Reaction	Volume Used	Final Concentration
Template DNA (2nM)	10µL	0.2nM
10X Pfu Polymerase Buffer with $MgCl_2$	10µL	1X
dNTP mix (2mM)	10µL	0.2mM
miR30 Forward Primer (10µM)	5µL	0.5µM
miR30 Reverse Primer (10µM)	5µL	0.5µM
Pfu Polymerase (2.5U/µL)	1µL	0.025U/µL
ddH_2O	54µL	
Total	100µL	

Table 3.7 PCR conditions for preparing shRNAmir-LMP constructs

PCR thermal cycle conditions for preparing shRNAmir-LMP constructs are shown in Table 3.8

Step	Temperature (^oC)	Time	
Initial Denaturation	94	1 min	
Denaturation	94	30 sec	30 cycles
Annealing	54	30 sec	
Extension	75	30 sec	
Final Extension	75	10 min	
Hold	4	∞	

Table 3.8 PCR thermal cycle conditions for preparing shRNAmir-LMP constructs

PCR products were run on 2% agarose gel and gel extracted and the band corresponded to 138 bp was isolated. Both the PCR products and the LMP vector were digested with EcoRI and XhoI restriction enzymes and ligated. The plasmids constructed were then analyzed with confirmation digestions.

3.2.6 Subcellular Localization

HeLa cells were used for subcellular localization experiments. Prior to their transfection with calcium phosphate, coverslides were attached to the surface of the plates and the cells were seeded those coverslides. Transfection of the DNA into HeLa cells was done according to the protocol explained in 3.2.3.3. After 48 hours from transfection, the medium was removed and the cover slips were washed with 1XPBS two times. 80% ethanol was then added to the plates and cells were incubated for 30 minutes at room temperature for fixation of the cells to the cover slips. 5µL of 99.8% glycerol was added on the slides and the cover slips were inverted on slides. The edges of the cover slip on the slide were then flushed with nail polish. After the nail polish was dry, the cells were visualized with the fluorescence microscope with appropriate magnification and appropriate filters.

3.2.7 Flow Cytometric Analysis

10^6 cells were used for each flow cytometric analysis. After centrifugation of the cells, the supernatant was removed and the cells were washed with PBS for two times. In order to detect TCR on the cell surface, the cells were incubated with H57PE at 4^oC for 30 minutes in dark. After incubation with antibody cells were washed with PBS two times and resuspended in 500µL PBS for analysis. The flow cytometric analysis of the cells was done by using BD FACSCanto. GFP and Venus proteins were excited by the argon laser and fleurescence was detected with FITC 530/30nm band pass filter. TCR levels were either detected with PE or Alexa-647 channel.

4. RESULTS

4.1 Recombination

4.1.1 Recombination Strategy

In the first part of this thesis, we conducted molecular biology experiments to generate a knockout construct which will be used to inactivate the CD3δ gene in the mouse genome. The main of strategy for the conditional knockout construct was to delete exonδ2 in which most of the CD3δ protein is encoded. In order to delete exonδ2, we wanted to insert two loxP sites. Therefore, the region between two loxP sites on either sides of this exon in mouse genomic DNA. As the bacteriophage Cre enzyme can delete the region between any two loxP sites (in our case exonδ2 of the mouse CD3δ gene), this construct can be used to generate a tissue and developmentally stage specific knockout of the CD3δ gene. This section is dedicated to the description of the generation of the CD3δ knockout targeting vector, which in future work will be used to generate these knockout mice.

To generate the CD3δ targeting vector, we used the recombineering technique to modify bacterial artificial chromosomes (BAC)[43-45]. The recombineering strategy consists of three steps, where CD3δ gene locus is sequentially modified in *E.coli*. In the first step, due to the difficulty of working with large BAC DNAs, we attempted to rescue a part of the CD3δ gene from a BAC by homologous recombination into a plasmid containing a thymodine kinase (TK) gene for further selection in embryonic stem cells (ESC). To rescue the CD3δ gene fragment form BAC RP23-432G9, we selected two regions of homology (R1 and R2) flanking exonδ1 and exonδ3. These

regions of homology were PCR amplified and inserted into the plasmid pKO917TK. Our strategy to rescue the region of interest from BAC RP23-432G9 into the plasmid NK6 (pKO917+R1+R2) by homologous recombination is shown in figure 4.1.

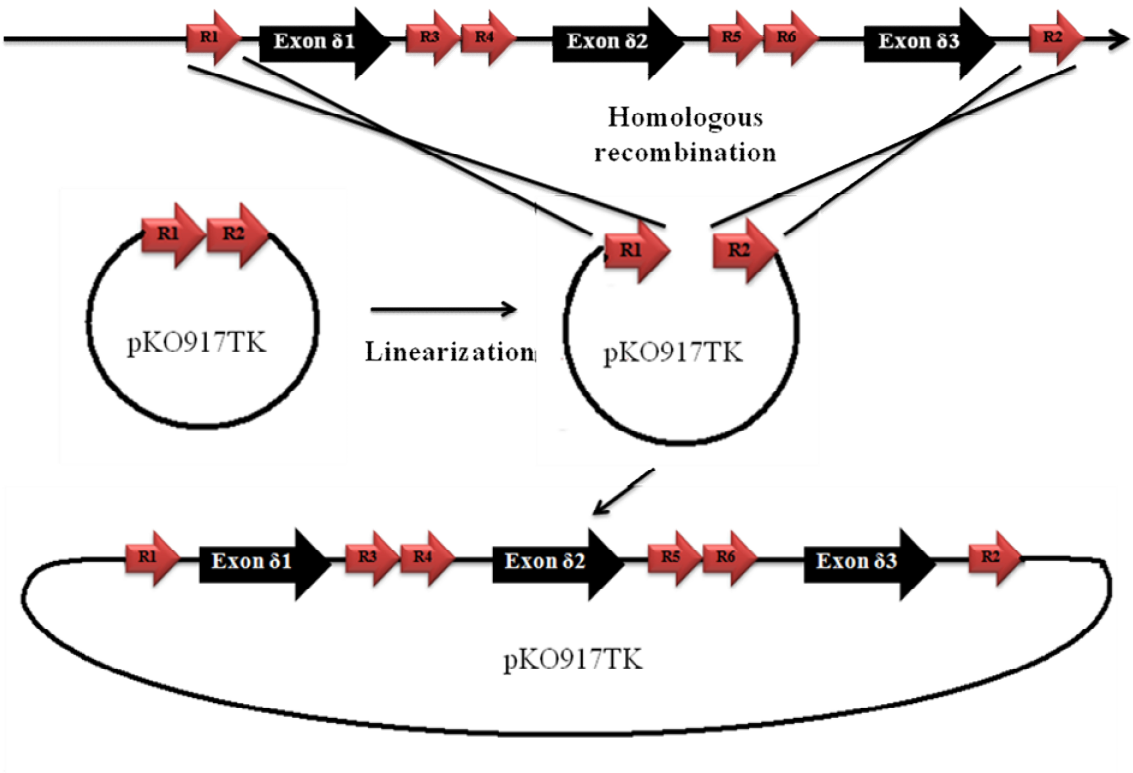

Figure 4.1 Schematic diagram describing the strategy to rescue the region of interest from BAC RP23-432G9 into the pKO917+R1+R2 plasmid by homologous recombination. The region between R1 and R2 homology regions is rescued from BAC RP23-432G9 into pKO917TK+R1+R2 by homologous recombination. Black arrows represent the exons and red arrows represent the homology regions.

The second step in the recombineering of the CD3δ gene locus was the insertion of loxP sites flanking CD3δ exonδ2. For this purpose, we constructed a plasmid (pLTM332+R3+R4) that will be used to insert loxP sites upstream of the CD3δ gene exonδ2. The first plasmid, contained two homology regions named R3 and R4, amplified from a region upstream of exonδ2 in the CD3δ gene. This plasmid contains a neomycin resistance gene (NEO) flanked by loxP sites in between these homology regions (R3 and R4). Our targeting strategy will recombine a cassette from plasmid pLTM332+R3+R4 into the CD3δ gene, followed by the deletion of NEO by activating the Cre enzyme in *E.coli* containing this plasmid DNA. This part of the strategy, with the second homologous recombination and deletion of NEO is shown in figure 4.2. The

deletion of the sequence between two loxP sites will generate a plasmid containing a single loxP site upstream of the CD3δ gene exonδ2.

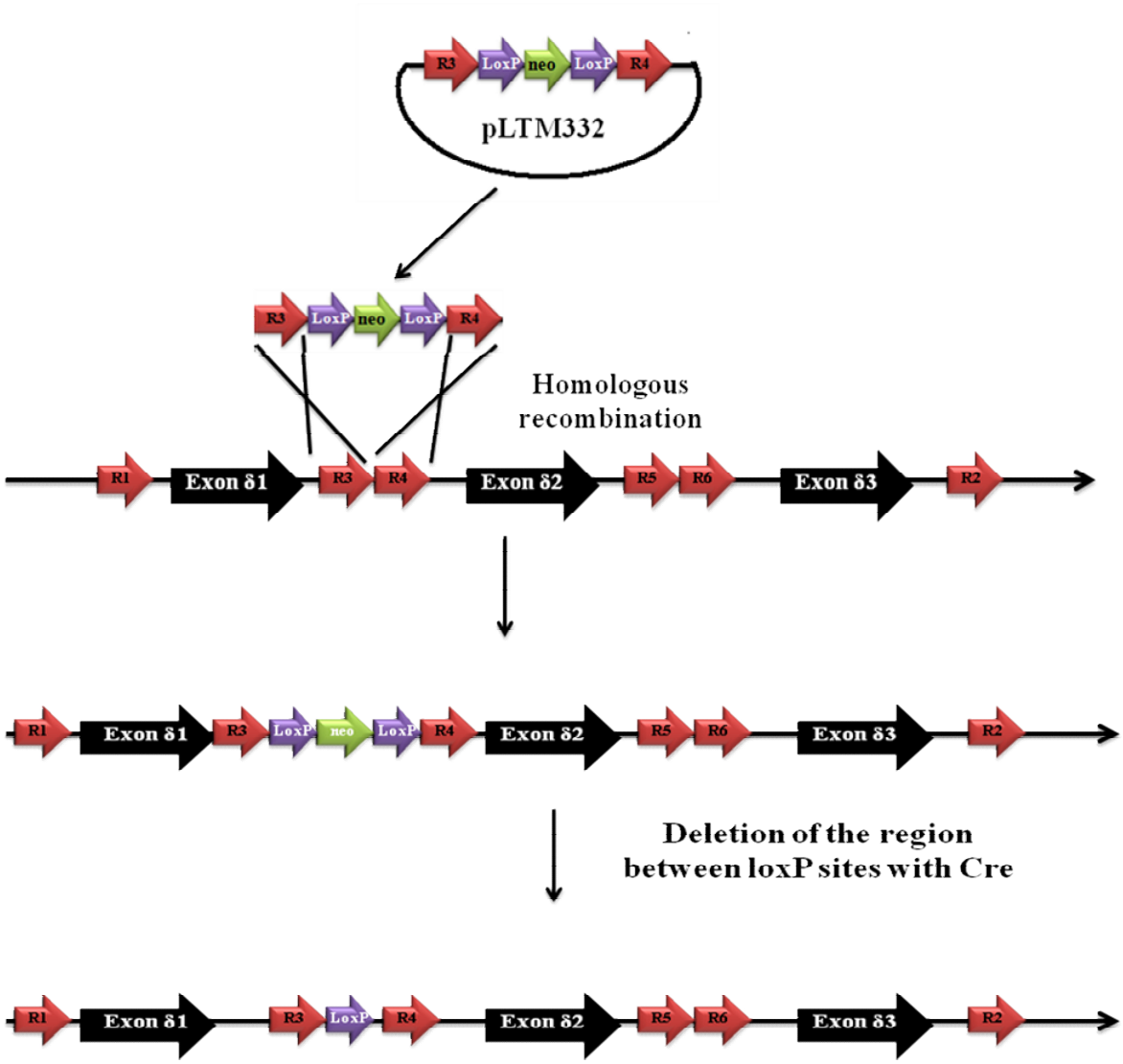

Figure 4.2 Schematic diagram describing homologous recombination reactions inserting a loxP site upstream of the CD3δ gene exonδ2. The R3-loxP-NEO-loxP-R4 cassette from plasmid pLTM332+R3+R4 will be inserted into the upstream region of CD3δ gene by homologous recombination. NEO will then be deleted by activating the Cre enzyme in *E.coli* containing this plasmid DNA and this will result in the generation of a plasmid containing a single loxP site upstream of CD3δ gene exonδ2. Bold black arrows represent the exons, red arrows represent homology regions, purple arrows represent loxP sites and green arrow represents the neomycin resistance gene.

Third step of recombineering involved the construction of a plasmid (pLTM260+R5+R6) containing homology regions named R5 and R6, amplified from the downstream region of CD3δ exonδ2, flanking two loxP sites (for Cre mediated excision), two Frt sites (for following Flp mediated excision) and a neomycin resistance gene. The strategy for recombineering this casette into the CD3δ gene locus is shown in figure 4.3. Briefly, after CD3δ gene containing plasmids will be modified by homologous recombination where a cassette derived from plasmid pLTM260+R5+R6 will be inserted downstream of the CD3δ gene exonδ2, with the help of homology regions R5 and R6. The NEO sequence in this cassette will be deleted by activating the Flp enzyme in *E.coli* containing this plasmid, which will delete sequences in between the two Frt sites. The deletion of these sequences will generate a plasmid containing a single Frt and a single loxP site located downstream of the CD3δ gene exonδ2. This loxP site and loxP site upstream of the exonδ2 generated in the second recombineering step will be used in future experiments to conditionally delete this exon of the CD3δ gene from its gene locus.

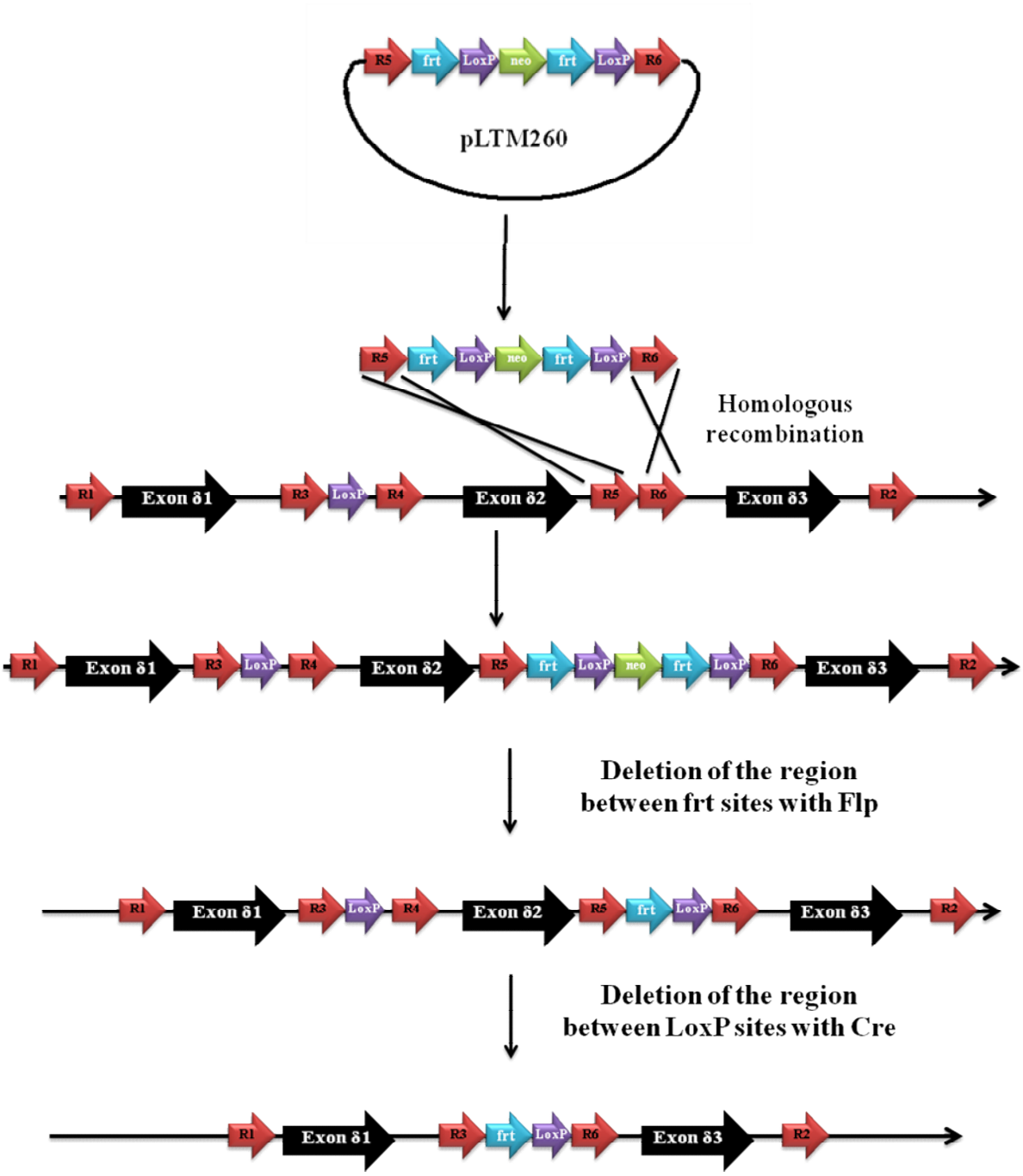

Figure 4.3 Schematic diagram describing homologous recombination reactions for inserting a loxP site downstream of the CD3δ gene exonδ2 and deletion of CD3δ gene exonδ2. R5-frt-loxP-NEO-frt-loxP-R6 cassette from plasmid pLTM260+R5+R6 will be inserted into the downstream region of CD3δ gene by homologous recombination. NEO will be then deleted by activating the Flp enzyme in *E.coli* containing this plasmid DNA and this will result in the generation of a plasmid containing a single loxP and a single Frt site upstream of CD3δ gene exonδ2. Bold black arrows represent the exons, red arrows represent the homology regions, purple arrows represent the loxP sites, blue arrows represent the Frt sites and green arrow represents the neomycin resistance gene.

4.1.2 Construction of Vectors for Recombination

4.1.2.1 Construction of the NK1 (pLTM332+R3) and NK2 (pLTM332+R3+R4) Plasmids

In this section, I will describe the experiments performed to construct the plasmids that are necessary to conduct the recombineering experiments whose strategy was detailed in section 4.1.1. First homology regions R3 and R4 were ligated into the pLTM332 vector which contains two loxP sites and a neomycin resistance gene. The first plasmid constructed for recombination experiments was named NK1 (pLTM332+R3) (shown in figure D.5). Before starting the construction of the plasmid, we performed diagnostic digests of pLTM332 with BglII – EcoRI and PvuI. According to the map of pLTM332 (shown in figure D.1), Bgl II – EcoRI double digestion should generate two bands of 1734 and 2961 bp and PvuI single digestion should generate two bands of 1045 and 3650 bp. The agarose gel containing the BglII – EcoRI and PvuI digested pLTM332 plasmid is shown in figure D.1.

The R3 homology region was previously amplified with PCR from BAC DNA containing the CD3δ gene (RP23-432G9) and ligated into the pTZ57R/T vector (Fermentas, InsTA cloning vector). The R3 homology region which is 245 bp long is flanked by a 5' SalI and a 3' XhoI restriction sites. In order to obtain the R3 fragment, the pTZ57R/T+R3 plasmid was digested with SalI – XhoI which generated two bands of 245 and 2892 bp where the 245 bp band corresponds to the R3 homology region. Therefore, the 245 bp band was gel extracted and purified for further ligation steps. The agarose gel for digestions and relevant controls are shown in figure D.2.

The SalI and XhoI restriction sites flanking the R3 homology region are compatible to each other. Therefore, the vector that received this insert, pLTM332 plasmid was only digested with SalI for the further ligation step. Digestion products

were loaded on 1% agarose gels and the linearized vector was gel extracted. In figure D.3, the linearization of the pLTM332 plasmid with SalI is shown.

The purified R3 fragment and linearized pLTM332 plasmid were compared before ligation. The ligation was performed using 1:10, 1:6, 1:3, 1:1 vector:insert ratios. In figure D.4, comparison of DNA fragments containing the purified R3 insert and linearized pLTM332 plasmid is shown. After ligation, 25 colonies were used to isolate plasmid DNAs. Due to the fact that R3 had compatible ends, there was the risk of multiple inserts being ligated into the plasmid. In addition to this, there was also the risk for the insert to be inserted in the wrong direction. We performed confirmation digests for identifying the number of inserts using XhoI – HindIII which generated three bands of 272, 1730 and 2944 bp. The XhoI site following the R3 fragment, which was destroyed after being ligated into the SalI site is shown as XhoI* in figure D.5. The orientation of the insert was confirmed with SmaI – KpnI double digestion where SmaI is introduced from the insert. A correct orientation of the insert would yield two bands of 237 and 4709 bp in a SmaI – KpnI digestion, whereas an incorrect orientation would generate two bands of 23 and 4923 bp. In figure D.5 a total size confirmation with XhoI – HindIII double digesiton and in figure D.5 b direction confirmation with SmaI – KpnI double digestion is shown.

The R4 homology region was previously amplified with PCR from BAC DNA containing the CD3δ gene (RP23-43G9) and ligated into pTZ57R/T vector (Fermentas, InsTA cloning vector). The R4 homology region which is 248 bp long is flanked by a 5' BamHI restriction site and a 3' Bgl II restriction site. In order to obtain the R4 fragment, the pTZ57R/T+R4 plasmid was digested with BamHI – Bgl II which generated two bands of 248 and 2892 bp where the 248 bp band corresponds to the R4 homology region. Therefore, the 248 bp band was gel extracted and purified for futher ligation steps. The agarose gel for digestions and single digestion controls for are shown in figure D.6.

The BamHI and Bgl II restriction sites flanking the R4 homology region are compatible to each other. Therefore, NK1 (pLTM332+R3) plasmid was only digested with BglII for the further ligation step. Digestion products were loaded on the 1% agarose gel and the linearized vector was gel extracted. In figure D.7, the linearization of NK1 (pLTM332+R3) with Bgl II is shown.

The purified R4 fragment and linearized NK1 (pLTM332+R3) were compared before ligation. The ligation was peformed using 1:10, 1:6, 1:3, 1:1 vector:insert ratios. In figure D.8, comparison of DNA fragments containing the purified R4 insert and linearized NK1 plasmid is shown. After ligation, 25 colonies were used to isolate plasmid DNAs. Due to the fact that R4 had compatible ends, there was the risk of multiple inserts being ligated into the plasmid. In addition to this, there was also the risk for the insert to be inserted in the wrong direction. We performed confirmation digests for identifynig the number of inserts using Sac II – XhoI which generated three bands of 319, 2002 and 2879 bp. Identification of the number of inserts was also confirmed with SacII – XbaI double digestion which generated two bands of 597 and 4603 bp. The orientation of the insert was confirmed with Bgl II - XhoI double digestion. A correct orientation of the insert would yield three bands of 307, 2002 and 2891 bp in a Bgl II – XhoI double digestion, whereas an incorrect orientation of the insert would generate two bands of 53 and 5147 bp. BamHI site at the beginnig of R4 was destroyed after being ligated into Bgl II site. Therefore in the figure 4.12 that BamHI site is shown as BamHI*. In additon to these, confirmation digests for NK1 (pLTM332+R3) was repeated with the correct colony for NK2 (pLTM332+R3+R4). In figure 4.4, confirmation digestion results one of the correct colonies is shown.

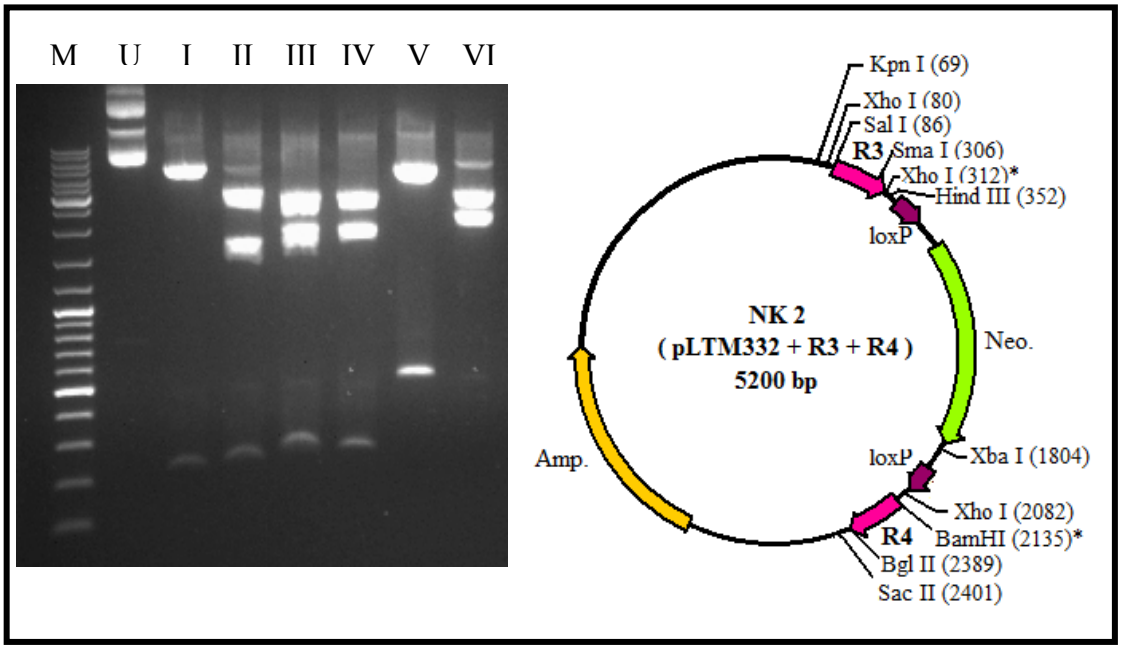

Figure 4.4 Confirmation digests of the NK2 (pLTM332+R3+R4) plasmid. The agarose gel on the left shows the confirmation digests of NK2 with SmaI – KpnI, XhoI – HindIII, Bgl II – XhoI, SacII – XhoI, SacII – XbaI and SalI – SacII double digestions Lane M shows the DNA size marker, lane U shows the undigested NK2, lane I shows SmaI – KpnI digested NK2, lane II shows XhoI – HindIII digested NK2, lane III shows the Bgl II – XhoI digested NK2, lane IV shows SacII – XhoI digested NK2, lane V shows SacII – XbaI digested NK2 and lane VI shows SalI – SacII digested NK2. The map of NK2, shown on the right, indicates that SmaI – KpnI double digestion should generate two bands of 239 and 4961 bp, XhoI – HindIII double digesiton should generate three bands of 302, 1730 and 3169 bp, Bgl II – XhoI double digestion should generate three bands of 307, 2002 and 2891 bp, SacII – XhoI double digestion should generate three bands of 319, 2002 and 2879 bp, SacII – XbaI double digestion should generate two bands of 597 and 4603 bp and SalI – SacII double digestion should generate two bands of 2315 and 2885 bp. (The XhoI site following the R3 fragment, which was destroyed after being ligated into the SalI site is shown as XhoI* and the BamHI site preceding the R4 fragment, which was destroyed after being ligated into the Bgl II site is shown as BamHI*)

4.1.2.2 Construction of the NK3 (pLTM260+R5) and NK4 (pLTM260+R5+R6) Plasmids

The R5 and R6 homology regions were ligated into the pLTM260 plasmid which contains two loxP sites, two frt sites and a neomycin resistance gene. The third plasmid constructed for recombination experiments was named NK3 (pLTM260+R5) (shown in figure D.14). Before starting the construction of the plasmid, we performed diagnostic digests of pLTM260 with SalI, XbaI and KpnI single digesitons. According to the map of pLTM260 (shown in figure D.10), SalI digestion should linearize pLTM260, XbaI digestion should generate three bands of 345, 1461 and 3011 bp and KpnI digestion should generate two bands of 1943 and 2874bp. The agarose gel containing the SalI, XbaI and KpnI single digested pLTM260 is shown in figure D.10.

The R5 homology region was previously amplified with PCR from BAC DNA containing the CD3δ gene (RP23-432G9) and ligated into the pTZ57R/T vector (Fermentas, InsTA cloning vector). The R5 homology region which is 216 bp long is flanked by a 5' SalI and a 3' XhoI restriction sites. In order to obtain the R5 fragment, pTZ57R/T+R5 plasmid was digested with SalI - XhoI which generated two bands of 216 and 2892 bp where the 216 bp band corresponds to the R5 homology region. Therefore, the 216 bp band was gel extracted and purified for futher ligation steps. The agarose gel for the double digestion and single digestion controls for are shown in figure D.11.

The SalI and XhoI restriction sites flanking the R5 homology region are compatible to each other. Therefore, the pLTM260 plasmid was only digested with SalI for the further ligation step. The digestion products were loaded on the 1% agarose gel and the linearized vector was gel extracted. In figure D.12, the linearization of the pLTM260 plasmids with SalI is shown.

The purified R5 fragment and linearized pLTM260 plasmid were compared before ligation. The ligation was performed using 1:10, 1:6, 1:3, 1:1 vector:insert ratios.

In figure D.13, comparison of DNA fragments containing the purified R5 insert and linearized pLTM260 plasmid is shown. After ligation, 25 colonies were used to isolate plasmid DNAs. Due to the fact that R5 had compatible ends, there was the risk of multiple inserts being ligated into the plasmid. In addition to this, there was also the risk for the insert to be inserted in the wrong direction. We performed confirmation digests for identifying the number of inserts using XhoI – HindIII which generated four bands of 22, 243, 1783 and 2991 bp. The XhoI site following the R5 fragment, which was destroyed after being ligated into the SalI site is shown as XhoI* in figure D.14. The orientation of the insert was confirmed with KpnI single digestion where an additional KnpI is introduced from the insert. A correct orientation of the insert would yield three bands of 227, 1938 and 2874 bp in a KpnI single digestion, whereas an incorrect orientation would generate three bands of 23, 2142 and 2874 bp. In figure D.14, confirmation digestion results one of the correct colonies is shown.

The R6 homology region was previously amplified with PCR from BAC DNA containing the CD3δ gene (RP23-432G9) and ligated into the pTZ57R/T vector (Fermentas, InsTA cloning vector). The R6 homology region which is 262 bp long is flanked by two SacII restriction sites. In order to obtain the R6 fragment, the pTZ57R/T+R6 plasmid was digested with SacII which generated two bands of 262 and 2892 bp where the 262 bp band corresponds to the R6 homology region. Therefore, the 262 bp band was gel extracted and purified for further ligation steps. The agarose gel for digestions and relevant controls are shown in figure D.15.

Due to the fact that the R6 homology region is flanked by two SacII restriction sites, the NK3 (pLTM260+R5) plasmid was only digested with SacII for the further ligation step. Digestion products were loaded on 1% agarose gels and the linearized vector was gel extracted. In figure D.16, the linearization of the NK3 (pLTM260+R5) plasmid with SacII is shown.

The purified R6 fragment and linearized NK3 (pLTM260+R5) plasmid were compared before ligation. The ligation was performed using 1:10, 1:6, 1:3, 1:1 vector:insert ratios. In figure D.17, comparison of DNA fragments containing the purified R6 insert and linearized NK3 (pLTM260+R5) plasmid is shown. After ligation, 25 colonies were used to isolate plasmid DNAs. Due to the fact that R6 has the same

ends, there was the risk of multiple inserts being ligated into the plasmid. In addition to this, there was also the risk for the insert to be inserted in the wrong direction. We performed confirmation digests for identifying the number of inserts using PvuII which generated four bands of 544, 844, 1408 and 2513 bp. The orientation of the insert was confirmed with BamHI – KpnI double digestion where BamHI is introduced from the insert. A correct orientation of the insert would yield two bands of 227, 262, 1938 and 2880 bp in an BamHI – KpnI digestion, whereas an incorrect orientation would generate three bands of 23, 227 and 1938 bp. In figure 4.5, confirmation digestion results one of the correct colonies is shown.

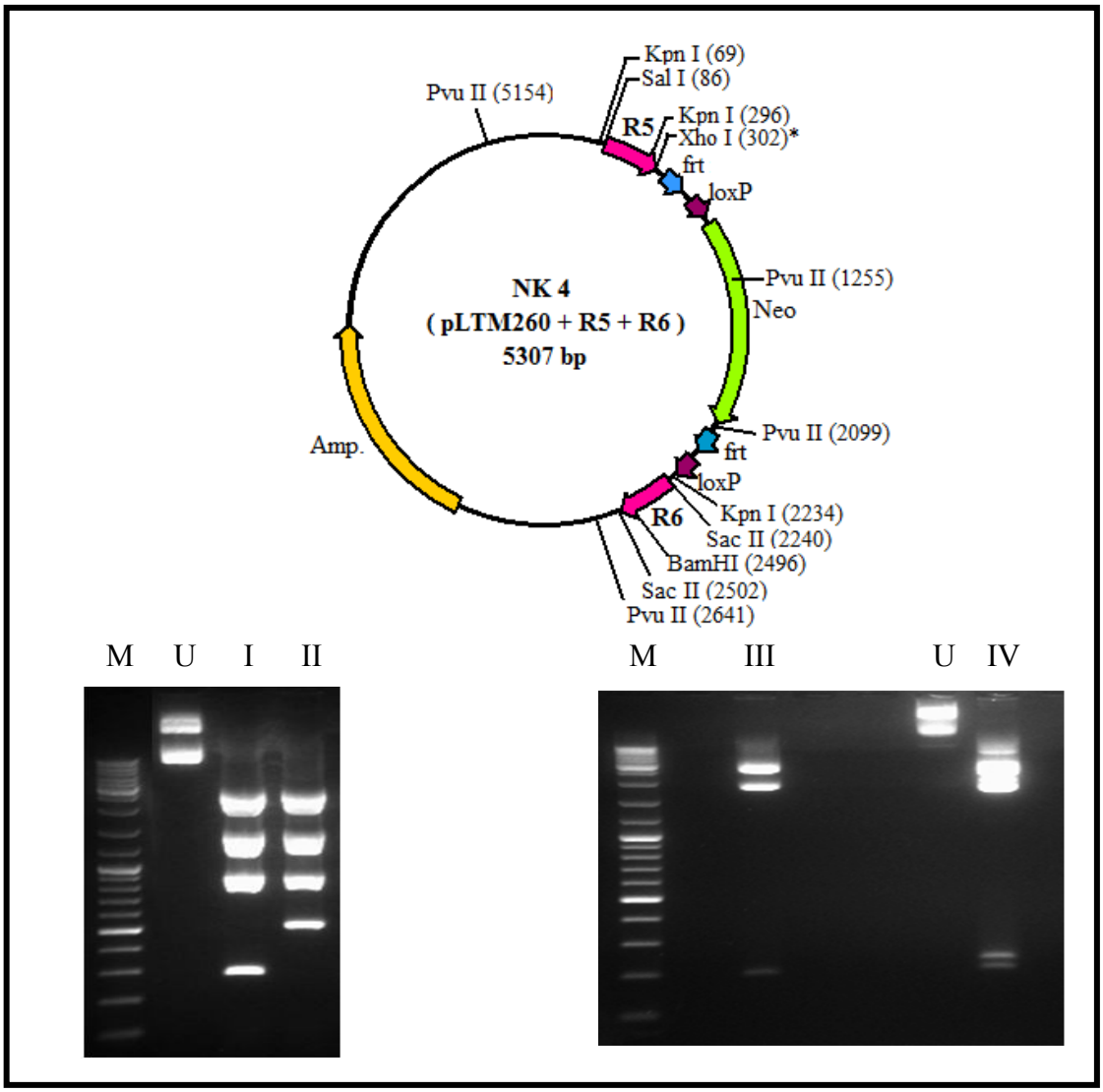

Figure 4.5 Confirmation digests of the NK4 (pLTM260+R5+R6) plasmid. The agarose gel on the left shows the confirmation digest of NK4 with PvuII whereas the agarose gel on the right shows the confirmation digest of NK4 with BamHI – KpnI. Lane M shows the DNA size marker, lane U shows the undigested NK4, lane I shows PvuII digested NK3, lane II shows PvuII digested NK4, lane III shows BamHI – KpnI digested NK3 and lane IV shows BamHI – KpnI digested NK4. The map of NK4, shown on the top, indicates that PvuII digestion of NK4 should generate four bands of 544, 844, 1408 and 2513 bp whereas PvuII digestion of NK3 (the plasmid without the R6 fragment) should generate four bands of 282, 844, 1408 and 2513 bp. BamHI – KpnI double digestion of NK4 should generate four bands of 227, 262, 1938 and 2880 bp whereas BamHI – KpnI double digestion of NK3 (the plasmid without the R6 fragment) should generate three bands of 227, 1938 and 2874 bp. (The XhoI site following the R5 fragment, which was destroyed after being ligated into the SalI site is shown as XhoI* and the BamHI site preceding the R6 fragment, which was destroyed after being ligated into the Bgl II site is shown as BamHI*)

4.1.2.3 Construction of the NK5 (pKO917TK+R1) and NK6 (pKO917TK+R1+R2) Plasmids

The R1 and R2 homology regions were ligated into the pKO917TK vector which contains a tyhmidine kinase (TK) gene for further selection in mouse. The fifth plasmid constructed for recombination experiments was named NK5 (pKO917TK+R5) (shown in figure D.23). Before starting the construction of the plasmid, we performed diagnostic digests of pKO917TK with NcoI, Bgl I, BamHI – SalI. According to the map of pKO917TK (shown in figure D.19), NcoI double digestion should generate three bands of 85, 295 and 3689 bp, Bgl I single digestion should generate three bands of 147, 1783 and 2059 bp and BamHI – SalI double digestion should generate two bands of 54 and 3935 bp. The agarose gel containing the NcoI, Bgl I and BamHI – SalI digested pKO917TK plasmid is shown in figure D.19.

The R1 homology region was previously amplified with PCR from BAC DNA containing the CD3δ gene (RP23-432G9) and ligated into the pTZ57R/T vector (Fermentas, InsTA cloning vector). The R1 homology region which is 620 bp long is flanked by a 5' BamHI and a 3' SalI restriction sites. In order to obtain the R1 fragment, the pTZ57R/T+R1 plasmid was digested with BamHI – SalI which generated three bands of 10, 620 and 2882 bp where the 620 bp band corresponds to the R1 homology region. Therefore, the 620 bp band was gel extracted and purified for further ligation steps. The agarose gel for digestions and relevant controls are shown in figure D.20.

The R1 homology region was flanked with BamHI and SalI restriction site.Therefore, the vector that received this insert, pKO917TK plasmid was digested with BamHI - SalI for the further ligation step. Digestion products were loaded on 1% agarose gels and the digested vector was gel extracted. In figure D.21, the digestion of the pKO91TK plasmid with BamHI - SalI is shown.

The purified R1 fragment and digested pKO917TK plasmid were compared before ligation. The ligation was performed using 1:10, 1:6, 1:3, 1:1 vector:insert ratios. In figure D.22, comparison of DNA fragments containing the purified R1 insert and digested pKO917TK plasmid is shown. After ligation, 25 colonies were used to isolate plasmid DNAs. Due to the fact that there was the risk of multiple inserts being ligated into the plasmid, we performed confirmation digests for identifying the number of inserts using XhoI – NotI which generated two bands of 643 and 3966 bp. Also we wanted to perform BamHI – SalI double digestion which would generate two bands of 620 and 3989 bp. In figure D.23, confirmation digestion results one of the correct colonies is shown.

The R2 homology region was previously amplified with PCR from BAC DNA containing the CD3δ gene (RP23-432G9) and ligated into the pTZ57R/T vector (Fermentas, InsTA cloning vector). The R2 homology region which is 640 bp long is flanked by a 5' SalI and a 3' NotI restriction sites. In order to obtain the R2 fragment, the pTZ57R/T+R2 plasmid was digested with SalI – NotI which generated three bands of 25, 640 and 2869 bp where the 640 bp band corresponds to the R2 homology region. Therefore, the 640 bp band was gel extracted and purified for further ligation steps. The agarose gel for digestions and relevant controls are shown in figure D.24.

The R2 homology region was flanked with SalI and NotI restriction site. Therefore, the NK5 (pko917TK+R1) plasmid was digested with SalI - NotI for the further ligation step. Digestion products were loaded on 1% agarose gels and the digested vector was gel extracted. In figure D.25, the digestion of the NK5 (pKO917TK+R1) plasmid with SalI - NotI is shown.

The purified R2 fragment and digested NK5 (pKO917TK+R1) plasmid were compared before ligation. The ligation was performed using 1:10, 1:6, 1:3, 1:1 vector:insert ratios. In figure D.26, comparison of DNA fragments containing the purified R2 insert and digested NK5 (pKO917TK+R1) plasmid is shown. After ligation, 25 colonies were used to isolate plasmid DNAs. Due to the fact that there was the risk

of multiple inserts being ligated into the plasmid, we performed confirmation digests for identifying the number of inserts using SalI- XmnI which generated three bands of 91, 1048 and 4110 bp. Also we wanted to perform SalI – NotI double digestion which would generate two bands of 640 and 4609 bp. In figure D.27, confirmation digestion results one of the correct colonies is shown.

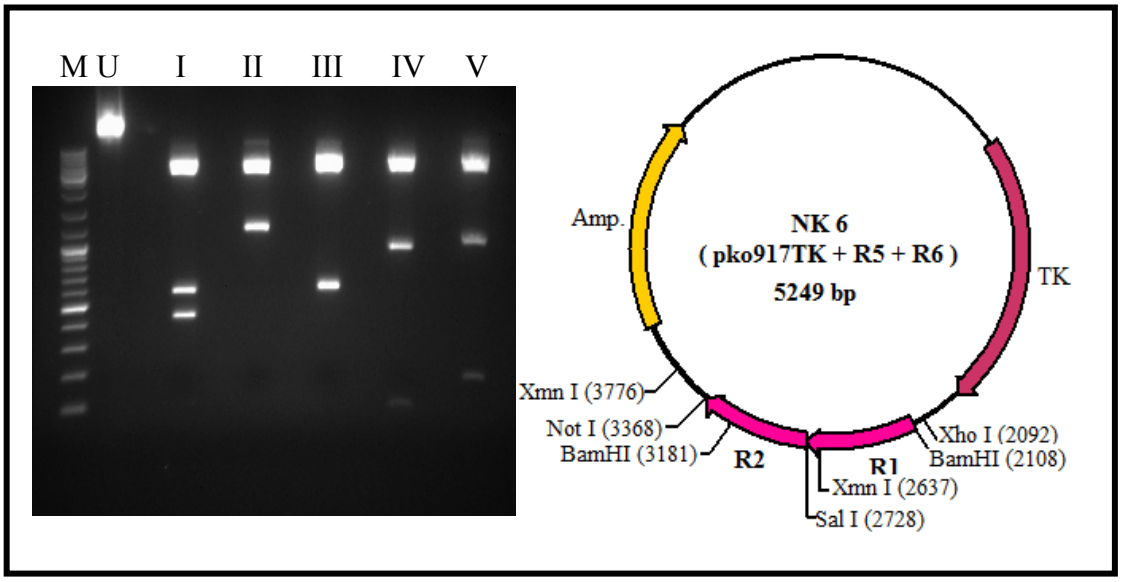

Figure 4.6 Confirmation digest of the NK6 (pKO917TK+R5+R6) plasmid. The agarose gel on the left shows the confirmation digest of NK6 with BamHI – SalI, XhoI – NotI, SalI – NotI, SalI – XmnI and BamHI – NotI. Lane M shows the DNA size marker, lane U shows the undigested NK6, lane I shows BamHI – SalI digested NK6, lane II shows XhoI – NotI digested NK6, lane III shows SalI – Not I digested NK6, lane IV shows SalI – XmnI digested NK6 and lane V shows BamHI – NotI digested NK6. The map of NK6, shown on the right, indicates that BamHI – SalI digestion should generate three bands of 453, 620 and 4176 bp, XhoI – NotI digestion should generate two bands of 1276 and 3973 bp, SalI – Not I digestion should generate two bands of 640 and 4609 bp, SalI – XmnI digestion should generate three bands of 91, 1048 and 4110 bp and BamHI – NotI digestion should generate three bands of 187, 1073 and 3989 bp.

4.2 Subcellular Localization of Rag1Ap1

4.2.1 Construction of Rag1Ap1 – Venus Fusion Plasmid

Rag1Ap1 cDNA was amplified by PCR without a stop codon in order to be fused to Venus sequence. Forward primer was containing a Bgl II restriction site and reverse primer was containing an XhoI restriction site. The 674 bp long PCR product corresponding to Rag1Ap1 sequence was flanked by BglII and XhoI restriction sites. PCR reaction was done as explained in section 3.2.1.2. The agarose gel containing of the PCR product and PCR controls were shown in figure E.1.

PCR product of RagAp1 without the stop codon was ligated into the pVenus-N1 plasmid which contains fluorescent Venus protein. The Rag1Ap1 – Venus fusion plasmid constructed for subcellular localization studies was named RVL (pVenus-N1+Rag1Ap1). Before starting the construction of the plasmid, we performed diagnostic digests of pVenus-N1 with NcoI and SalI – NotI digestions. According to the map of pVenus-N1 (shown in figure E.2), NcoI digestion should generate four bands of 317, 703, 1809 and 1904 bp and SalI – NotI double digestion should generate two bands of 762 and 3971 bp. The agarose gel containing the NcoI and SalI – NotI digested pVenus-N1 is shown in figure E.2.

PCR product of Rag1Ap1 was flanked with The BglII and XhoI restriction sites. Therefore, pVenus-N1 plasmid was digested with BglII – XhoI for the further ligation step. After digestion, the digestion products were loaded on the 1% agarose gel and digested vector was gel extracted. In figure E.3, the double digestion of the pVenus-N1 with Bgl II and XhoI is shown.

The purified Rag1Ap1 PCR product and digested pVenus-N1 plasmid were compared before ligation. The ligation was performed using 1:10, 1:6, 1:3, 1:1 vector:insert ratios. In figure E.4, comparison of DNA fragments containing the purified Rag1Ap1 fragment and digested pVenus-N1 plasmid is shown. After ligation, 25 colonies were used to isolate plasmid DNAs. We performed confirmation digests for identifying the number of inserts using Bgl II – Not I which generated two bands of 1466 and 3941 bp. Also we wanted to perform BglII – XhoI double digestion which yield two bands of 678 and 4729 bp. In figure 4.7, confirmation digestion results one of the correct colonies is shown.

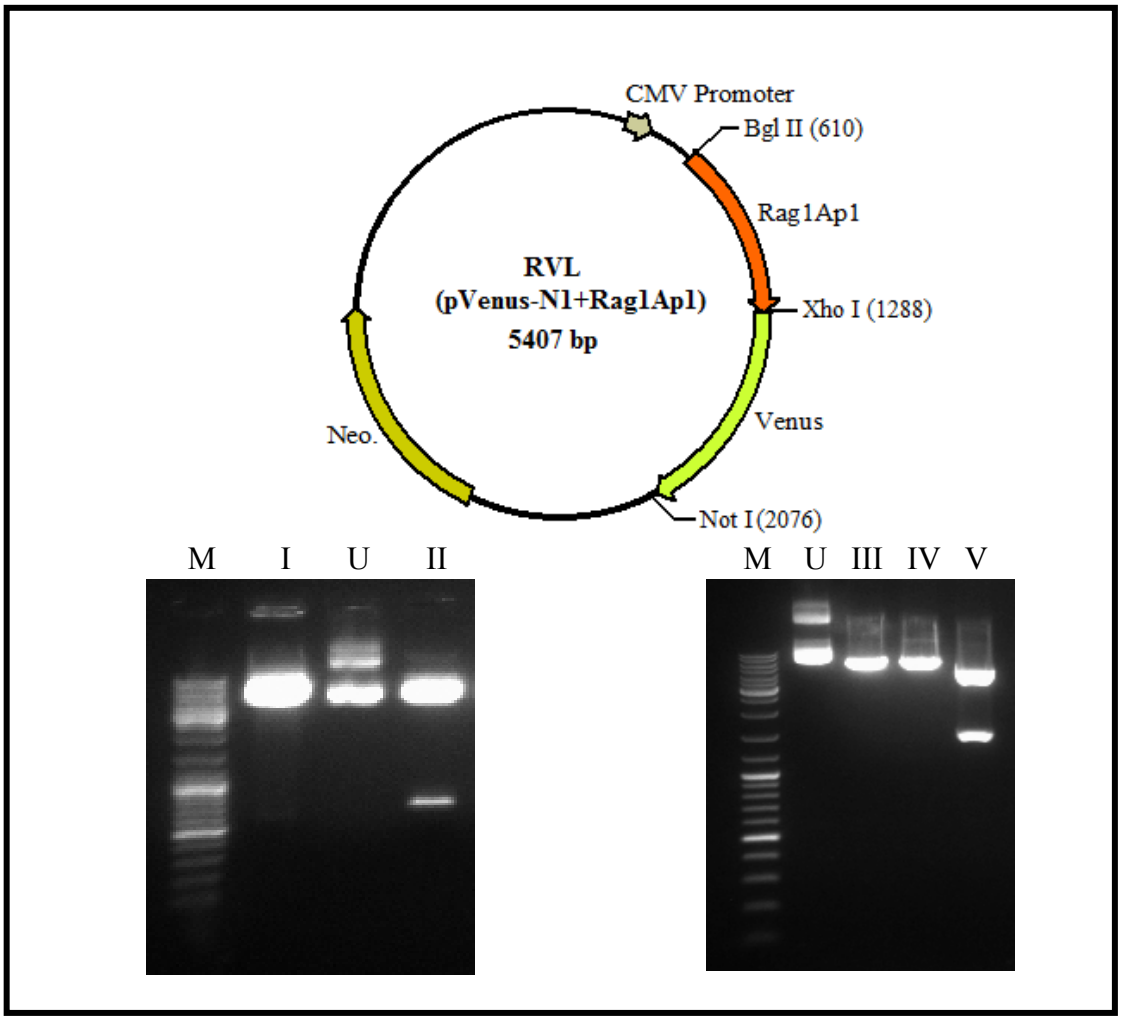

Figure 4.7 Confirmation digests of the RVL (pVenus-N1+Rag1Ap1) plasmid. The agarose gel on the left shows the confirmation digest of RVL with Bgl II – XhoI whereas the agarose gel on the right shows the confirmation digests of RVL with Bgl II, NotI and Bgl II – NotI. Lane M shows the DNA size marker, lane U shows the undigested RVL, lane I shows Bgl II – XhoI digested pVenus-N1, lane II shows Bgl II – XhoI digested RVL, lane III shows Bgl II digested RVL, lane IV shows NotI digested RVL and lane V shows Bgl II – NotI digested RVL. The map of RVL, shown on the top, indicates that Bgl II – XhoI digestion of RVL should generate two bands of 678 and 4729 bp, whereas Bgl II – XhoI digestion of pVenus-N1 should generate two bands of 4 and 4729 bp. Bgl II digestion and NotI digestion of RVL should linearize RVL and Bgl II – NotI double digestion should generate two bands of 1466 and 3941 bp.

The expression of fusion protein was examined using the western blotting technique. Briefly, pVenus-N1 plasmid and RVL (pVenus-N1+Rag1Ap1) fusion plasmid were transfected into HEK293T cells. 48 hours after transfection, transfected cells were lysed and lysates were immunoblotted with anti-GFP antibodies. In figure 4.8 a typical western blot result is shown.

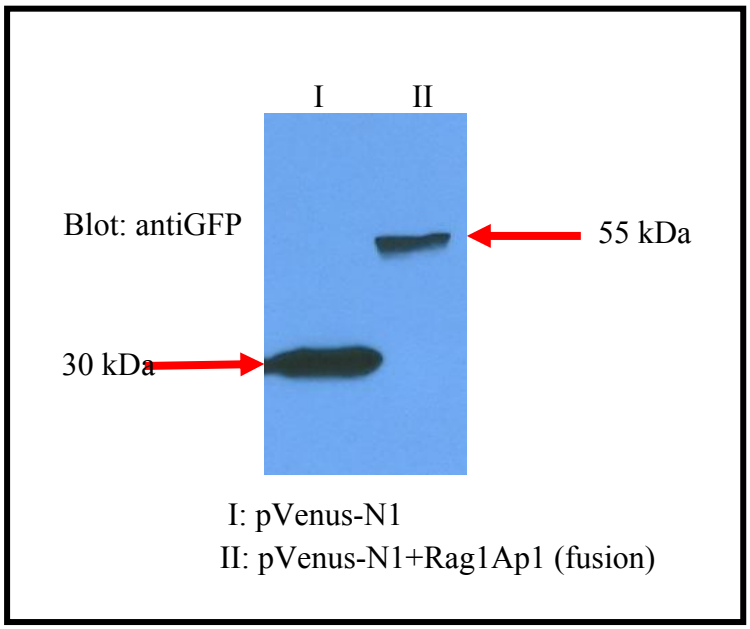

Figure 4.8 Detection of Rag1Ap1-Venus fusion proteins. Plasmids encoding Venus and Venus - Rag1Ap1 fusion proteins were transfected into HEK293T cells and lysates were blotted with anti-GFP antibodies to detect a shift in Venus protein mobility indicating Rag1Ap1 expression.

The anti-GFP antibody recognizes the yellow fluorescent variant Venus protein because of homology between these proteins as well. Lane I in figure 4.8 shows the expression of 30kDa Venus protein. In the second lane, Rag1Ap1-Venus fusion plasmid (pVenus-N1+Rag1Ap1) can be seen as a 55kDa band. The shift in the molecular weight, 25kDa, also corresponds to the calculated weight of the Rag1Ap1 protein.

4.2.2 Subcellular Localization of Rag1Ap1

The RVL (pVenus-N1+Rag1Ap1) plasmid was transfected into Hela cells in order to visualize the subcellular localization of Rag1Ap1 protein. Figure 4.9 shows the fluorescent microscope image of the Rag1Ap1 protein in HeLa cells.

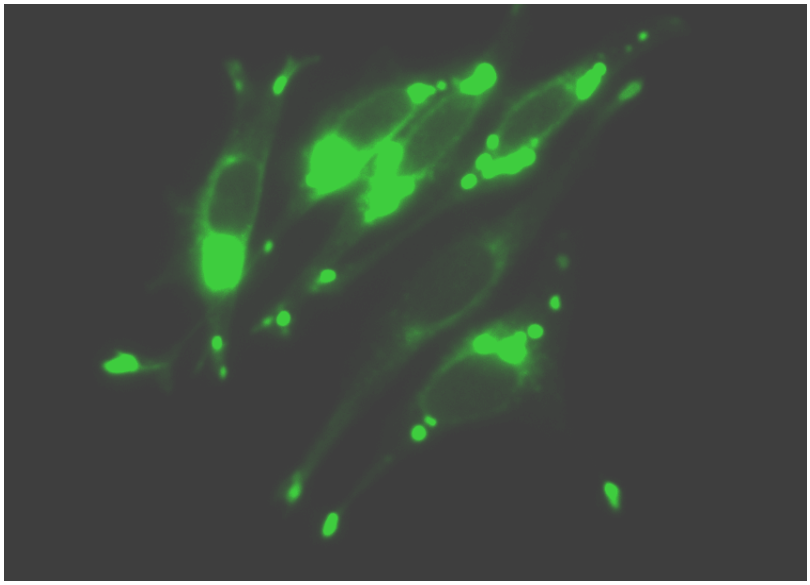

Figure 4.9 Detection of the Rag1Ap1 – Venus protein in HeLa cells with fluorescent microscopy (40X magnification). Transfected HeLa cells mounted on slides were analyzed on an Olympus BX70 upright microscope. Green fluorescence of Venus proteins were detected using a WIBA filter set.

To determine that fluorescence observed in these images is derived specifically from the Venus tagged Rag1AP1 protein, we analyzed untransfected HeLa cells with a confocal microscope. The background fluorescence profile coming from untransfected HeLa cells can be seen in figure 4.10. This background fluorescence was mostly localized in distinct spots in the nucleus. An emission wavelength profile (from 450 to 70 nm) did not match the expected profile for the Venus protein, which allowed us to conclude that this fluorescence was non-specific.

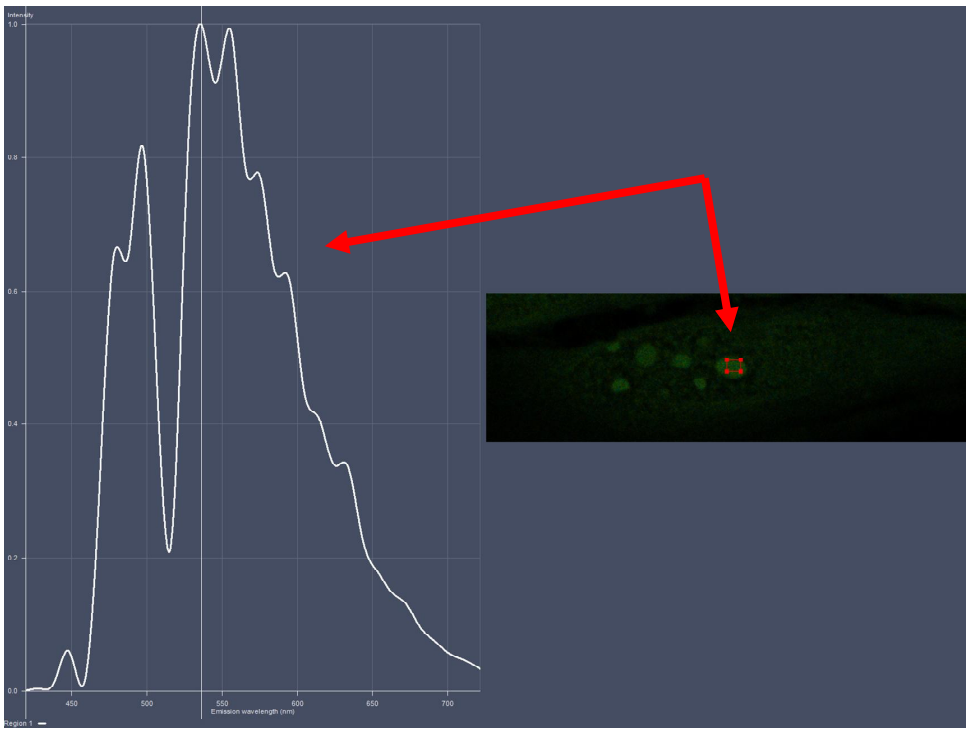

Figure 4.10 Analysis of untransfected HeLa cells by confocal microscopy. HeLa cells, mounted on slides were analyzed on a Zeiss LSM710 microscope. On the left, an emission wavelength profile (from 450 to 70 nm) indicates background fluorescence of Hela cells. On the right, the image of a single cell where the red box indicates the area in which the background emission wavelength profile was calculated.

After analysing the background flourescence, we analyzed Rag1Ap1 – Venus fusion plasmid transfected HeLa cells and detected specific Venus protein fluorescence Again, an emission wavelength profile (from 450 to 70 nm) indicated that nuclear spots were non-specific but cytoplasmic fluorescence matching the emission profile of Venus protein demonstrated that Rag1Ap1 – Venus fusion proteins were localized in cytoplasmic compartments.

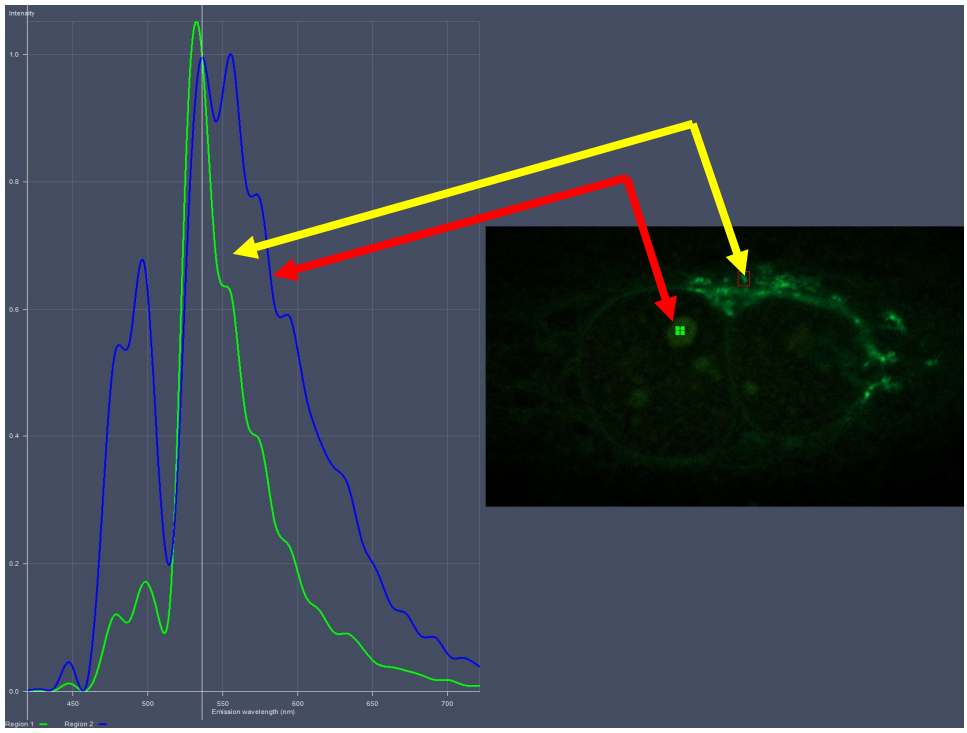

Figure 4.11 Confocal microscope analysis of Rag1Ap1 – Venus transfected HeLa cells. The red arrow shows the background profile and the yellow arrow shows the exact match of the profile of the Venus protein fluorescence.

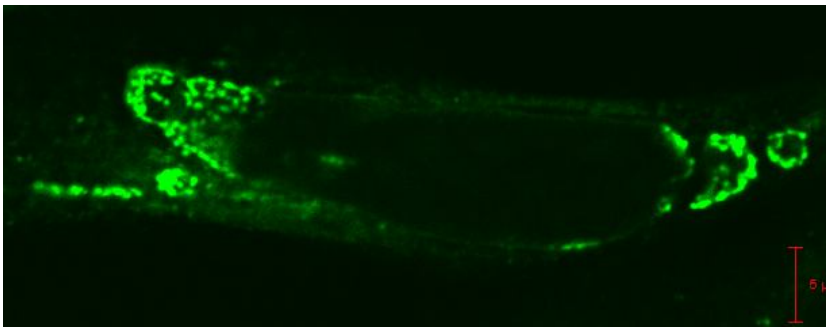

Figure 4.12 Detection of the Rag1Ap1 – Venus protein in HeLa cells with confocal microscopy (63X magnification).

Detailed confocal microscopic analysis indicated that Rag1Ap1 – Venus fusion protein localized to regions immediately outside of the nucleus. This continuous localization starting from the outer boundaries of the nucleus up to the cell membrane indicated that Rag1Ap1 likely localized in the endoplasmic reticulum of these transfected HeLa cells. Detailed analysis of the cytoplasmic region containing specific Rag1Ap1-Venus fluorescence indicated that the part of the cytoplasm containing fluorescent spots spanned an area of 37 um^2. Confocal microscope imaging allowed the measurement of the diameter of the individual fluorescent spots in this cytoplasmic region and these Rag1Ap1 containing spots range from 0.33um to 0.76um. These detailed analyses are shown in figure 4.13

Figure 4.13 shows the zoom to the left part of figure 4.12 to see the protein closer.

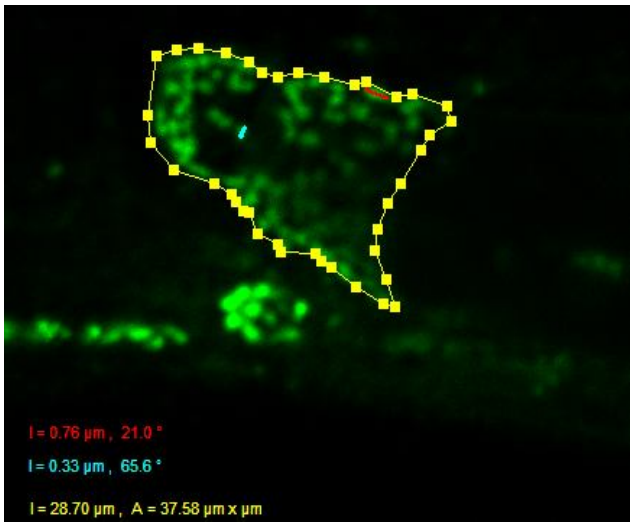

Figure 4.13 Zoom to Rag1Ap1

4.3 Identification of the Rag1Ap1 – CD3 delta Interaction in HEK293T Cells

Rag1Ap1 was known to interact with CD3δ in HEK293T cells, which do not express a TCR. However, if the cell expresses TCR on the cell surface, it was not known whether the interaction becomes stronger or weaker. In order to test this, Rag1Ap1 and CD3δ were overexpressed in HEK293T cells in both the presence and absence of TCR subunits.

For this experiment, pHA-Mex+Rag1Ap1, pcDNA3.1MycCD3δ, pMIGIITCRab and pMIGIITCRdgez plasmids were used. Before starting the experiment, diagnostic digests of the plasmids encoding these proteins were conducted. We performed diagnostic digests of the pHA-Mex+Rag1Ap1 plasmid with BamHI and NcoI single digestions (shown in figure F.1). BamHI single digestion generated three bands of 218, 1088 and 4085 bp and NcoI single digestion generated three bands of 700, 1904 and 2787 bp. In this plasmid HA tag was fused to the N-terminal of Rag1Ap1. The agarsoe gel containing BamHI digested and NcoI digested pHA-Mex+Rag1Ap1 and the map pf pHA-Mex+Rag1Ap1 are shown in figure F.1.

We performed diagnostic digests of the pcDNA3.1Myc-CD3δ plasmid with XmnI and XhoI – HindIII digestions (shown in figure 4.43). XmnI single digestion generated three bands of 946, 1652 and 3381 bp and XhoI – HindIII double digestion generated two bands of 525 and 5479 bp. In this plasmid myc tag was fused to C-terminal of CD3δ. The agarose gel containing XmnI digested and XhoI – HindIII digested pcDNA3.1Myc-CD3δ and the map of pcDNA3.1Myc-CD3δ is shown in figure F.2.

Another plasmid used for this experiment was pMIGIITCRab which is used for TCRα and TCRβ expression. We performed diagnostic digests of the pMIGIITCRab plasmid with BglII – BstXI and BglII – XhoI (shown in figure F.3). BglII – BstXI double digestion generated two bands of 1259 and 6854 bp and BglII – XhoI double digestion generated 1803 and 6310 bp bands. The agarose gel containing BglII – BstXI and BglII – XhoI digested pMIGIITCRab plasmid and the map is shown in figure F.3.

The pMIGIITCRdgez plasmid was also used for the expression of CD3δ, γ, ε and ζ. The diagnostic digests of the pMIGIITCRdgez plasmid was performed with EcoRI – BglII and BglII – SalI double digesitons. According to the map of pMIGIITCRdgez plasmid (shown in fig F.4) , EcoRI – BglII double digestion generated two bands of 1149 and 7495 bp and BglII – SalI double digestion generated two bands of 2524 and 6120 bp were expected. The agarose gel containing EcoRI – BglII and BglII – SalI and digested plasmid map is shown in figure F.4.

To identify the context dependence of the CD3δ-Rag1Ap1 interaction, the CD3δ-Myc, HA-Rag1Ap1, pMIGIITCRab and pMIGIITCRdgez expression plasmids were transfected into HEK293T cells. The pcDNA-GFP plasmid was used as a transfection control. 48 hours after transfection, the cells were lysed and lysates immunoprecipitated with an antiHA immunoprecipitation kit (Sigma). Lysates separated on acyrlamide gels were immunoblotted with anti-c-myc-HRP antibodies in a western blot experiment. In figure 4.14 blots of IP and lysates are shown.

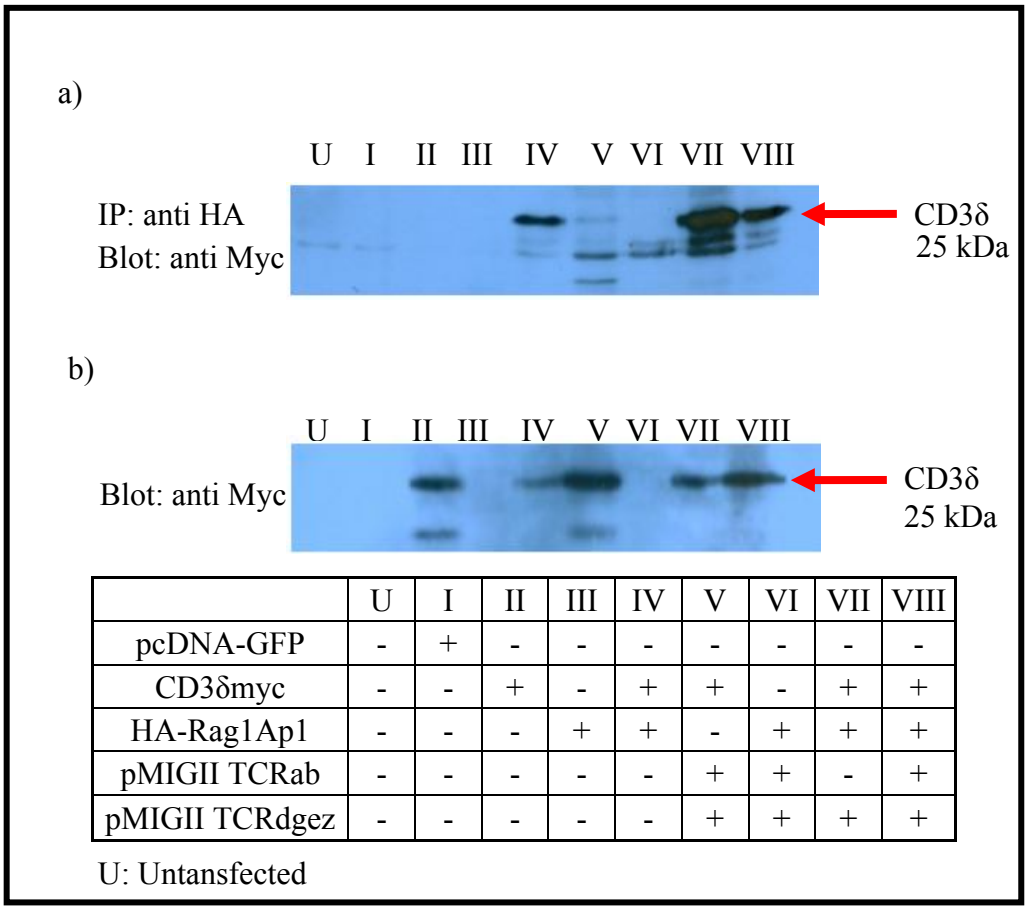

	U	I	II	III	IV	V	VI	VII	VIII
pcDNA-GFP	-	+	-	-	-	-	-	-	-
CD3δmyc	-	-	+	-	+	+	-	+	+
HA-Rag1Ap1	-	-	-	+	+	-	+	+	+
pMIGII TCRab	-	-	-	-	-	+	+	-	+
pMIGII TCRdgez	-	-	-	-	-	+	+	+	+

U: Untansfected

Figure 4.14 IP and western blot results for demonstrating the Rag1Ap1 – CD3δ interaction.

In this experiment HA immunoprecipitation of the lysates brings down all proteins associated with the HA tagged Rag1Ap1. Anti-myc western blotting reveals that CD3d is present in these immunoprecipitations. In figure 4.14a lanes IV, VII and VIII have a 25kDa CD3δ band which results from the interaction of Rag1Ap1 and CD3δ. As a specificity control we tried to detect the presence of CD3d even in cells that do not express Rag1AP1 and in figure 4.14b lanes II, IV, V, VII and VIII have the 25kDA CD3δ band which shows the presence of CD3δ in these lysates.

Comparison of the CD3δ-Rag1Ap1 interaction in cells with or without TCR expression, reveals that there is no significant difference in this interaction. To confirm the expression of the TCR on the HEK293T cell surface upon pMIGIITCRab and

pMIGIITCRdgez transfection, we performed flow cytometric analysis. Staining the cell surface with H57-Biotin (TCR antibody) followed by streptavidin alexa-647, 48 hours after transfection revealed that TCR can be expressed on the surface of these transfected cells. Our flow cytometer analysis is shown in fig 4.15. The detailed analysis of this experiment is shown in figure G.1 in Appendix G. Here the mean fluorescence intensity of Alexa647 fluoresence increases from 61 in control transfected cells to 181 in pMIGIITCRab and pMIGIITCRdgez transfected cells. This analysis was performed on the same cells that were analyzed by western blotting in figure 4.15. Thus, the CD3δ-Rag1Ap1 interaction can take place with the same efficiency in the presence or absence of TCR expression.

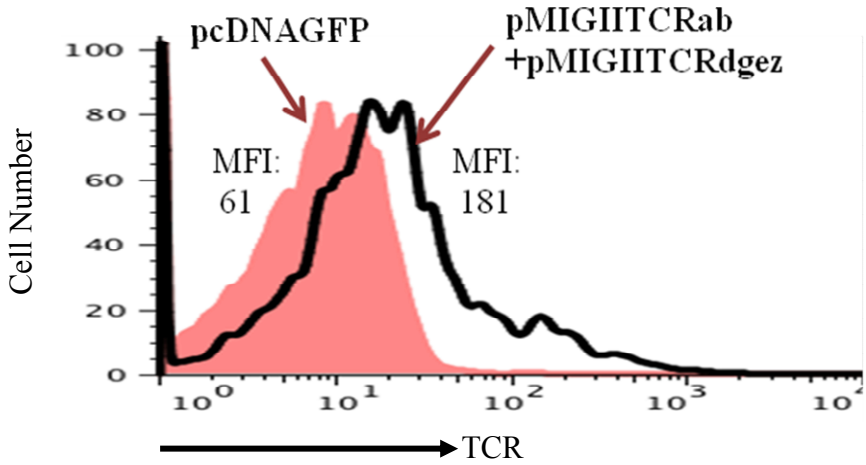

Figure 4.15 Flow cytometric analysis of TCR expression in transfected HEK293T cells. An overlay of Alexa647 fluorescence on cells transfected either with a control pCDNA3GFP plasmid or the pMIGIITCRab and pMIGIITCRdgez plasmids encoding the subunits of the TCR. MFI increases of 3 fold (from 61 to 181) indicate the presence of the TCR on the surface of the transfected cells.

4.4 Identification of the Effect of Rag1Ap1 Overexpression in T Lymphocytes

We examined the interaction of CD3δ and Rag1Ap1 in the presence of TCR on cell surface of HEK293T cells in section 4.3. However, in these experiments, the TCR was expressed on the surface of HEK293T cells artificially by overexpressing TCR subunits. In this section, we wanted to analyze the effect of Rag1Ap1 overexpression on TCR expression in T lymphocytes which express endogenous TCR on their cell surface.

For overexpression, we used the pVenus-N1+Rag1Ap1 plasmid. The construction of this plasmid was explained in 4.2.1. This plasmid was transfected into the VL3-3M2 cell line which is a double positive T lymphocyte line. 48 hours after transfection, the cells were analyzed by flow cytometry. VL3-3M2 cells were stained with H57-PE (TCR antibody) prior to flow cytometer analysis. We identified live cells by forward scatter, side scatter and 7AAD exclusion. We analyzed the expression of TCR on Venus positive cells by electronic gating. The details of this experiment are shown in Appendix H.

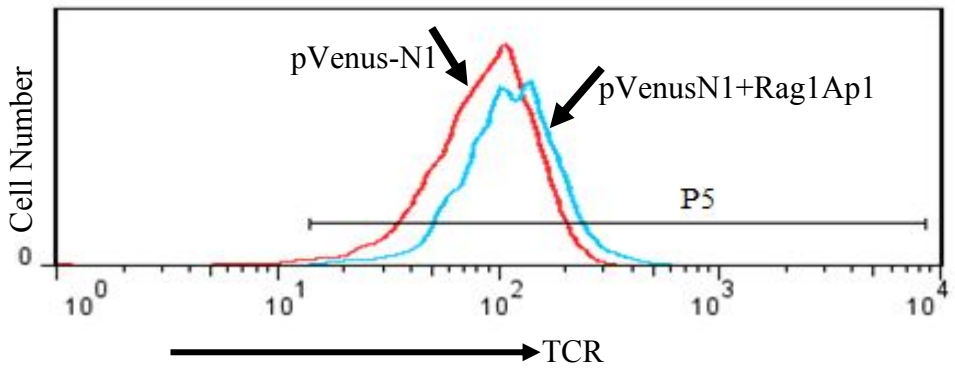

Figure 4.16 Overlay of TCR expression levels in Rag1Ap1 overexpressing VL3-3M2 cells. Venus expressing live cells (by FSC, SSC and 7AAD exclusion) were electronically gated and PE fluorescence in this population was analyzed in different population.

Flow cytometric analysis of TCR expression levels on VL3-3M2 cells either expression of empty pVenus-N1 or pVenusN1+Rag1Ap1 indicate that in the presence of Rag1Ap1 the level of TCR on the cell surface increases. MFI analysis of TCR expression indicates that TCR expression increases from 93 to 136 in the presence of Rag1Ap1.

4.5 Identification of the Effect of Rag1Ap1 Silencing by shRNAmir in T lymphocytes

4.5.1 Construction of shRNAmir Expression Plasmids

To further study the importance of Rag1Ap1 on TCR expression, we decided to silence Rag1Ap1 expression by shRNA mediated silencing. To characterize the shRNA expression plasmid MSCV-LMP, we performed diagnostic digests with Bgl I and Pvu II. The map of MSCV-LMP (shown in figure I.1), indicates that Bgl I single digestion will yield 131, 436, 608, 1118, 2459 and 3142 bp bands, and PvuII single digestion will yield 356, 2364 and 5174 bp bands. The outcome of Bgl I and PvuII diganostic digests are shown in figure I.1.

shRNAmir sequences against Rag1Ap1 were amplified by PCR. We used three different 97mer oligos as templates for PCR to generate 3 shRNAmirs targeting different areas of the cDNA to silence Rag1Ap1. These 97mer oligos were amplified with a forward primer introducing an XhoI restriciton site and a reverse primer introducing an EcoRI restriction site resulting in a 138 bp long PCR product flanked by XhoI and EcoRI restriction sites (shown in figure I.2). The PCR product and the MSCV-LMP plasmid were digested with EcoRI and XhoI and gel extracted for ligation (shown in figure I.3). Ligations were performed with 1:10, 1:6, 1:3, 1:1 vector:insert ratios. In figure I.4, gel photos of the inserts and purified vectors before ligation are shown.

For each ligation, 25 colonies were taken and DNAs were isolated. We performed confirmation digests for the ligation using XhoI – SacII which should generate two bands of 985 and 7019 bp for the correct ligation whereas 875 and 7019 bp for empty MSCV-LMP. Figure 4.17 shows the confirmation digests of the constructed shRNAmir plasmids 1/4, 1/8, 2/2, 2/7, 3/2 and 3/8.

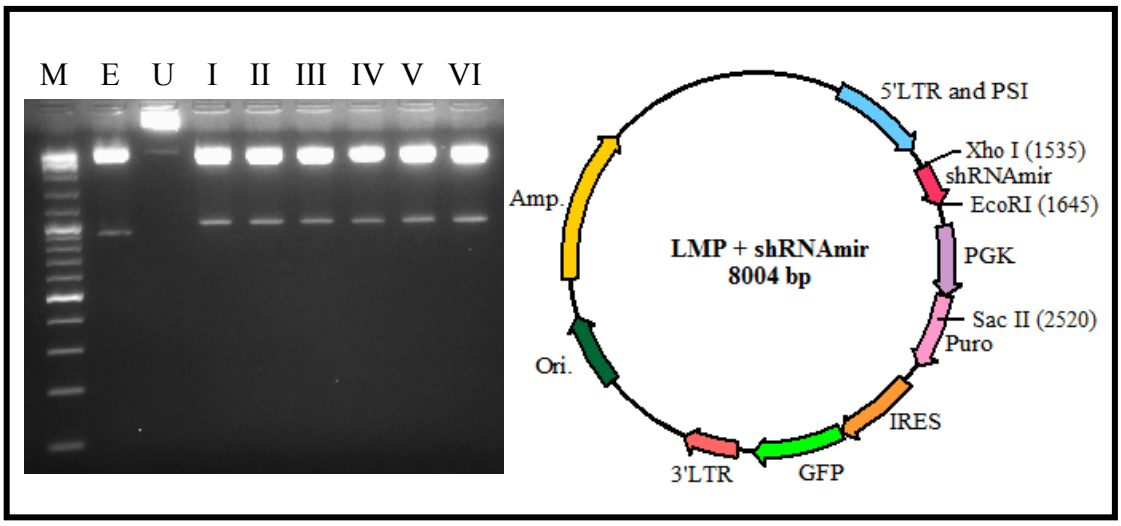

Figure 4.17 Confirmation digests of LMP+shRNAmir plasmids. The agarose gel on the left shows the confirmation digest of LMP+shRNAmir plasmids with XhoI – SacII. Lane M shows the DNA size marker,lane E shows XhoI – SacII double digested LMP, lane U shows the undigested shRNAmirplasmid 1/4, lane I shows XhoI – SacII double digested shRNAmir plasmid 1/4, lane II shows XhoI – SacII double digested shRNAmir plasmid 1/8, lane III shows XhoI – SacII double digested shRNAmir plasmid 2/2, lane IV shows XhoI – SacII double digested shRNAmir plasmid 2/7 and lane V shows XhoI – SacII digested shRNAmir plasmid 3/2 and lane VI shows XhoI – SacII double digested shRNAmir plasmid 3/8. The map of shRNAmir plasmids, shown on the right, indicates that XhoI – SacII doulbe digestions of shRNAmir plasmids should generate two bands of 985 and 7019 bp.

4.5.2 Transfection of shRNAmir Expression Plasmids to VL3-3M2 Cells

shRNAmir plasmids which are explained in 4.5.1, were transfected into VL3-3M2 cells. 48 hours after transfection, transfected cells were analyzed by flow cytometry for the expression of surface TCR. Live VL3-3M2 cells were identified by FSC, SSC and 7AAD exclusion criteria as described before. VL3-3M2 cells express TCR on their cell surface. This is demonstrated by a dramatic increase in fluorescence when cells were stained with H57-PE (TCR antibody) compared to unstained cells (the details of this

experiment are shown in Appendix J). When we compared TCR expression levels on the surface of empty MSCV-LMP expressing cells compared to shRNAmir expressing cells, the level of TCR was lower in some cell lines. Specifically of the three shRNA candidates shRNAmir2/7, 3/2 and 3/8 resulted in the downregulation of TCR, while the other shRNAs did not affect TCR expression. This may be because in some transfections, shRNA levels may be lower than others.

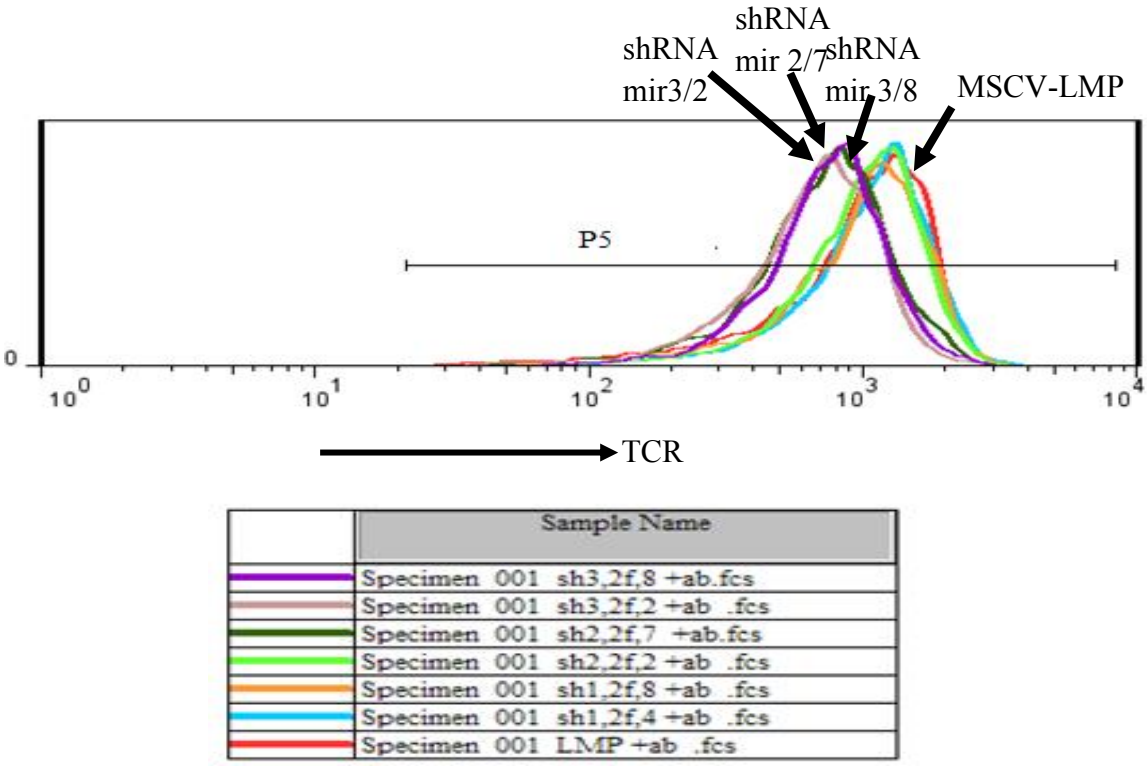

Figure 4.18 Overlay of TCR expression level histogram of shRNAmir transfected cells

In conclusion when all six candidate shRNAmirs were compared, shRNAmir3/2 was the most effective in downregulating surface TCR expression level. This is seen as a 1.5 fold decrease in surface TCR (by MFI decreases from 1066 to 643). Thus overexpressing shRNAs targeting Rag1Ap1 can downregulate surface TCR expression and the potential role of Rag1Ap1 as a chaperone of TCR assembly by binding to at least the CD3d subunit indicates that this interaction is critical for maintaining the levels of surface TCR on T lymphocytes.

5. DISCUSSION

T-cell immune response starts with the engagement of the TCR and the CD4 or CD8 co-receptors by cognate antigen presented on MHC molecules by antigen presenting cells. All T-cell activation events such as proliferation, cytotoxic killing, cytokine secretion and induction of programmed cell death are initiated by signals emanating from the TCR-CD3 complex on the cell surface of T lymphocytes. TCR is composed of TCRα and TCRβ which are responsible for ligand binding and CD3δ, CD3γ, CD3ε and TCRζ which are responsible for signal transduction. Among these subunits, CD3δ is unique because inactivation of CD3δ does not prevent the transition of immature T-cells from the DN stage to the DP stage in the thymus. [41]

The preTCR receptor that is composed of preTCRα, TCRβ and CD3 subunits is responsible for signaling the transition of immature cells from the DN to DP stages. DN cells express neither CD4 nor CD8 co-receptors on the cell surface and these co-receptors are not required for preTCR signaling, unlike TCR signaling. Therefore, CD3δ might be a critical subunit for co-receptor dependent signaling of T-cell receptors.

In the first part of the project, the main aim was to prepare a conditional knockout construct. Bacterial artificial chromosome (BAC) which is widely used in large genome sequence analysis was used to modify the CD3δ exon2 locus. The reason to use a BAC was that it includes the entire gene and all the long-range controlling elements associated to this gene which enables the control of gene expression from this DNA molecule in the cells that contain it with a pattern similar to the expression of the endogenous CD3δ genes . However, conducting molecular biology experiments on such

a large DNA molecule was difficult because of its high molecular weight. Because of these difficulties, we first wanted to rescue the region of interest by homologous recombination in *E.coli* to a plasmid containing a thymidine kinase (TK) gene for further selection. At the time of submission of this thesis, we generated all of the plasmids necessary for the recombinational rescue of the region of interest from this CD3δ containing BAC. Plasmids necessary for recombineering loxP and Frt sites into the CD3δ gene locus were prepared using PCR amplified homology sequences ligated into the appropriate plasmid. As mentioned in the recombination strategy in 4.1.1, R1 and R2 homology regions were cloned into the pKO917TK plasmid which has a TK selection marker. Also, R3 and R4 homology regions were cloned into pLTM332 plasmid that has two loxP sites and a neomycin resistance gene. Similarly, R5 and R6 homology regions were cloned into pLTM260 plasmid that has two loxP, two frt sites and a neomycin resistance gene as mentioned in 4.1.2.

In the second part of the project, we focused on a protein called Rag1Ap1, which is known to have an interaction with CD3δ. The Rag1Ap1 protein is not a thoroughly studied protein so that not much is known about it. Therefore, we first wanted to learn where this protein is localized in the cell. For this purpose, Rag1Ap1 – Venus yellow fluorescent protein fusion proteins were expressed in HeLa cells and transfected cells were visualized under fluorescent and confocal microscopes. To confirm that the fluorescent signal detected under the confocal microscope originated from the Rag1Ap1 – Venus fusion protein we analyzed the fluorescence profile of spots, in an analysis shown in figures 4.37 and 4.40. In these images the Rag1Ap1 – Venus fusion protein was localized outside of the nucleus in spots in the cytoplasm. While co-localization with organelle markers would definitively demonstrate the precise localization of this protein, this finding indicates that the sub-cellular localization of the Rag1Ap1 protein is mostly in the ER. This finding is interesting as the ER is also the organelle in which TCR subunits assemble. Thus, we hypothesized that Rag1Ap1 protein can be an ER chaperone protein that might affect TCR assembly and cell surface expression. To be sure that the fluorescent protein detected in our microscopy experiments was indeed the Rag1Ap1 – Venus fusion, we analyzed the lysates of transfected cells by western blotting. A difference in the mobility of the Venus fluorescent protein and the Rag1Ap1 – Venus fusion protein indirectly demonstrates that the 25kDa Rag1Ap1 protein indeed is expressed in these cells. (shown in figure 4.36).

To identify structural features in the Rag1Ap1 protein that may be important for its potential chaperone function in the ER, we performed structure predictions of Rag1Ap1 using bioinformatic tools. We predicted the location of the transmembrane domains of this protein using the programs uniprot, sosui, tmpred and tmhmm. These different programs predict that the number of transmembrane domains in the Rag1Ap1 protein could be either 5, 6 or 7. This is significant because the number of transmembrane domains influences the intracellular or ER luminal localization of the N- and C-termini of the protein. Except for the tmhmm program, all prediction programs predicted that the N-terminus of the protein was exposed to the ER luminal space (corresponding to extra-cellular space). Contrary to this prediction, when the Rag1Ap1 protein was originally identified in a yeast two hybrid assay, it was fused to a ubiquitin moiety on its N-terminus which must have been exposed to the cytoplasmic space to interact with the CD3δ bait protein in this assay. The subcellular localization analysis of Rag1Ap1 – Venus fusion protein by microscopy indicated that the Venus protein must be exposed to the cytoplasm. Thus, various experimental findings indicate that both the N- and C-termini of the Rag1Ap1 protein are exposed to cytoplasm. When these results are analyzed in the light of the bioinformatic predictions of the model built by the tmhmm software seems to be the most accurate structure prediction for this protein.

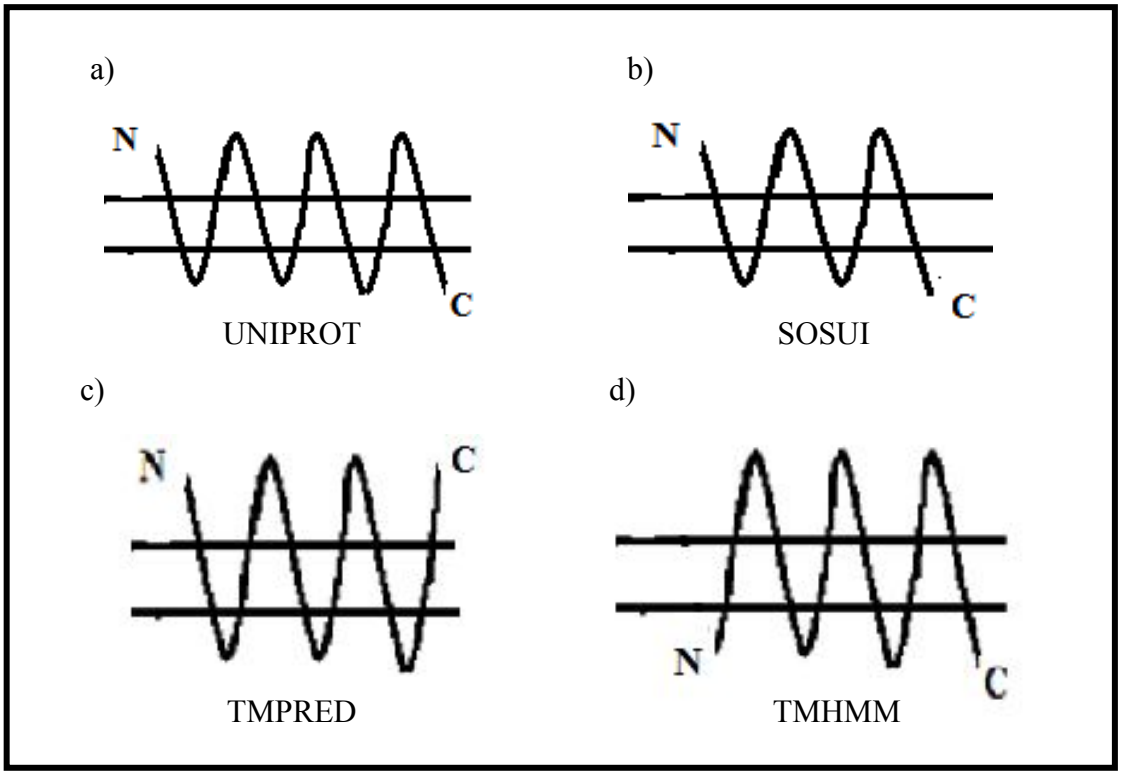

Figure 5.1 Transmembrane domain prediction of Rag1Ap1 with bioinformatic tools. Two horizontal lines indicate the bilipid membrane of the ER. In each schematic, ER lumen (ie, extracellular space) is on top and cytoplasm is below the membrane.

We wanted to confirm the Rag1Ap1-CD3δ interaction and also test the ability of this interaction to persist under different conditions. As CD3δ is normally a part of the TCR complex, it's interaction with the putative Rag1Ap1 chaperone may not persist under conditions where a full TCR is assembled. Alternatively Rag1Ap1 may continue to bind to CD3δ when this subunit is assembled into a full TCR. To differentiate these possibilities, we transfected CD3δ-Myc and HA-Rag1Ap1 plasmids into HEK293T cells in the presence and absence of expression plasmids encoding other TCR subunits. Immunoprecipitaion with anti-HA antibodies and immunoblotting with anti-Myc antibodies confirmed that the interaction between Rag1Ap1 and CD3δ was not altered when myc-tagged CD3δ was expressed in the same cell as a full TCR. Although the assembly of this myc-tagged CD3δ into a full TCR was not biochemically confirmed, we examined the surface expression of TCRbeta by staining with H57 TCR antibodies and analyzed by flow cytometry. As described in figure 1.5, surface expression of TCRbeta can only occur when all TCR subunits assemble into this multisubunit complex. In our experiments, 20.7% to 28.3% of HEK293T cells transfected with TCR

expression plasmids expressed TCR on the cell surface. Further microscopy experiments will reveal the subcellular localization of the Rag1Ap1-CD3δ interaction in the presence of surface TCR.

In order to confirm our hypothesis that Rag1Ap1 may have a role in TCR assembly and cell surface expression, we overexpressed Rag1Ap1 in T lymphocytes. For this purpose, we used VL3-3M2 cells which naturally express TCR on the cell surface. Compared to VL3-3M2 cells transfected with the empty pVenus-N1 plasmid, pVenusN1+Rag1Ap1 transfected cells showed a slight increase in TCR expression.

We also wanted to examine the effects on TCR surface expression in cells that have low levels of Rag1Ap1 protein. To silence Rag1Ap1 expression, we amplified bioinformatically identified shRNAmir sequences against Rag1Ap1 by PCR and cloned these shRNAs into a retroviral expression plasmid named MSCV-LMP. The MSCV-LMP plasmid can be used to produce retroviruses which express shRNAmirs in infected cells. Unfortunately, previous experiments demonstrated that VL3-3M2 cells could not be infected. For this reason we used the shRNA mir expressing pLMP plasmids to transfect VL3 cells. We generated 3 different MSCV-LMP-shRNAmir plasmids that target different regions of the Rag1Ap1 cDNA. Of these different shRNAs, shRNAmir 2/7, shRNAmir 3/2 and shRNAmir 3/8 significantly decreased the TCR expression levels on transfected cells, compared to the TCR levels of empty pLMP transfected cells. The most effective shRNA was shRNAmir3/2 which decreased the TCR expression level approximately 1.5 fold.

These experiments, demonstrate that while endogenous Rag1Ap1 levels are not limiting, this potential chaperone is necessary for surface TCR expression. As Rag1Ap1 binds to the CD3δ subunit, and is localized in our experiments in the ER compartment, it likely plays a role in TCR assembly. When levels of this chaperone protein decrease, the assembly of CD3de dimmers or TCRa-CD3de trimers may be perturbed. It is also likely that if Rag1Ap1 functions as a chaperone, it binds to the other TCR and CD3 subunits. A possible scenario describing the effect of Rag1Ap1 silencing on TCR surface expression is shown in Figure 5.2.

a)

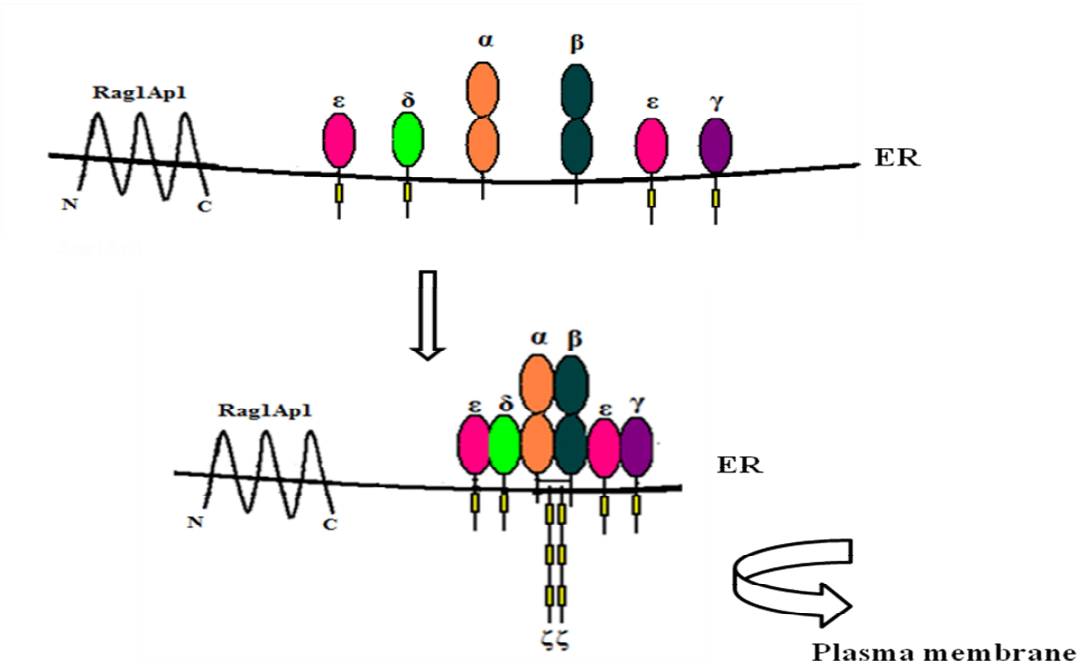

b)

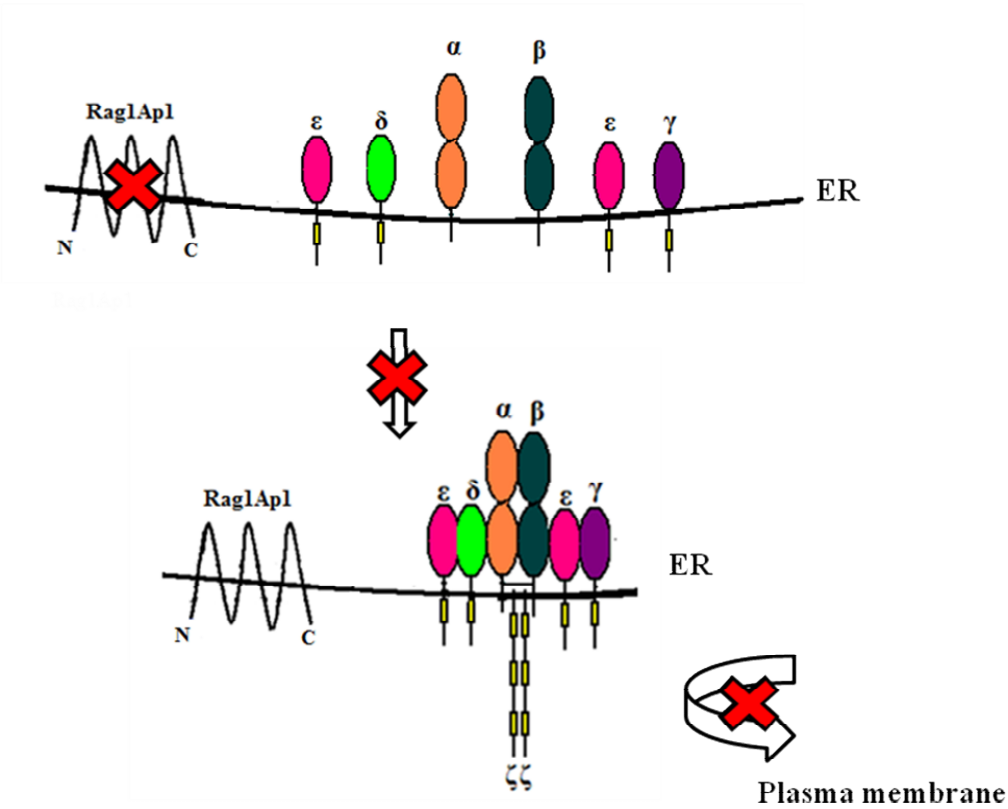

Figure 5.2 Schematic representation of the effect of a) overexpression and b) shRNA mediated silencing of Rag1ap1 on TCR expression.

6. CONCLUSION

The T-cell receptor (TCR) complex is a multi-subunit complex that consists of TCRα and TCRβ subunits which are responsible for ligand binding and CD3δ, CD3γ, CD3ε and TCRζ subunits, which are responsible for signal transduction. CD3δ is different from other subunits of the TCR complex because only its inactivation does not affect the transition of the immature T cells from the DN to the DP stage. To identify the specific functions of the CD3d subunit, in this project we aimed to prepare a CD3δ conditional knockout construct and we also characterized the interaction of CD3δ with the novel Rag1Ap1 protein.

For the first part of the project, we prepared the plasmids required for recombination: NK1 (pLTM332+R3+R4), NK3 (pLTM260+R5+R6) and NK6 (pko917TK+R1+R2). The identity of these plasmids was confirmed by restriction digestion and DNA sequencing. Experiments to generate the final CD3d gene targeting construct by recombination in *E.coli* bacteria were ongoing at the time of the submission of this thesis.

The second part of the project involved the investigation of a protein called Rag1Ap1 which was previously identified in Dr. Erman's laboratory as a CD3δ interacting protein. Rag1Ap1 was fused to the Venus fluorescent protein and this fusion protein was analyzed by fluorescent and confocal microscopy for sub-cellular localization. Interaction of CD3δ and Rag1Ap1 was confirmed by immunoprecipitation and immunoblotting. The role of Rag1Ap1 in TCR assembly was examined by overexpressing and silencing this protein. These experiments demonstrate that Rag1Ap1 is not limiting yet its expression is necessary for surface TCR expression.

REFERENCES

1. Kuby, J., Kindt, T. J., Goldsby, R. A. & Osborne, B. A. Immunology (W.H. Freeman, New York, 2007)
2. Janeway, C., Travers, P., Walport, M. & Shomchick, M. Immunobiology: the immune system in health anddisease (Current Biology ; Garland Pub., London ; San Francisco New York, 2005).
3. Abbas, A. K. & Lichtman, A. H. Cellular and molecular immunology (Saunders,Philadelphia, PA, 2005)
4. O'Neill, A. J. Immunity's early warning system. Scientific American 292, 25 (2005).
5. Basset, C., et al. Innate immunity and pathogen - host interaction. Vaccine 21, 2-12 (2003).
6. Fearon, D., T. & Locksley, R. M. The instructive role of innate immunity in the acquired immune response. Science 272, 50-53 (1996).
7. Davis, D. M., & Dustin, M. L. What is the importance of immunological synapse? Trends in Immunology 25, 323-27 (2004).
8. Baker, B. M., Gagnon, S. J., Biddison, W. E. & Wiley, D. C. Conversion of a T cell antagonist into an agonist by repairing a defect in the TCR/peptide/MHC interface:implications for TCR signaling. Immunity 13, 475-484 (2000).
9. Grakoui, A., Bromley, S. K., Sumen, C., Davis, M. M., Shaw, A. S., Allen, P. M. & Dustin, M. L. A molecular machine controlling T cell activation. Science 285, 221-27 (1999).
10. Herman, A., Kappler, J. W., Marrack, P. & Pullen, A. M., superantigens: mechanism of T-cell stimulation and role in immune response. Annual rewiev of immunology 9,745 (1991).
11. Myung, P. S., Boerthe, N. J. & Koretzky, G. A., Adapter proteins in lymphocyte antigen- receptor signaling. Current opinion in Immunology 12, 256 (2000).

12. Trambas, C. M., & Griffiths, G. M., Delivering the kiss of death. Nat. Immunol. 4, 399-403 (2003).
13. Kuhns, M. S., Davis, M. M. & Garcia, K. C. Deconstructing the form and function of the TCR/CD3 complex. Immunity 24, 133-9 (2006).
14. Fernandez-Miguel, G. et al. Multivalent structure of an alphabetaT cell receptor. Proc. Natl. Acad. Sci. USA 96, 1547-52 (1999).
15. de la Hera, A., Muller, U., Olsson, C., Isaaz, S., & Tunnacliffe, A. Structure of the T cell antigen receptor (TCR): two CD3 epsilon subunits in a functional TCR/CD3 complex. J Exp Med 173, 7-17 (1991).
16. Wegener, A. M., Letourneur, F., Hoeveler, A., Brocker, T., Luton, F., & Malissen, B. The T cell receptor/CD3 complex is composed of at least two autonomous transduction modules. Cell 68, 83-95 (1992).
17. Punt, J.A., Roberts, J.L., Kearse, K.P.,& Singer, A. Stoichiometry of the T cell antigen receptor (TCR) complex: each TCR/CD3 complex contains one TCR alpha, one TCR beta, and two CD3 epsilon chains. J Exp Med 180, 587-93 (1994).
18. Osman,N., Turner,H., Lucas,S., Reif, K., & Cantrell, D., A. The protein interactions of the immunoglobulin receptor family tyrosine-based activation motifs present in the T cell receptor z subunits and theCD3 γ, δ and ε chains. Eur. J. Immunol. 26, 1063–1068(1996).
19. Huang, Y. & Wange R. L. T cell receptor signaling: beyond complex complexes. Journal of Biochemical Chemistry 279, 2827-30 (2004).
20. Palacios, E. H. & Weiss, A. Function of the Src-family kinases, Lck and Fyn, in Tcell development and activation. Oncogene 23, 7990-8000 (2004).
21. Cantrell, D. T cell antigen receptor signal transduction pathways. Annu Rev Immunol 14, 259-74 (1996).
22. Call, M.E., Pyrdol, J. & Wucherpfennig, K.W. Stoichiometry of the T-cell receptor-CD3 complex and key intermediates assembled in the endoplasmic reticulum. Embo J 23, 2348-57 (2004).
23. Kearse, K., P., Roberts, J., L. & Singer, A. TCR alpha-CD3 delta epsilon association is the initial step in alpha beta dimer formation in murine T cells and is limiting in immature CD4+ CD8+ thymocytes. Immunity 2, 391-9 (1995).
24. Call, M.E., Pyrdol, J., Wiedmann, M. & Wucherpfennig, K., W. The organizing principle in the formation of the T cell receptor-CD3 complex. Cell 111, 967-79 (2002).

25. Rothenberg, E., V., Yui, M. A., & Telfer, J., C. T cell developmental biology. In fundamental immunology, 5th ed., W. Paul, ed. Lippincott Williams and Wilkins, Philadelphia (2002)
26. Bhandoola, A., von Boehmer, H., Petrie, H. T., & Zuniga-Pflucker, J. C. Commitment and developmental potential of extrathymic and intrathymic T cell precursors: plenty to choose from. Immunity 26, 678-89 (2007).
27. Petrie, H. T. Early commitment: T cell progenitors in the blood. Immunity 26, 7-8(2007)
28. Groettrup, M., & von Boehmer, H. A role for a pre-T-cell receptor in T-cell development. Immunol Today 14, 610-4 (1993).
29. Pan, Q., Brodeur, J. F., Drbal, K., & Dave, V. P. Different role for mouse and human CD3delta/epsilon heterodimer in preT cell receptor (preTCR) function: human CD3delta/epsilon heterodimer restores the defective preTCR function in CD3gamma- and CD3gammadelta-deficient mice. Mol Immunol 43, 1741-50 (2006).
30. Love, P. E., Lee, J., & Shores, E. W. Critical relationship between TCRsignaling potential and TCR affinity during thymocyte selection. J Immunol 165, 3080-7 (2000).
31. Palmer, E .2003 negative selection – clearing out the bad apples from the T cell repertoire. Nature Review of Immunology 2:383-91
32. Singer, A. & Bosselut, R. CD4/CD8 coreceptors in thymocyte development, selection, and lineage commitment: analysis of the CD4/CD8 lineage decision. *Adv Immunol* **83**, 91-131 (2004)
33. Ellmeier, W., Sawada, S., & Littman, D.R. The regulation of CD4 and CD8 coreceptor gene expression during T cell development. Annu Rev Immunol 17, 523-54 (1999)
34. Bommhardt, U., Beyer, M., Hunig, T., & Reichardt, H. M. Molecular and cellular mechanisms of T cell development. Cell Mol Life Sci 61, 263-80 (2004).
35. Rothenberg, E., V. 2000 Stepwise specification of lymphocye developmental lineages. Current Opin. Gen. Dev. 10 370

36. Amsen, D., & Kruisbeek, A. M. Thymocyte selection: not by TCR alone.Immunol Rev 165, 209-29 (1998).
37. Chen, W. The late stage of T cell development within mouse thymus. Cell Mol Immunol 1, 3-11 (2004).
38. Gobel, T. W., & Dangy, J. P. Evidence for a stepwise evolution of the CD3 family. J Immunol 164, 879-83 (2000).
39. Dave, V.P. Hierarchical role of CD3 chains in thymocyte development. Immunol Rev 232: 22–33 (2009).
40. Wang, B. et al. T lymphocyte development in the absence of CD3 epsilon or CD3 gamma delta epsilon zeta. J Immunol 162, 88-94 (1999).
41. Dave, V. P., Cao, Z., Browne, C., Alarcon, B., Fernandez-Miguel, G., Lafaille, J., de la Hera, A., Tonegawa, S. & Kappes, D. J. CD3 delta deficiency arrests development of the alpha beta but not the gamma delta T cell lineage. Embo J. 16, 1360-70 (1997).
42. Dave, V.P. et al. Altered functional responsiveness of thymocyte subsets from CD3delta-deficient mice to TCR-CD3 engagement. Int Immunol 10, 1481-90 (1998).
43. Liu,P., Jenkins,N.A. & Copeland,N.G. A highly efficient recombineering- based method for generating conditional knockout mutations. Genome Res., 13, 476–484 (2003).
44. Cotta-de-Almeida,V., Schonhoff,S., Shibata,T., Leiter,A. & Snapper,S.B. A new method for rapidly generating gene-targeting vectors by engineering BACs through homologous recombination in bacteria. Genome Res., 13, 2190–2194 (2003).
45. Copeland,N.G., Jenkins,N.A. & Court,D.L. Recombineering:a powerful new tool for mouse functional genomics. Nature Rev.Genet., 2, 769–779 (2001).
46. Szymczak, A.L., Workman, C.J., Wang, Y., Vignali, K.M., Dilioglou, S., Vanin, E.F. & Vignali, D.A.A. Correction of multi-gene deficiency *in vivo* using a single 'self-cleaving' 2A peptide – based retroviral vector. Nature Biotech., 22, 589-594 (2004).
47. Szymczak, A.L. & Vignali, D.A.A. Development of 2A peptide-based strategies in the design of multicistronic vectors. Exper. Opin. Biol. Ther., 5, 627-638 (2005).

APPENDIX

APPENDIX A: Chemicals Used In The Study

Chemicals and Media Components	Supplier Company
Acetic Acid	Merck, Germany
Acid Washed Glass Beads	Sigma, Germany
Acrylamide/Bis-acrylamide	Sigma, Germany
Agarose	peQLab, Germany
Anti c-Myc Antibody	Roche, Germany
Anti-GFP Antibody	Roche, Germany
Anti-HA Affinity Matrix	Roche, Germany
Anti-Myc Peroxidase	Roche, Germany
Ammonium Persulfate	Sigma, Germany
Ammonium Sulfate	Sigma, Germany
Ampicillin Sodium Salt	CellGro, USA
Bacto Agar	BD, USA
Bacto Tryptone	BD, USA
Boric Acid	Molekula, UK
Bradford Reagent	Sigma, Germany
Bromophenol Blue	Sigma, Germany
Chloramphenicol	Gibco, USA
D-Glucose	Sigma, Germany
Distilled water	Milipore, France
DMEM	PAN, Germany
DMSO	Sigma, Germany
DNA Gel Loading Solution, 5X	Quality Biological, Inc, USA
DPBS	CellGro, USA

EDTA	Applichem, Germany

Chemicals and Media Components	Supplier Company
Ethanol	Riedel-de Haen, Germany
Ethidium Bromide	Sigma, Germany
Fetal Bovine Serum (FBS)	Biological Industries, Israel
Glycerol Anhydrous	Applichem, Germany
Glycine	Applichem, Germany
HBSS	CellGro, USA
HEPES	Applichem, Germany
Hydrochloric Acid	Merck, Germany
Isopropanol	Riedel-de Haén, Germany
Kanamycin Sulfate	Gibco, USA
LB Agar	BD, USA
LB Broth	BD, USA
L-Glutamine	Hyclone, USA
Liquid nitrogen	Karbogaz, Turkey
Magnesium Chloride	Promega, USA
2-Mercaptoethanol	Sigma, Germany
Methanol	Riedel-de Haen, Germany
Monoclonal Anti-HA Antibody	Sigma, Germany
Penicillin-Streptomycin	Sigma, Germany
Phenol-Chloroform-Isoamylalcohol	Amersco, USA
PIPES	Sigma, Germany
Potassium Acetate	Merck, Germany
Potassium Chloride	Fluka, Germany
Potassium Hydroxide	Merck, Germany
Protease Tablets (EDTA-free)	Roche, Germany
ProtG Sepharose	Amersco, USA
RNase A	Roche, Germany
RPMI 1640	PAN, Germany
SDS Protein Gel Loading Pack	Fermentas, Germany
SDS Pure	Applichem, Germany

Chemicals and Media Components	Supplier Company

Skim Milk Powder	Fluka, Germany
Sodium Azide	Amresco, USA
Sodium Chloride	Applichem, Germany
TEMED	Applichem, Germany
Tris Buffer Grade	Amresco, USA
Tris Hydrochloride	Amresco, USA
Triton X100	Promega, USA
Tween20	Sigma, Germany
SuperSignal West Pico Chemiluminescent Substrate	Thermo Scientific, USA

APPENDIX B: Equipment Used In The Study

Equipment	Company
Autoclave	Hirayama,Hiclave HV-110,Japan
Balance	Sartorius, BP221S, Germany
	Schimadzu, Libror EB-3200 HU, Japan
Cell Counter	Cole Parmer, USA
Centrifuge	Eppendorf, 5415D, Germany
	Hitachi, Sorvall RC5C Plus, USA
CO_2 Incubator	Binder,Germany
Deepfreeze	-80^{o}C, Forma,Thermo ElectronCorp.,USA
	-20^{o}C,Bosch,Turkey
Distilled Water	Millipore, Elix-S, France
Electrophoresis Apparatus	Biogen Inc., USA
	Biorad Inc., USA
Elecroporation Cuvettes	Eppendorf, Germany
Electroporator	BTX-ECM630, Division of Genetronics, Inc, USA
Filter Membranes	Millipore,USA
Flow Cytometer	BDFACSCanto,USA
Gel Documentation	Biorad, UV-Transilluminator 2000, USA
Heater	ThermomixerComfort,Eppendorf,Germany
Hematocytometer	Hausser Scientific,Blue Bell Pa.,USA
Ice Machine	Scotsman Inc., AF20, USA
Incubator	Memmert, Modell 300, Germany
	Memmert, Modell 600, Germany
Laminar Flow	Kendro Lab. Prod., Heraeus, HeraSafe HS12, Germany
Liquid Nitrogen Tank	Taylor-Wharton,3000RS,USA
Magnetic Stirrer	VELP Scientifica, ARE Heating Magnetic Stirrer, Italy
Microliter Pipettes	Gilson, Pipetman, France
	Eppendorf, Germany

Microscope	Olympus CK40,Japan
	Olympus CH20,Japan
	Olympus IX70,Japan
	Zeiss Confocal LSM710, German
Microwave Oven	Bosch,Turkey
pH meter	WTW, pH540 GLP MultiCal, Germany
Power Supply	Biorad, PowerPac 300, USA
Refrigerator	Bosch,Turkey
Shaker Incubator	New Brunswick Sci., Innova 4330, USA
Spectrophotometer	Schimadzu, UV-1208, Japan
	Schimadzu, UV-3150, Japan
Thermocycler	Eppendorf, Mastercycler Gradient, Germany
Vortex	Velp Scientifica,Italy

APPENDIX C: DNA and Protein Molecular Weight Marker

Gene Ruler ^{TM} DNA Ladder Mix
Fermentas, Germany

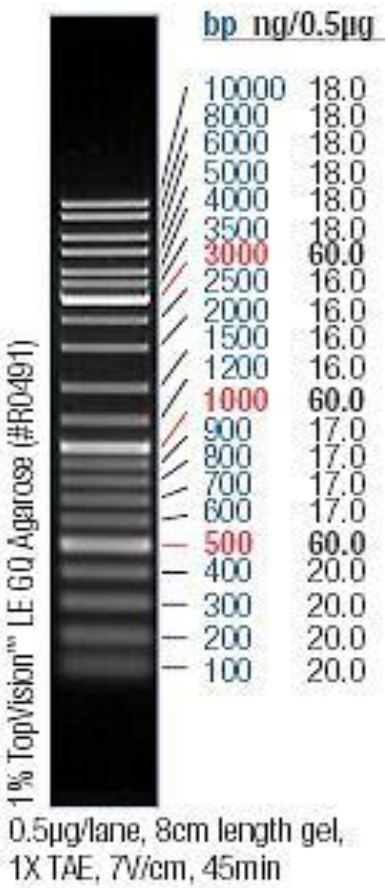

Page Ruler^{TM} Prestained Protein
Ladder Fermentas, Germany

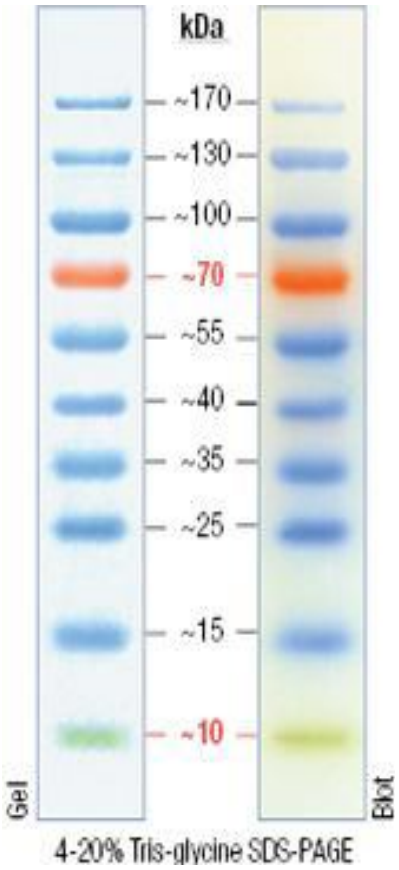

APPENDIX D: Construction of Plasmids for Recombination

According to the recombination strategy detailed in Section 4.1.1, the first plasmid we prepared was NK1 (pLTM332+R3). After diagnostic digestion of the pLTM332 parent plasmid, the R3 homology region which was purified from the pTZ57R/T+R3 plasmid (shown in figure D.2) and linearized pLTM332 (shown in figure D.3) were ligated. The correct construction of the NK1 (pLTM332+R3) plasmid was confirmed with restriction digestions (shown in figure D.5).

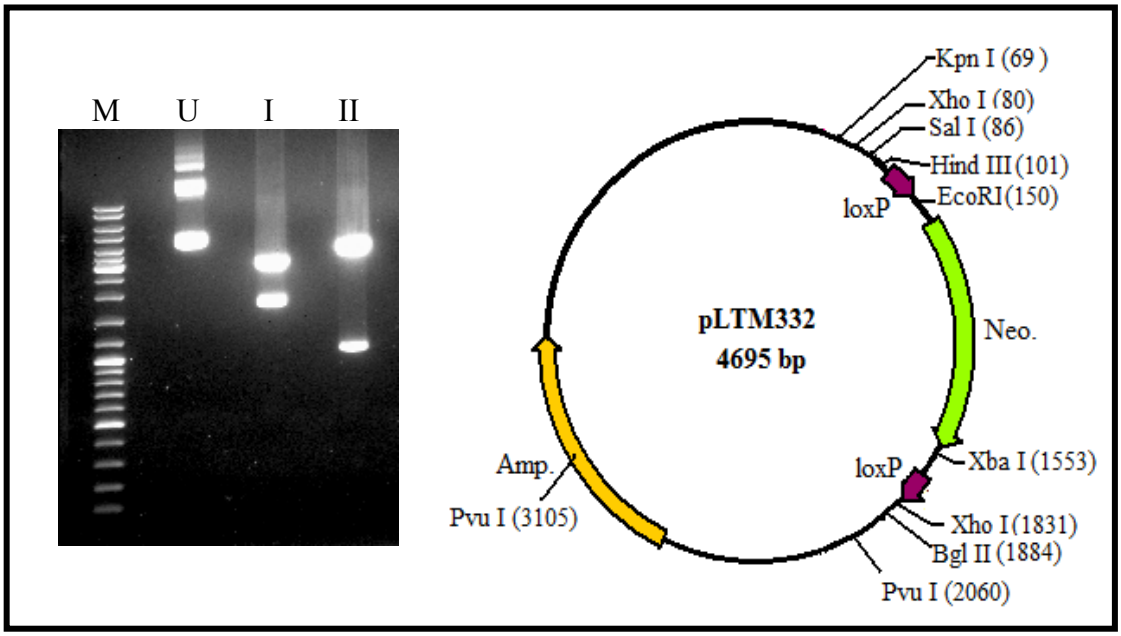

Figure D.1 Diagnostic digests of the pLTM332 plasmid. The agarose gel on the left shows the diagnostic digests of pLTM322 with BglII – EcoRI and PvuI. Lane M shows the DNA size marker, lane U shows the undigested pLTM332, lane I shows BglII-EcoRI double digested pLTM332 and lane II shows PvuI digested pLTM332. The map of pLTM332, shown on the right, indicates that Bgl II – EcoRI double digestion should generate two bands of 1734 and 2961 bp and PvuI digestion should generate two bands of 1045 and 3650 bp. The bands corresponding to these sizes are shown with arrows.

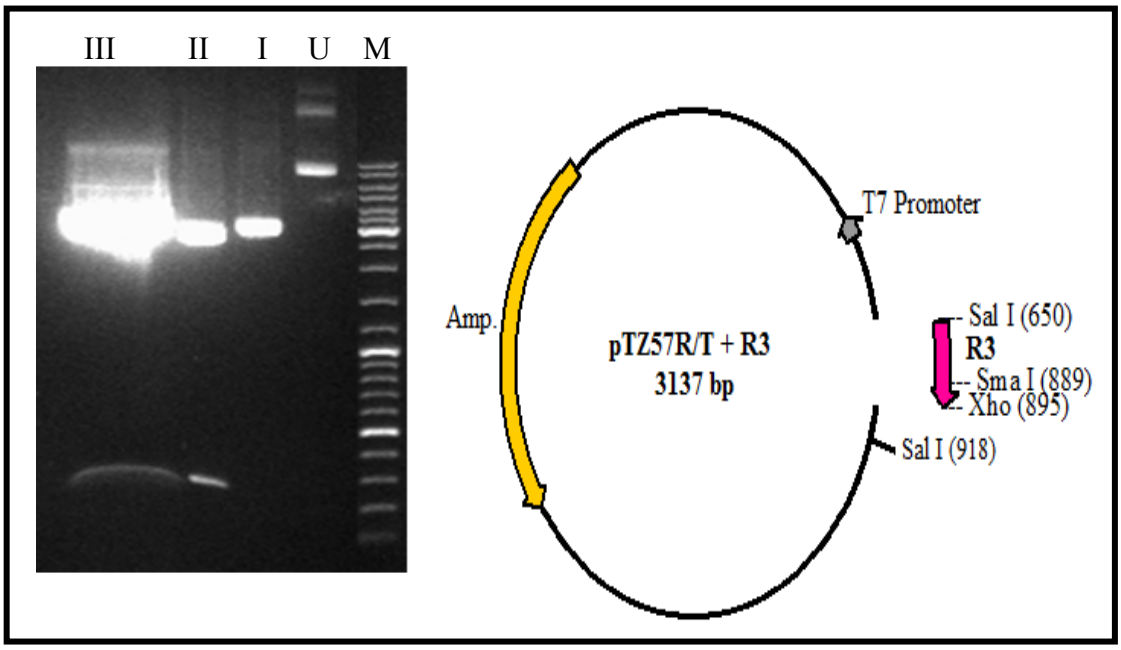

Figure D.2 Digestion of the pTZ57R/T+R3 vector with XhoI – SalI to obtain the R3 homology region. The agarose gel on the left shows the digesiton of pTZ57R/T+R3 vector with XhoI – SalI double digesiton. Lane M shows the DNA size marker, lane U shows the undigested pTZ57R/T+R3 vector, lane I shows XhoI digested pTZ57R/T+R3 vector, lane II shows SalI digested pTZ57R/T+R3 vector and lane III shows XhoI – SalI double digested pTZ57R/T+R3 vector. The map of pTZ57R/T+R3, shown on the right, indicates that XhoI digestion should linearize the vector, SalI digestion should generate two bands of 268 and 2896 bp and XhoI – SalI double digestion should generate two bands of 245 and 2892 bp.

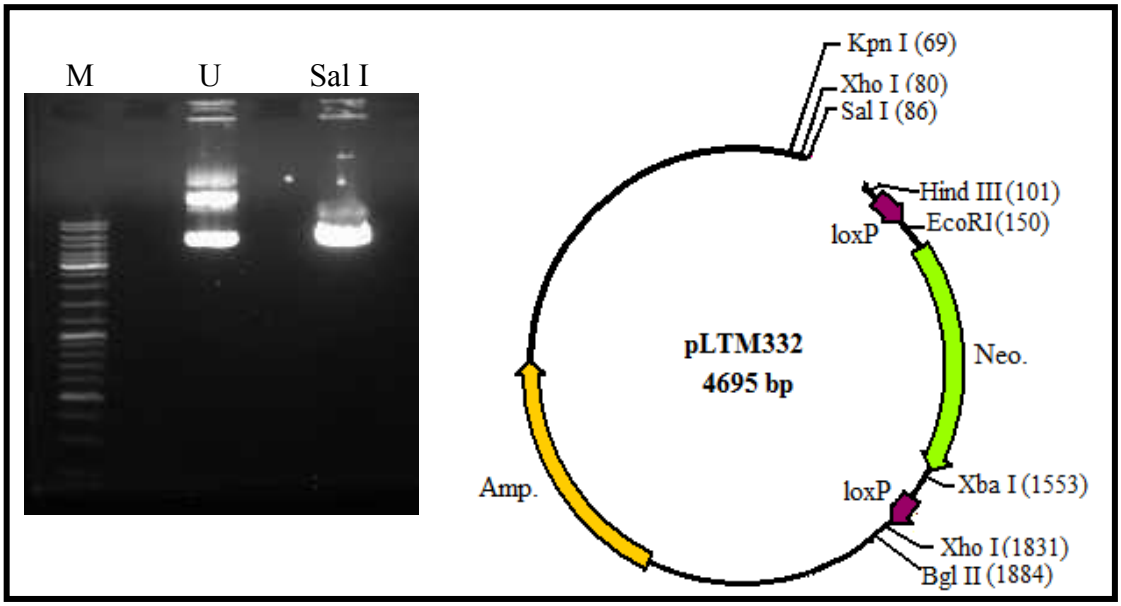

Figure D.3 Linearization of the pLTM332 plasmid with SalI. The agarose gel on the left shows the digestion of pLTM332 with SalI. Lane M shows the DNA size marker, lane U shows the undigested pLTM332 and lane SalI shows SalI digested pLTM332. Schematic representation of linearization of pLTM332 with SalI is shown on the right.

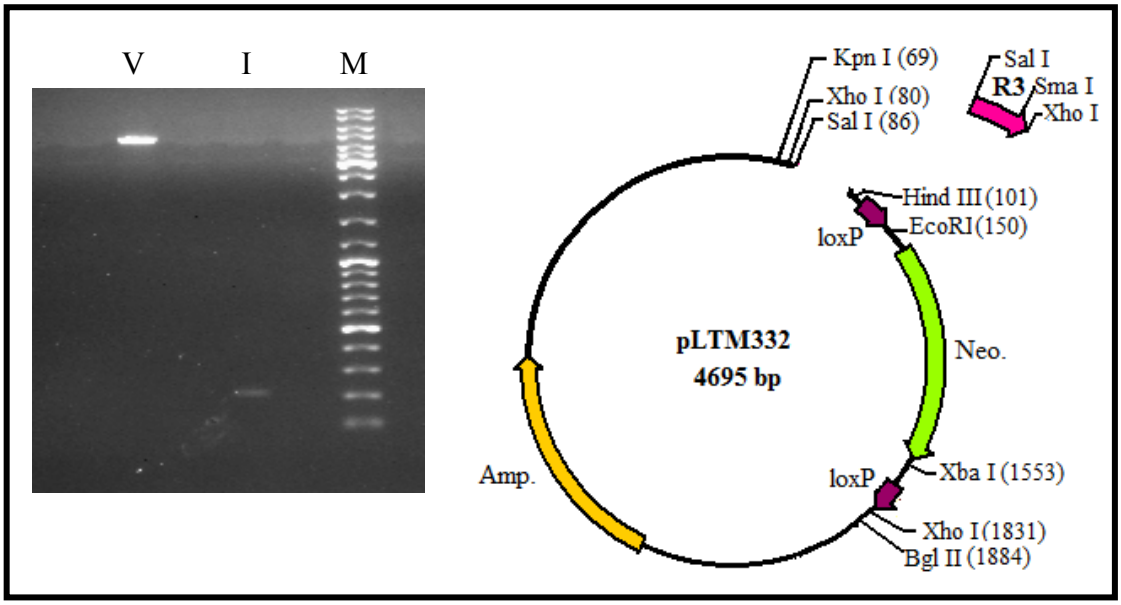

Figure D.4 Comparison of DNA fragments containing the purified R3 insert and the linearized pLTM332 vector before ligation. The agarose gel on the left shows the comparison of vector (pLTM332) and insert (R3) before ligation. Lane V shows linearized pLTM332, lane I shows R3 and lane M shows the DNA size marker. Schematic representation of comparison of pLTM332 and R3 before ligation is shown on the right.

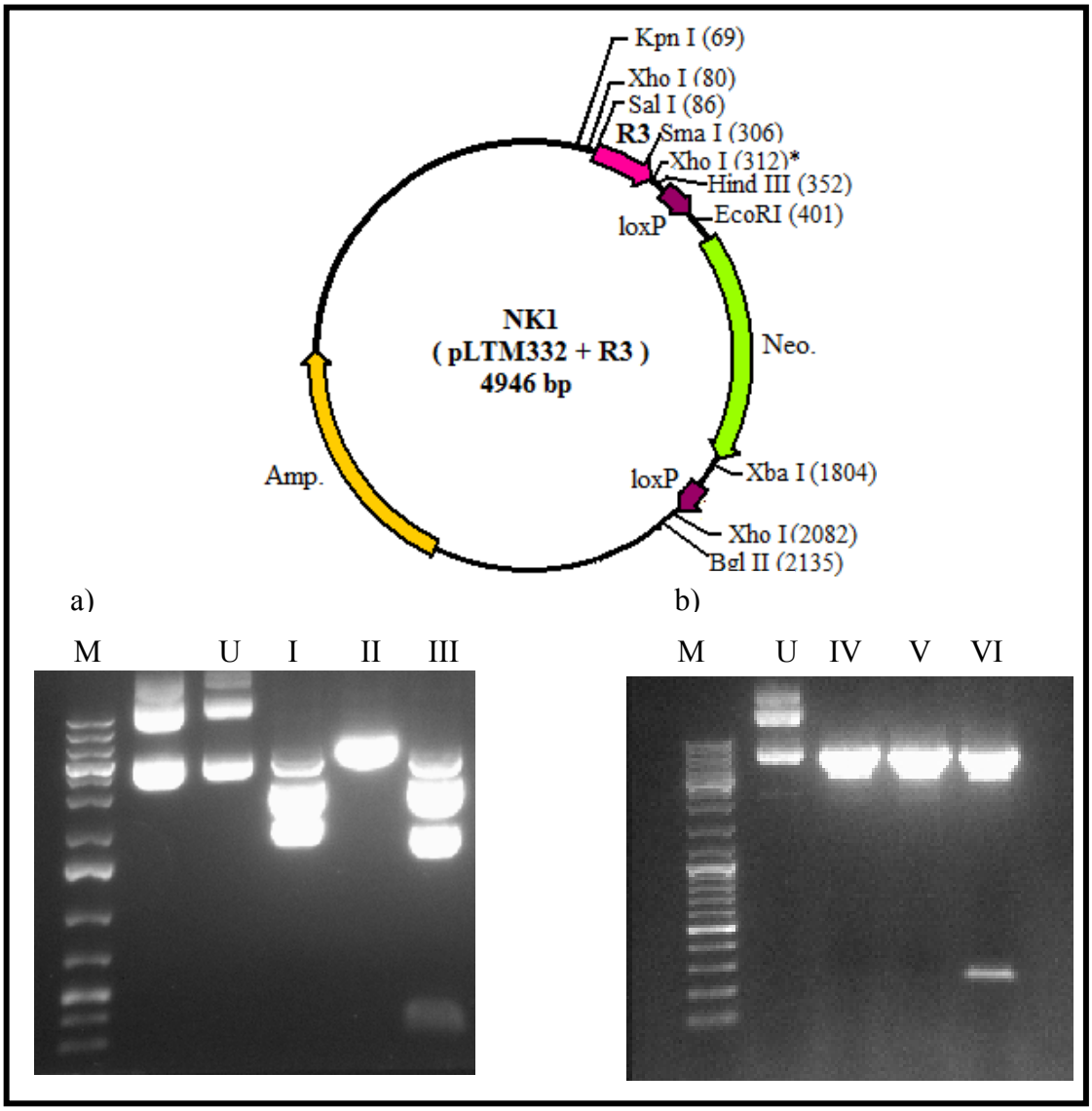

Figure D.5 Confirmation digests of the NK1 plasmid. a) Confirmation of the size of the insert with XhoI – HindIII double digestion and b) Confirmation of the direction of the insert with SmaI – KpnI double digestion. The agarose gel on the left shows the confirmation digest of NK1 with XhoI – HindIII wheras the agarose gel on the right shows the confirmation digest of NK1 with SmaI – KpnI. Lane M shows the DNA size marker, lane U shows the undigested NK1, lane I shows XhoI digested NK1, lane II shows HindIII digested NK1, lane III shows the XhoI – HindIII digested NK1, lane IV shows SmaI digested NK1, lane V shows Kpn1 digested NK1 and lane VI shows SmaI - KpnI digested NK1. The map of NK1, shown on the top, indicates that XhoI digestion should generate two bands of 2002 and 2944 bp, HindIII should linearize NK1, XhoI – HindIII double digestion should generate three bands of 272, 1730 and 2944 bp, SmaI digestion and KpnI digestion should linearize NK1 and SmaI - KpnI digestion should generate two bands of 237 and 4709 bp. (The XhoI site following the R3 fragment, which was destroyed after being ligated into the SalI site is shown as XhoI*.)

According to the recombination strategy detailed in Section 4.1.1, the second plasmid we prepared was NK2 (pLTM332+R3+R4). The R4 homology region which was purified from the pTZ57R/T+R4 plasmid (shown in figure D.6) and linearized NK1 plasmid (shown in figure D.7) were ligated. The correct construction of the NK2 (pLTM332+R3+R4) plasmid was confirmed with restriction digestions (shown in figure D.9).

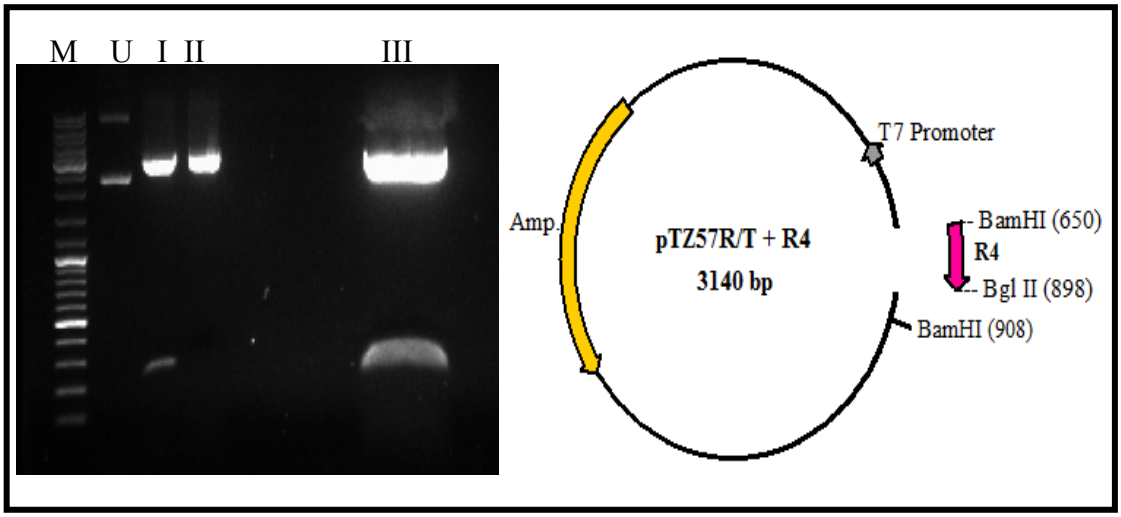

Figure D.6 Digestion of the pTZ57R/T+R4 vector with BamHI – Bgl II to obtain the R4 homology region. The agarose gel on the left shows the BamHI – Bgl II double digestion of pTZ57R/T+R4 plasmid. Lane M shows the DNA size marker, lane U shows the undigested pTZ57R/T+R4 plasmid, lane I shows BamHI digested pTZ57R/T+R4, lane II shows BglII digested pTZ57R/T+R4 and lane III shows BamHI – Bgl II digested pTZ57R/T+R4. The map of pTZ57R/T+R4 plasmid, shown on the right, indicates that BamHI digestion should generate two bands of 258 and 2882 bp, Bgl II digestion should linearize pTZ57R/T+R4 plasmid and BamHI – Bgl II digestion should generate two bands of 248 and 2892 bp.

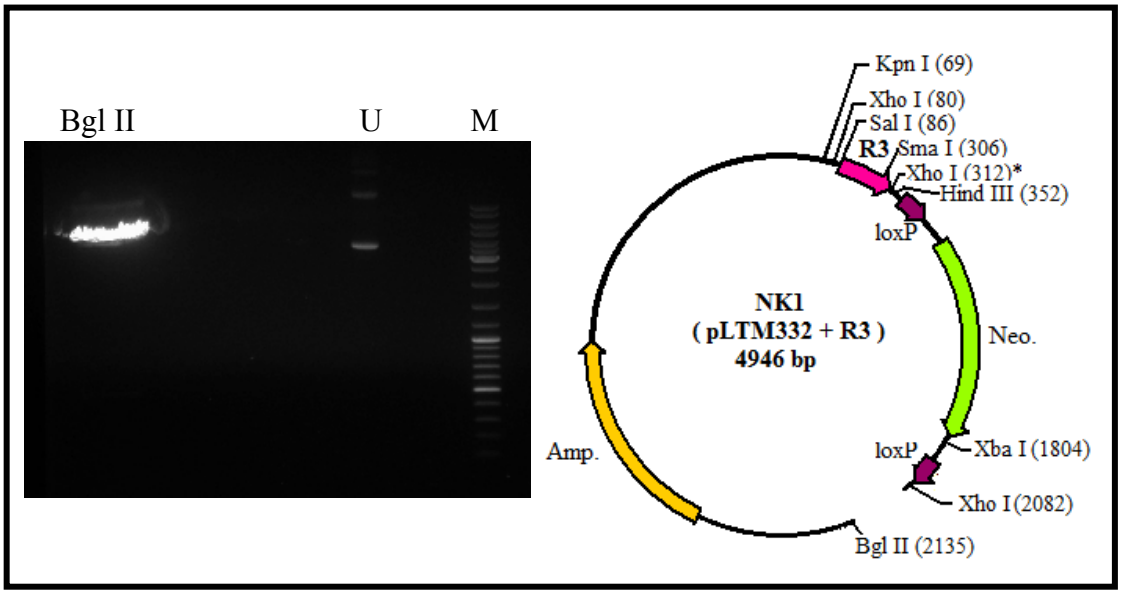

Figure D.7 Linearization of the NK1 (pLTM332+R3) plasmid with Bgl II. The agarose gel on the left shows linearization of NK1 with BglII. Lane M shows the DNA size marker, lane U shows the undigested NK1 and lane Bgl II shows Bgl II digested NK1. Schematic representation of linearization of NK1 is shown on the right.

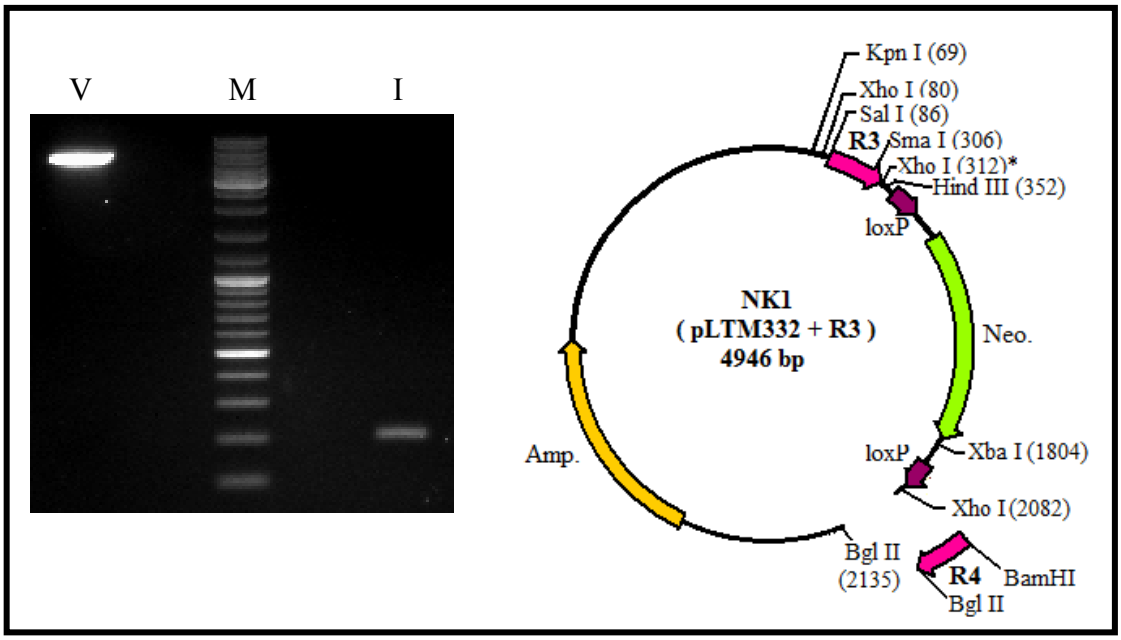

Figure D.8 Comparison of DNA fragments containing the purified R4 insert and linearized NK1 (pLTM332+R3) vector before ligation. The agarose gel on the left shows the comparison of vector (NK1) and insert (R4) before ligation. Lane V shows linearized NK1, lane I shows R4 and lane M shows the DNA size marker. Schematic representation of comparison of NK1 and R4 before ligation is shown on the right.

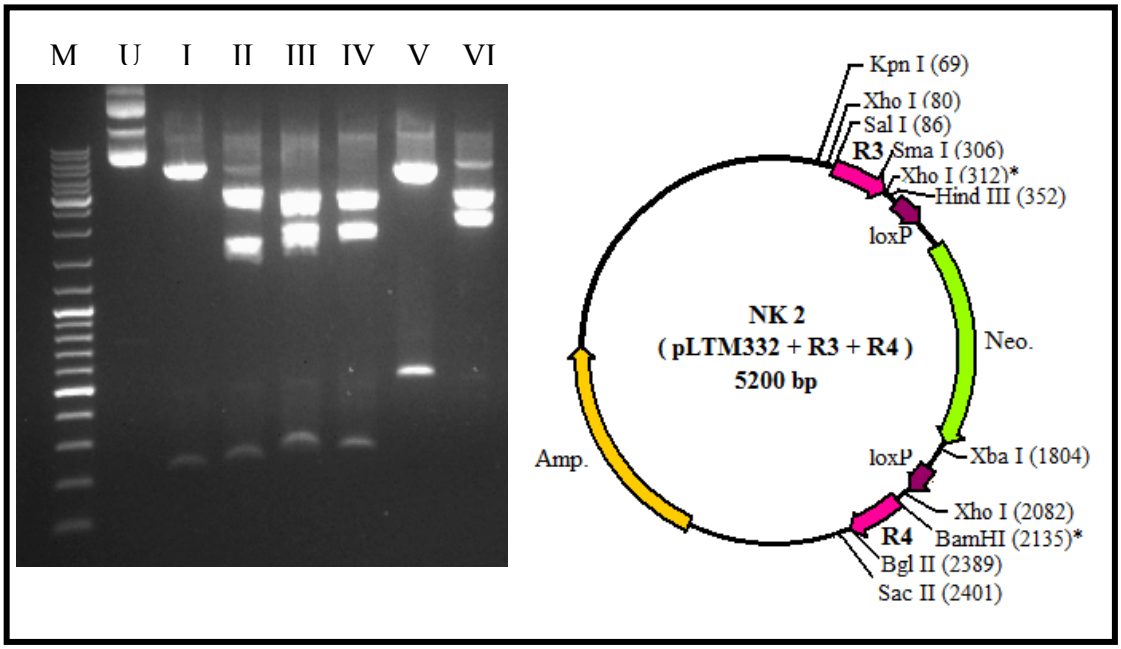

Figure D.9 Confirmation digests of the NK2 (pLTM332+R3+R4) plasmid. The agarose gel on the left shows the confirmation digests of NK2 with SmaI – KpnI, XhoI – HindIII, Bgl II – XhoI, SacII – XhoI, SacII – XbaI and SalI – SacII double digestions Lane M shows the DNA size marker, lane U shows the undigested NK2, lane I shows SmaI – KpnI digested NK2, lane II shows XhoI – HindIII digested NK2, lane III shows the Bgl II – XhoI digested NK2, lane IV shows SacII – XhoI digested NK2, lane V shows SacII – XbaI digested NK2 and lane VI shows SalI – SacII digested NK2. The map of NK2, shown on the right, indicates that SmaI – KpnI double digestion should generate two bands of 239 and 4961 bp, XhoI – HindIII double digesiton should generate three bands of 302, 1730 and 3169 bp, Bgl II – XhoI double digestion should generate three bands of 307, 2002 and 2891 bp, SacII – XhoI double digestion should generate three bands of 319, 2002 and 2879 bp, SacII – XbaI double digestion should generate two bands of 597 and 4603 bp and SalI – SacII double digestion should generate two bands of 2315 and 2885 bp. (The XhoI site following the R3 fragment, which was destroyed after being ligated into the SalI site is shown as XhoI* and the BamHI site preceding the R4 fragment, which was destroyed after being ligated into the Bgl II site is shown as BamHI*)

The third plasmid we prepared was NK3 (pLTM260+R5). After diagnostic digestion of the pLTM260 parent plasmid, the R5 homology region which was purified from the pTZ57R/T+R5 plasmid (shown in figure D.11) and linearized pLTM260 (shown in figure D.12) were ligated. The correct construction of the NK3 (pLTM260+R5) plasmid was confirmed with restriction digestions (shown in figure D.14).

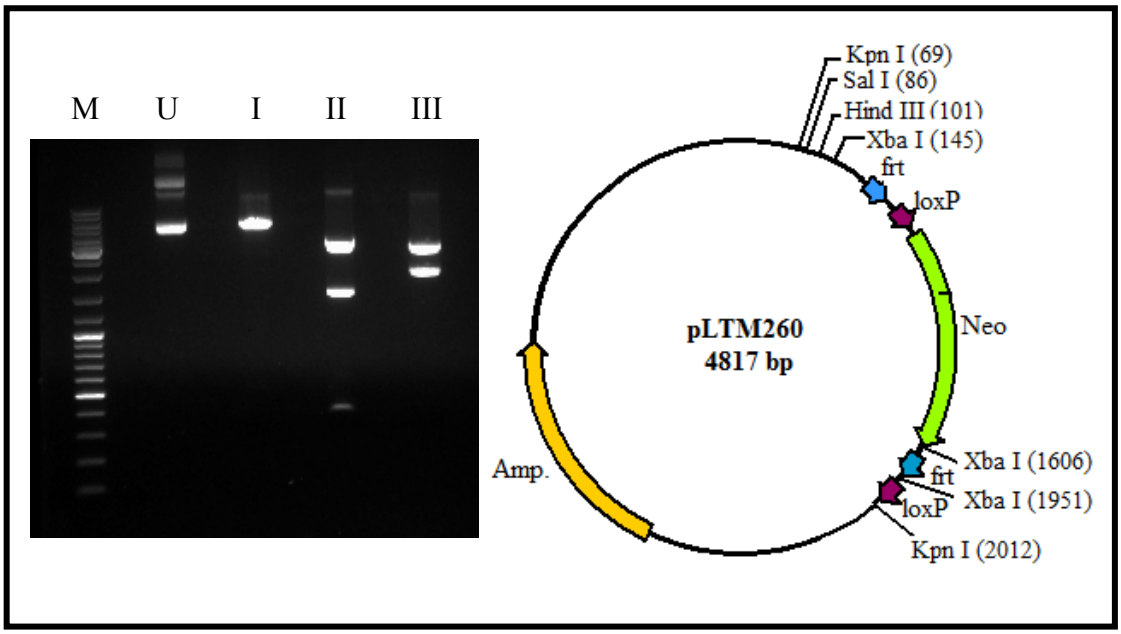

Figure D.10 Diagnostic digests of the pLTM260 plasmid. The agarose gel on the left shows the diagnostic digests of pLTM260 with SalI, XbaI and KpnI. Lane M shows the DNA size marker, lane U shows the undigested pLTM260, lane I shows SalI digested pLTM260 and lane II shows XbaI digested pLTM260 and lane III shows KpnI digested pLTM260. The map of pLTM260, shown on the right, indicates that SalI digestion should linearize pLTM260, XbaI digestion should generate three bands of 345, 1461 and 3011 bp, KpnI digestion should generate two bands of 1943 and 2874bp.

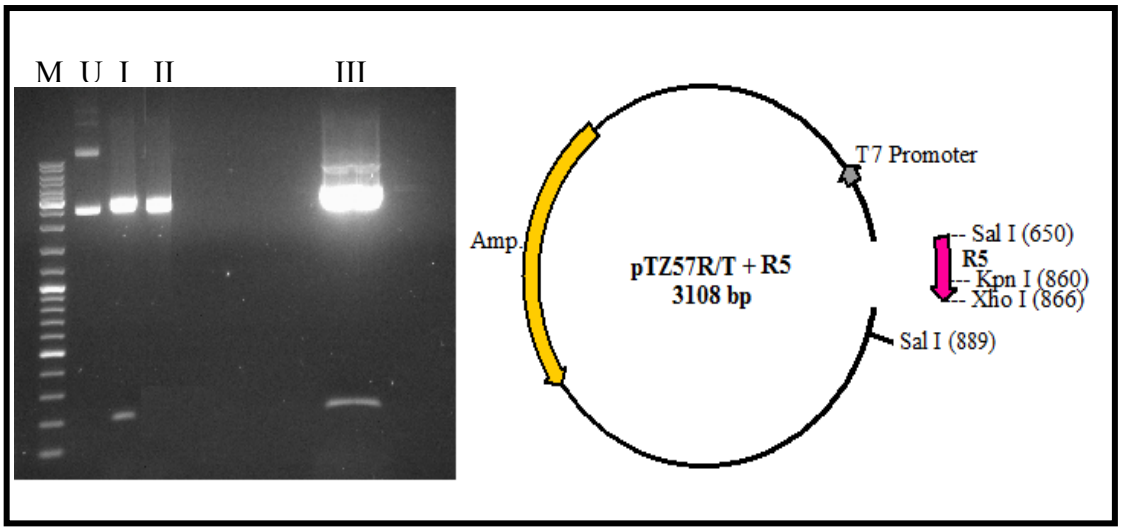

Figure D.11 Digestion of the pTZ57R/T+R5 vector SalI – XhoI to obtain the R5 homology region. The agarose gel on the left shows the double digestion of the pTZ57R/T+R5 plasmid with SalI – XhoI. Lane M shows the DNA size marker, lane U shows the undigested pTZ57R/T+R5, lane I shows SalI digested pTZ57R/T+R5, lane II shows XhoI digested pTZ57R/T+R5 and lane III shows SalI – XhoI digested pTZ57R/T+R5. The map of pTZ57R/T+R5, shown on the right, indicates that SalI digestion should generate two bands of 239 and 2869 bp, XhoI digestion should linearize pTZ57R/T+R5 and SalI – XhoI double digestion should generate two bands of 216 and 2892 bp.

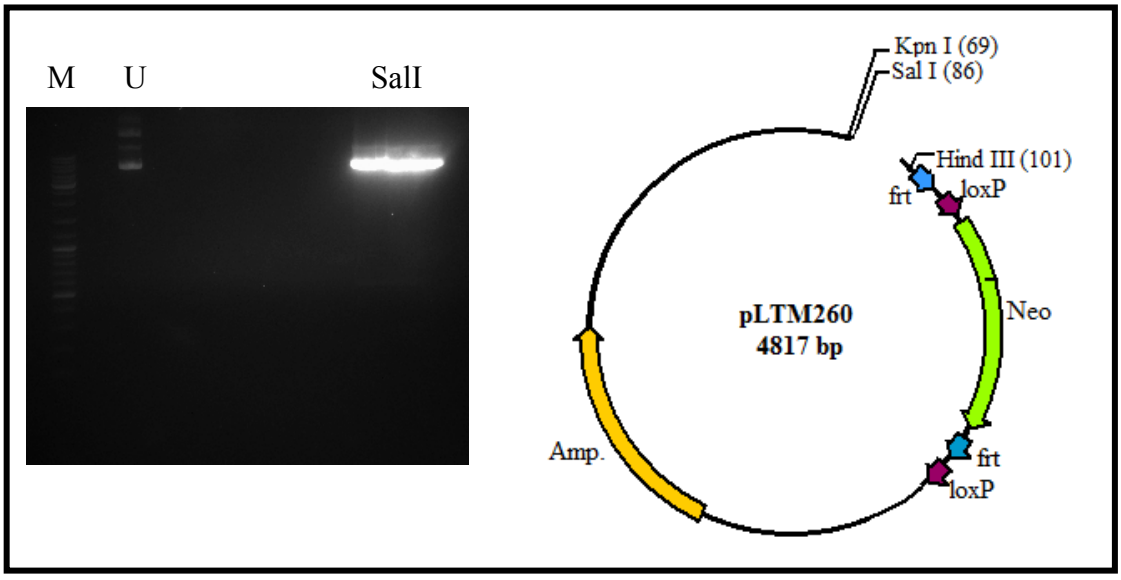

Figure D.12 Linearization of the pLTM260 plasmid with Sal I. The agarose gel on the left shows the digestion of pLTM260 with SalI. Lane M shows the DNA size marker, lane U shows the undigested pLTM260 and lane SalI shows SalI digested pLTM260. Schematic representation of linearization of pLTM260 with SalI is shown on the right.

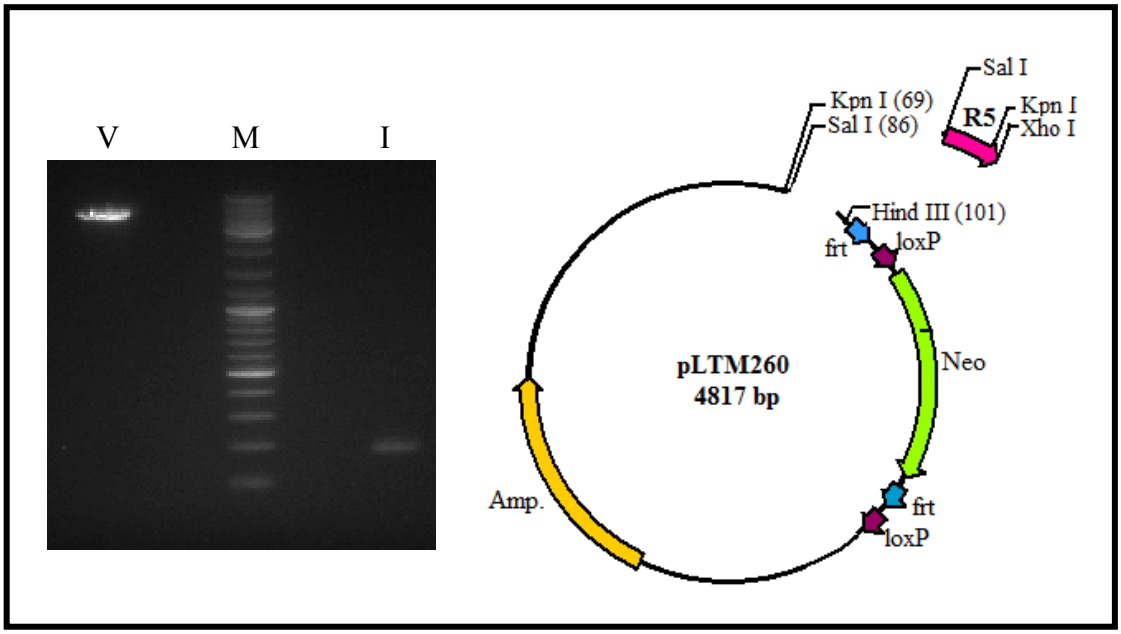

Figure D.13 Comparison of DNA fragments containing the purified R5 insert and linearized pLTM260 vector before ligation. The agarose gel on the left shows the comparison of vector (pLTM260) and insert (R5) before ligation. Lane V shows linearized pLTM260, lane I shows R5 and lane M shows the DNA size marker. Schematic representation of comparison of pLTM260 and R5 before ligation is shown on the right.

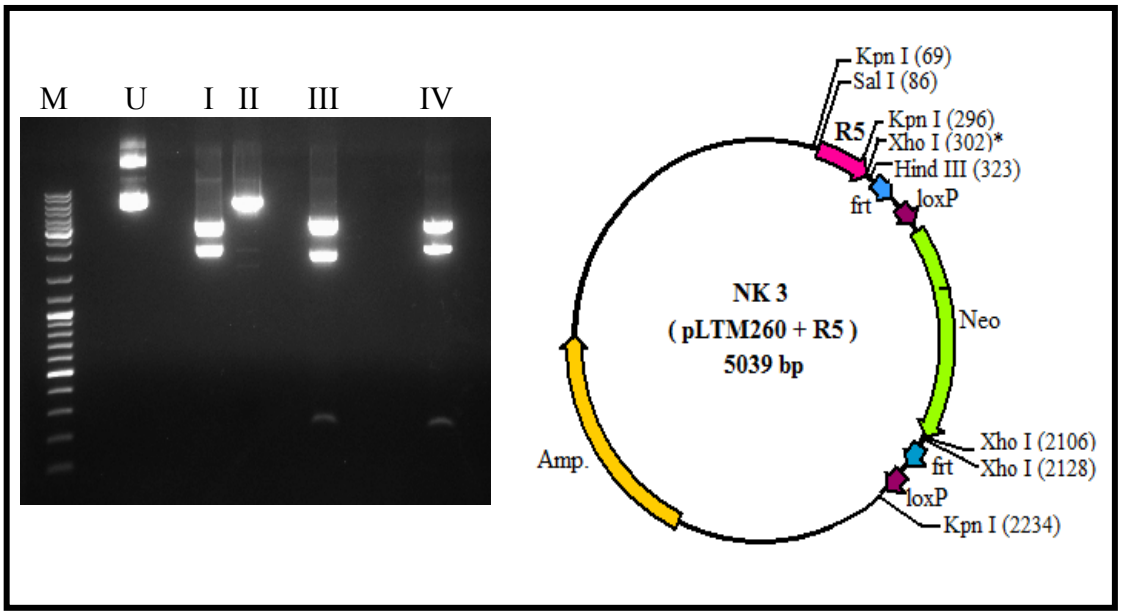

Figure D.14 Confirmation digests of the NK3 (pLTM260+R5) plasmid. The agarose gel on the left shows the confirmation digest of NK3 with XhoI – HindIII and KpnI digestions. Lane M shows the DNA size marker, lane U shows the undigested NK3, lane I shows XhoI digested NK3, lane II shows HindIII digested NK3, lane III shows the XhoI – HindIII digested NK3 and lane IV shows KpnI digested NK3. The map of NK3, shown on the top, indicates that XhoI digestion should generate three bands of 22, 2026 and 3013 bp, HindIII digestion should linearize NK3, XhoI – HindIII double digestion should generate four bands of 22, 243, 1783 and 2874 bp and KpnI digestion should generate three bands of 227, 1938 and 2874 bp. (The XhoI site following the R5 fragment, which was destroyed after being ligated into the SalI site is shown as XhoI*.)

The fourth plasmid we prepared was NK4 (pLTM260+R5+R6). The R6 homology region which was purified from the pTZ57R/T+R6 plasmid (shown in figure D.15) and linearized NK3 (shown in figure D.16) were ligated. The correct construction of the NK4 (pLTM260+R5+R6) plasmid was confirmed with restriction digestions (shown in figure D.18).

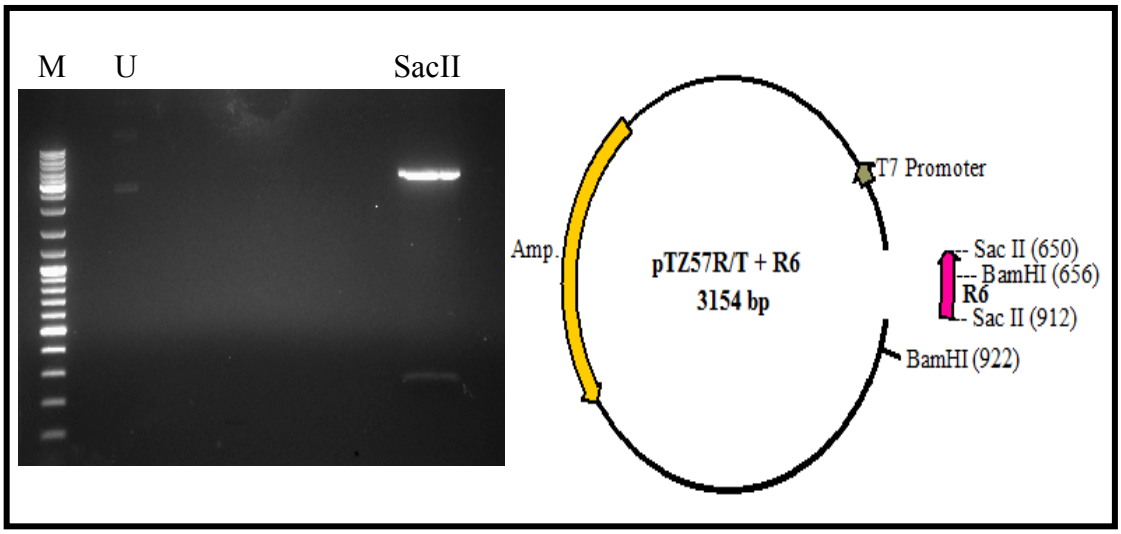

Figure D.15 Digestion of the pTZ57R/T+R6 plasmid with Sac II to obtain the R6 homology region. The agarose gel on the left shows the digestion of pTZ57R/T+R6 plasmid with SacII. Lane M shows the DNA size marker, lane U shows the undigested pTZ57R/T+R6 plasmid and lane SacII shows SacII digested pTZ57R/T+R6. The map of the pTZ57R/T+R6 plasmid, shown on the right, indicates that SacII digestion should generate two bands of 262 and 2892 bp.

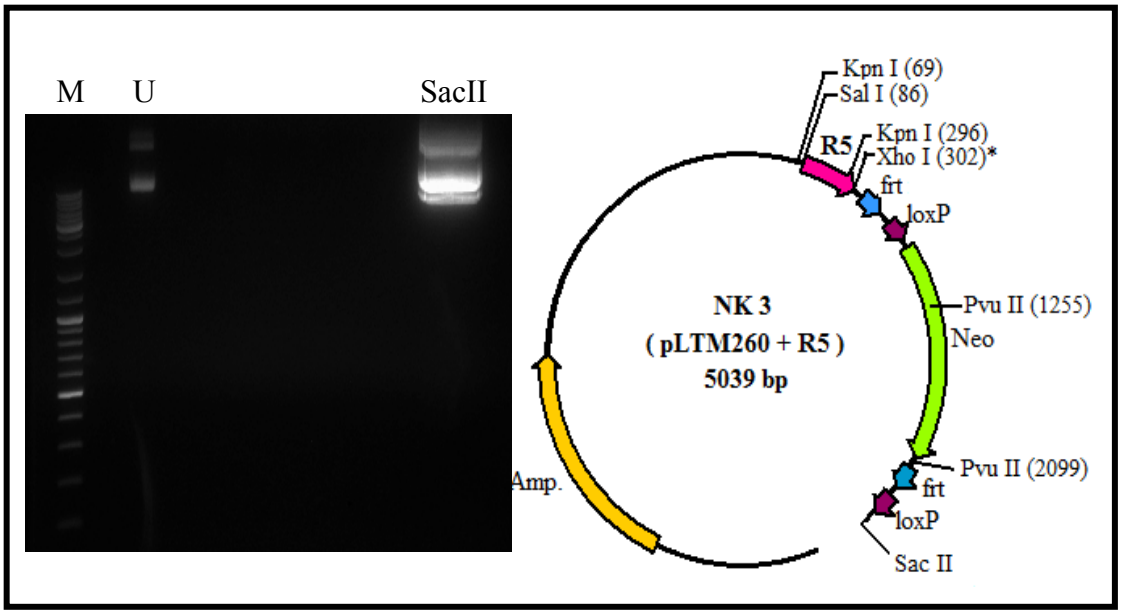

Figure D.16 Linearization of the NK3 (pLTM260+R5) plasmid with Sac II. The agarose gel on the left shows linearization of NK3 with SacII. Lane M shows the DNA size marker, lane U shows the undigested NK3 and lane SacII shows SacII digested NK3. Schematic representation of linearization of NK3 is shown on the right.

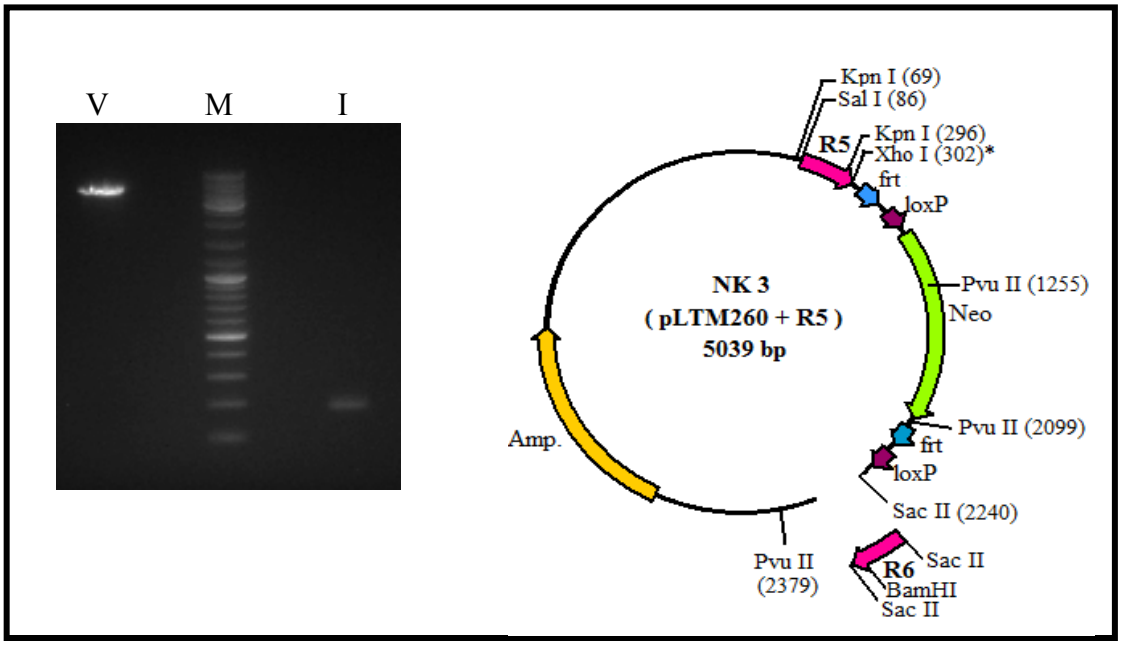

Figure D.17 Comparison of DNA fragments containing the purified R6 insert and linearized NK3 (pLTM260+R5) vector before ligation. The agarose gel on the left shows the comparison of vector (NK3) and insert (R6) before ligation. Lane V shows linearized NK3, lane I shows R6 and lane M shows the DNA size marker. Schematic representation of comparison of NK3 and R6 before ligation is shown on the right.

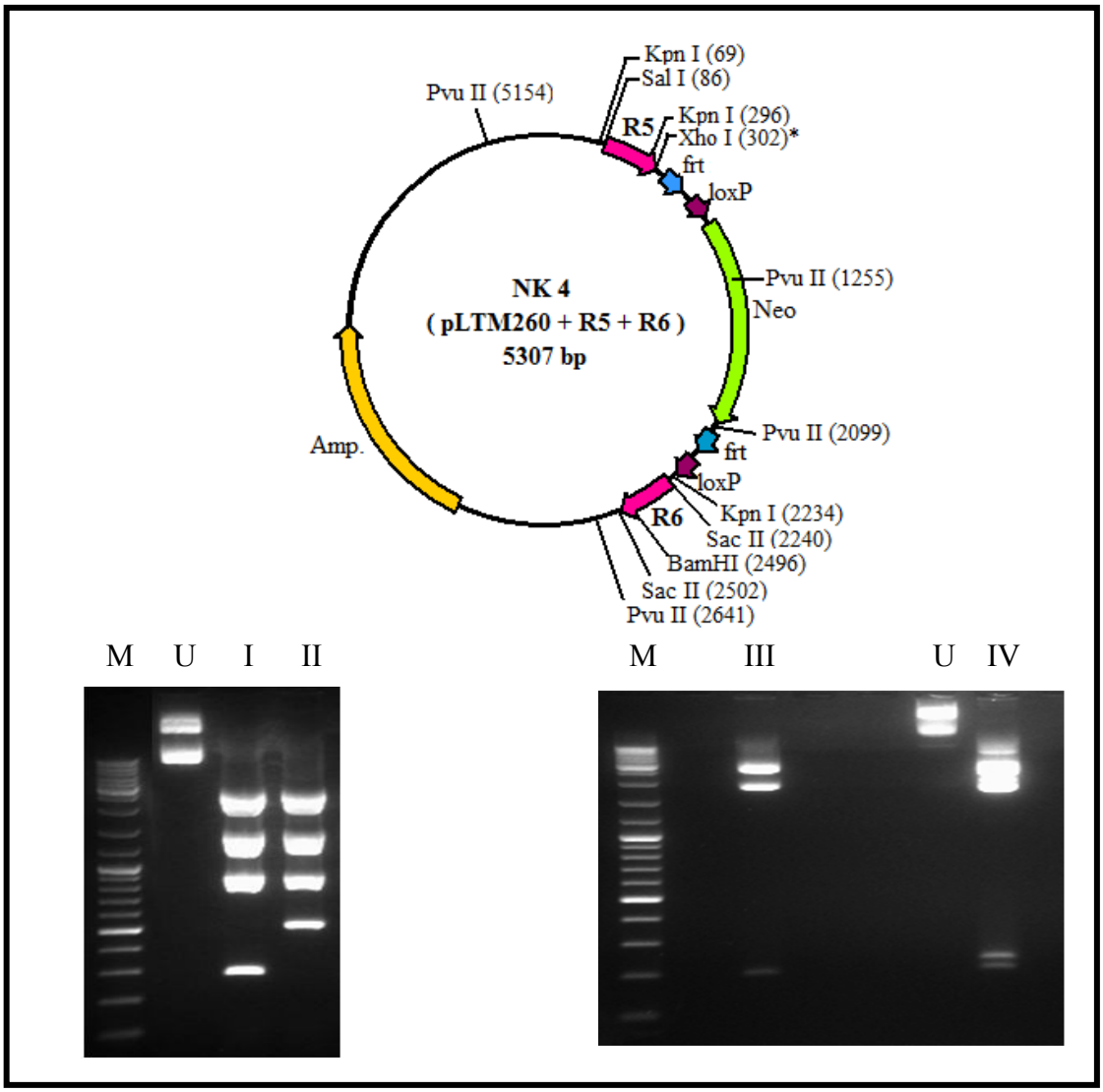

Figure D.18 Confirmation digests of the NK4 (pLTM260+R5+R6) plasmid. The agarose gel on the left shows the confirmation digest of NK4 with PvuII whereas the agarose gel on the right shows the confirmation digest of NK4 with BamHI – KpnI. Lane M shows the DNA size marker, lane U shows the undigested NK4, lane I shows PvuII digested NK3, lane II shows PvuII digested NK4, lane III shows BamHI – KpnI digested NK3 and lane IV shows BamHI – KpnI digested NK4. The map of NK4, shown on the top, indicates that PvuII digestion of NK4 should generate four bands of 544, 844, 1408 and 2513 bp whereas PvuII digestion of NK3 (the plasmid without the R6 fragment) should generate four bands of 282, 844, 1408 and 2513 bp. BamHI – KpnI double digestion of NK4 should generate four bands of 227, 262, 1938 and 2880 bp whereas BamHI – KpnI double digestion of NK3 (the plasmid without the R6 fragment) should generate three bands of 227, 1938 and 2874 bp. (The XhoI site following the R5 fragment, which was destroyed after being ligated into the SalI site is shown as XhoI* and the BamHI site preceding the R6 fragment, which was destroyed after being ligated into the Bgl II site is shown as BamHI*)

The fifth plasmid we prepared for recombination strategy was NK5 (pKO917TK+R1). After diagnostic digestion of the pKO917TK parent plasmid, the R1 homology region which was purified from the pTZ57R/T+R1 plasmid (shown in figure D.20) and linearized pKO917TK (shown in figure D.21) were ligated. The correct construction of the NK5 (pKO917TK+R1) plasmid was confirmed with restriction digestions (shown in figure D.23).

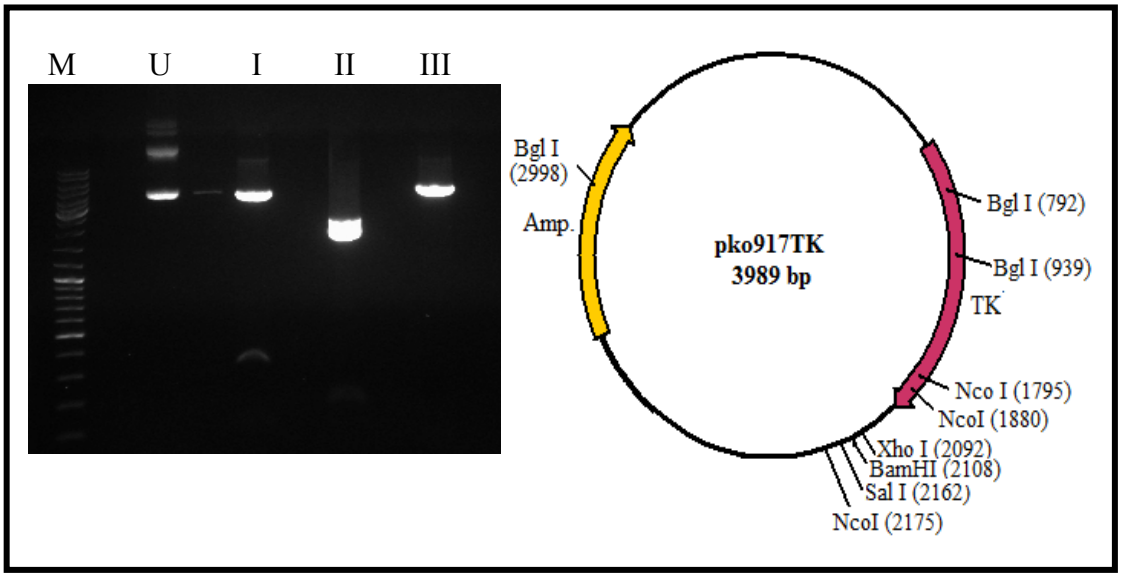

Figure D.19 Diagnostic digests of the pKO917TK plasmid. The agarose gel on the left shows the diagnostic digests of pKO917TK with NcoI, Bgl I and BamHI – SalI. Lane M shows the DNA size marker, lane U shows the undigested pKO917TK, lane I shows NcoI digested pKO917TK, lane II shows Bgl I digested pKO917TK and lane III shows BamHI – SalI double digested pKO917TK. The map of pKO917TK, shown on the right, indicates that NcoI digestion should generate three bands of 85, 295 and 3689 bp, Bgl I digestion should generate three bands of 147, 1783 and 2059 bp and BamHI – SalI double digestion should generate two bands of 54 and 3935 bp.

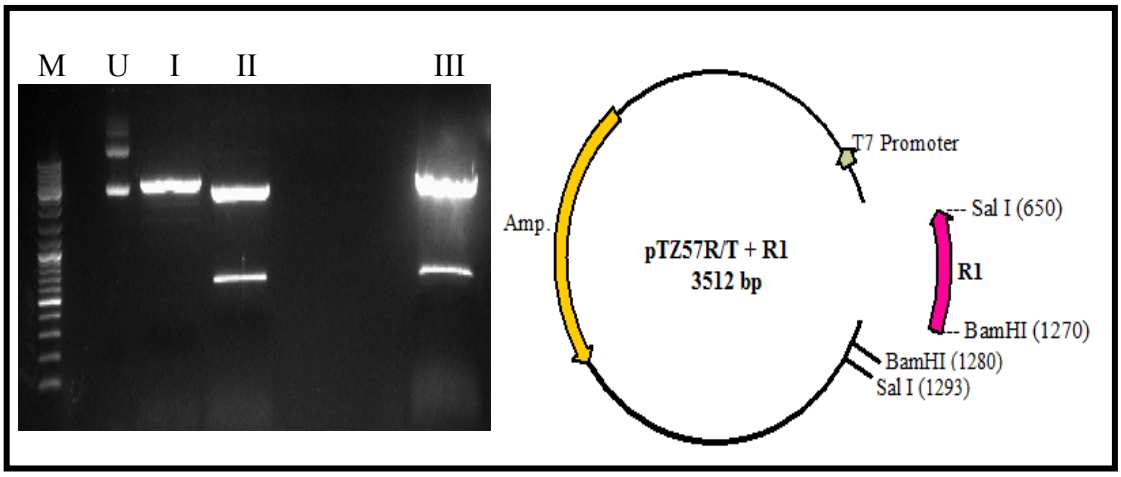

Figure D.20 Digestion of pTZ57R/T+R1 vector with BamHI – SalI to obtain R1 homology region. The agarose gel on the left shows the digesiton of pTZ57R/T+R1 vector with BamHI – SalI double digesiton. Lane M shows the DNA size marker, lane U shows the undigested pTZ57R/T+R1 vector, lane I shows BamHI digested pTZ57R/T+R1 vector, lane II shows SalI digested pTZ57R/T+R1 vector and lane III shows BamHI – SalI double digested pTZ57R/T+R1 vector. The map of pTZ57R/T+R1, shown on the right, indicates that BamHI digestion should generate two bands of 10 and 3502 bp, SalI digestion should generate two bands of 643 and 2869 bp and BamHI – SalI double digestion should generate three bands of 10, 620 and 2882 bp.

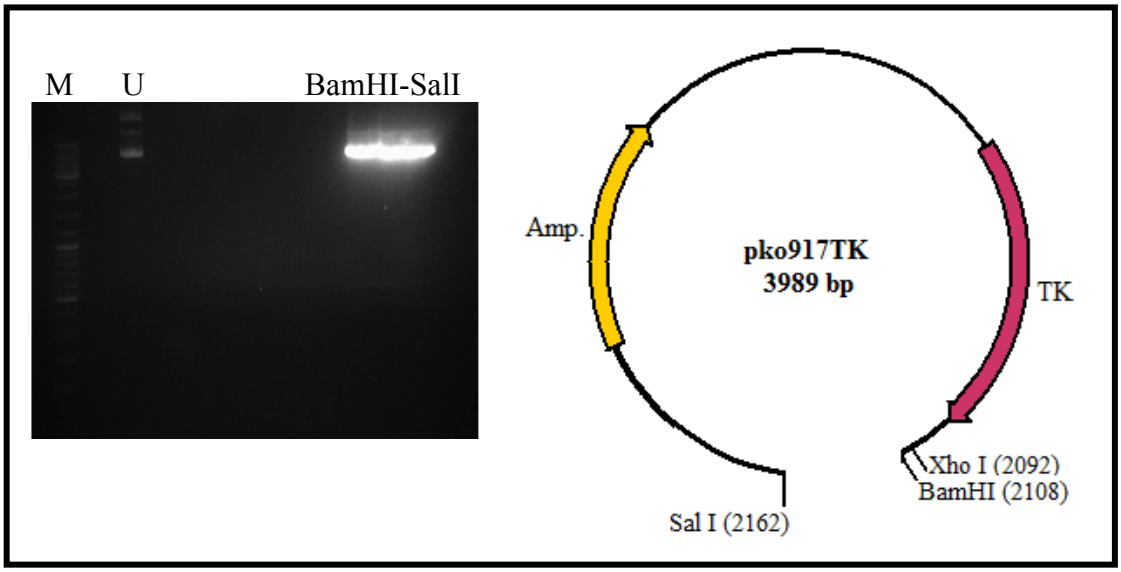

Figure D.21 Digestion of pKO917TK with BamHI – SalI. The agarose gel on the left shows the double digestion of pKO917TK with BamHI – SalI. Lane M shows the DNA size marker, lane U shows the undigested pKO917TK and lane BamHI – SalI shows BamHI – SalI digested pKO917TK. Schematic representation of BamHI – SalI digested pKO917TK is shown on the right.

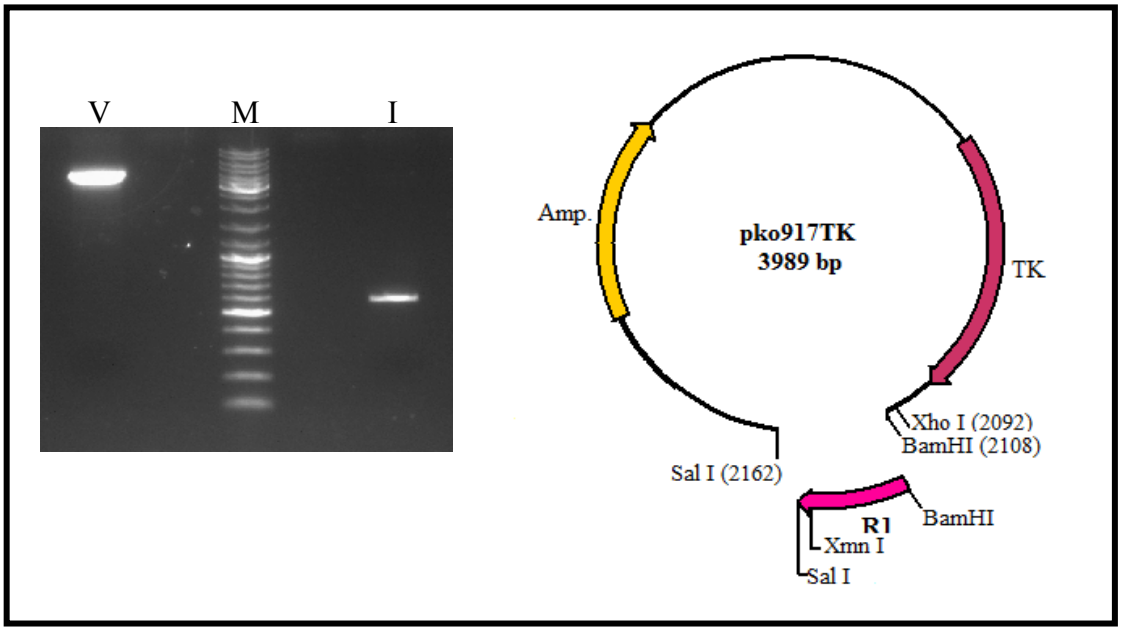

Figure D.22 Comparison of DNA fragments containing the purified R1 insert and digested pKO917TK vector before ligation. The agarose gel on the left shows the comparison of vector (pKO917TK) and insert (R1) before ligation. Lane V shows digested pKO917TK, lane I shows R3 and lane M shows the DNA size marker. Schematic representation of comparison of pKO197TK and R1 before ligation is shown on the right.

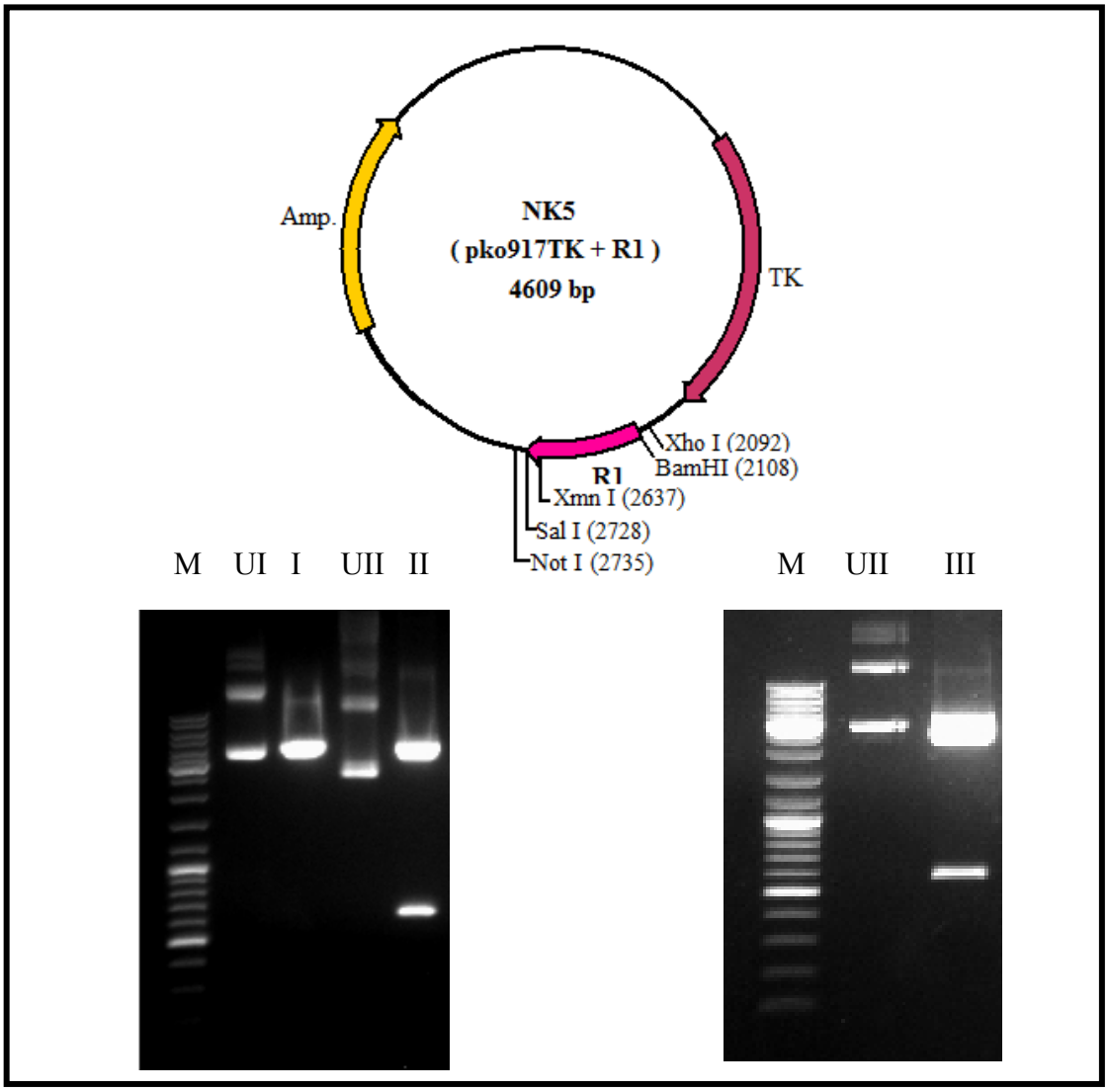

Figure D.23 Cofirmation digests of the NK5 (pKO917TK+R1) plasmid. The agarose gel on the left shows the confirmation digest of NK5 with XhoI – NotI wheras the agarose gel on the right shows the confirmation digest of NK5 with BamHI – SalI. Lane M shows the DNA size marker, lane UI shows the undigested pKO917TK, lane I shows XhoI – NotI digested pKO917TK, lane UII shows the undigested NK5, lane II shows XhoI – NotI digested NK5 and lane III shows the BamHI – SalI digested NK5. The map of NK5, shown on the top, indicates that XhoI – NotI double digestion of NK5 should generate two bands of 643 and 3966 bp whereas XhoI – NotI double digestion of empty pKO917TK plasmid should generate two bands of 61 and 3912 bp. Also, BamHI – SalI double digestion of NK5 should generate two bands of 620 and 3989 bp.

The sixth plasmid we prepared was NK6 (pKO917TK+R1+R2). The R2 homology region which was purified from the pTZ57R/T+R2 plasmid (shown in figure D.24) and digested NK5 (shown in figure D.25) were ligated. The correct construction of the NK6 (pKO917TK+R1+R2) plasmid was confirmed with restriction digestions (shown in figure D.27).

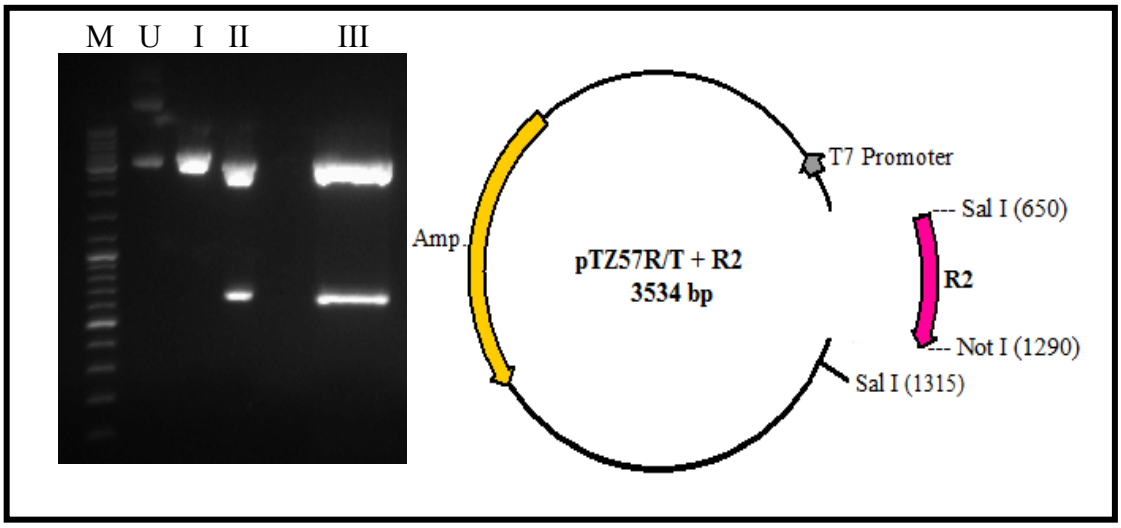

Figure D.24 Digestion of the pTZ57R/T+R2 vector SalI – NotI to obtain the R2 homology region. The agarose gel on the left shows the digesiton of pTZ57R/T+R2 vector with NotI – SalI double digesiton. Lane M shows the DNA size marker, lane U shows the undigested pTZ57R/T+R2 vector, lane I shows NotI digested pTZ57R/T+R2 vector, lane II shows SalI digested pTZ57R/T+R2 vector and lane III shows NotI – SalI double digested pTZ57R/T+R2 vector. The map of pTZ57R/T+R2, shown on the right, indicates that NotI digestion should linearize pTZ57R/T+R2, SalI digestion should generate two bands of 665 and 2869 bp and NotI – SalI double digestion should generate three bands of 25, 640 and 2869 bp.

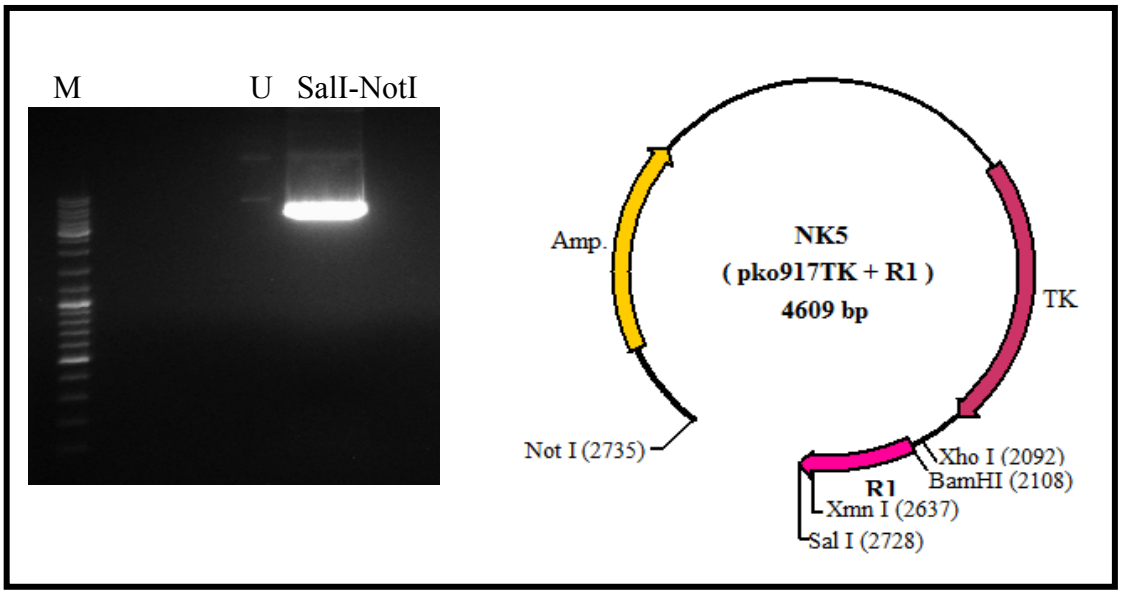

Figure D.25 Digestion of NK5 (pKO917TK+R1) with SalI – NotI. The agarose gel on the left shows double digestion of NK5 with SalI – NotI. Lane M shows the DNA size marker, lane U shows the undigested NK3 and lane SacII – NotI shows SacII – NotI digested NK5. Schematic representation of SacII – NotI double digested NK5 is shown on the right.

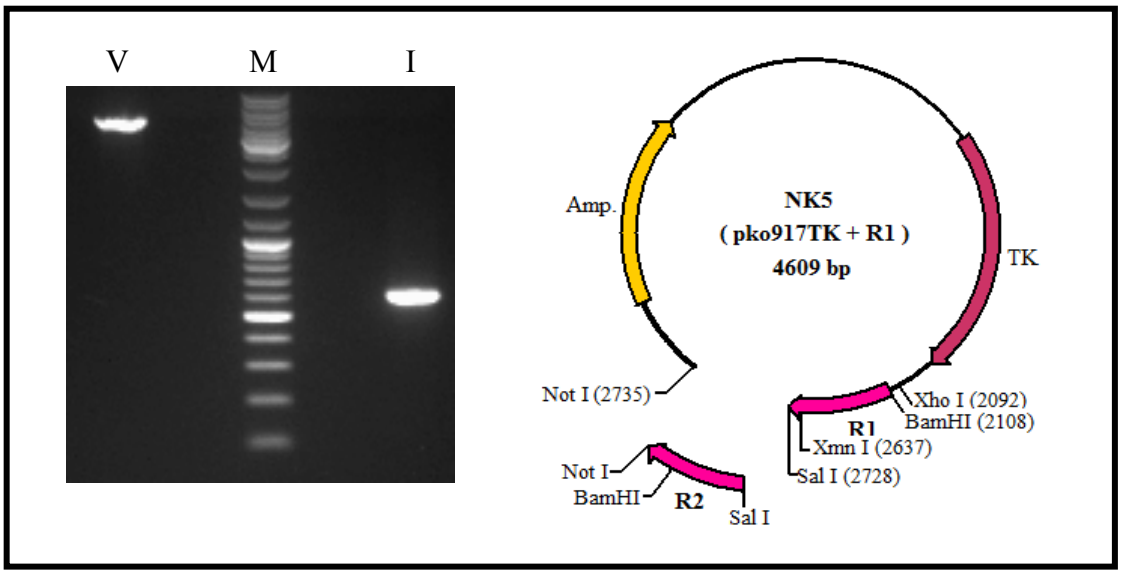

Figure D.26 Comparison of DNA framents containing the purified R2 insert and digested NK5(pKO917TK+R1) vector before ligation. The agarose gel on the left shows the comparison of vector (NK5) and insert (R2) before ligation. Lane V shows digested NK5, lane I shows R2 and lane M shows the DNA size marker. Schematic representation of comparison of NK5 and R2 before ligation is shown on the right.

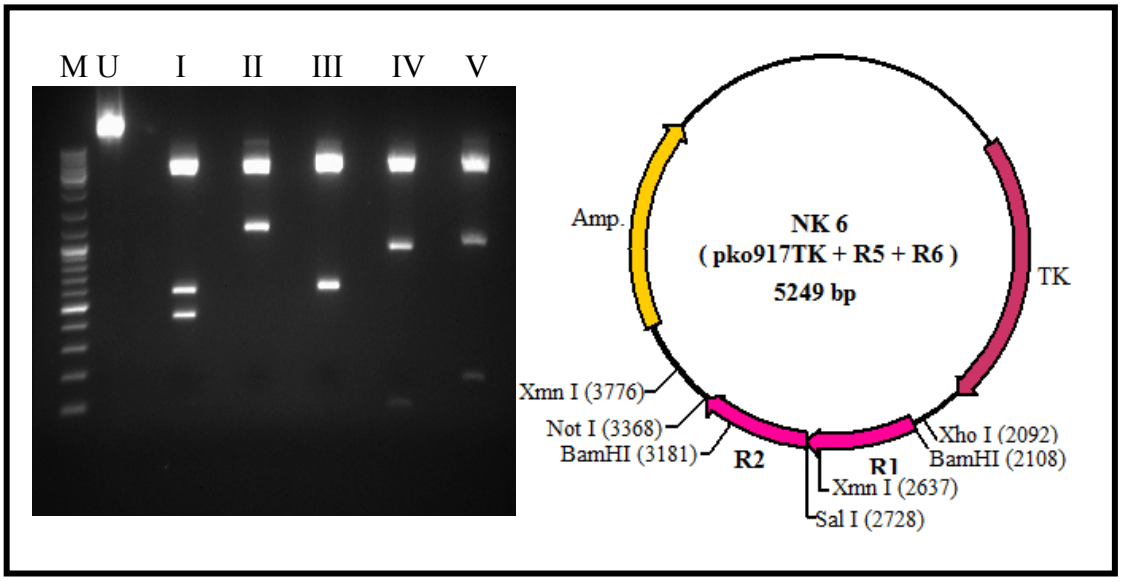

Figure D.27 Confirmation digest of the NK6 (pKO917TK+R5+R6) plasmid. The agarose gel on the left shows the confirmation digest of NK6 with BamHI – SalI, XhoI – NotI, SalI – NotI, SalI – XmnI and BamHI – NotI. Lane M shows the DNA size marker, lane U shows the undigested NK6, lane I shows BamHI – SalI digested NK6, lane II shows XhoI – NotI digested NK6, lane III shows SalI – Not I digested NK6, lane IV shows SalI – XmnI digested NK6 and lane V shows BamHI – NotI digested NK6. The map of NK6, shown on the right, indicates that BamHI – SalI digestion should generate three bands of 453, 620 and 4176 bp, XhoI – NotI digestion should generate two bands of 1276 and 3973 bp, SalI – Not I digestion should generate two bands of 640 and 4609 bp, SalI – XmnI digestion should generate three bands of 91, 1048 and 4110 bp and BamHI – NotI digestion should generate three bands of 187, 1073 and 3989 bp.

APPENDIX E: Costruction of the Rag1Ap1 – Venus Fusion Plasmid

For subcellular localization and overexpression studies of the Rag1Ap1 protein, we constructed a Rag1Ap1 – Venus fusion plasmid. Rag1Ap1 sequence was amplified by PCR witout a stop codon and fused to the N-terminus of flourescent Venus protein sequence in the pVenus-N1 plasmid. The correct construction of RVL (pVenus-N1+Rag1AP1) plasmid was confirmed with digestions shown in figure E.5

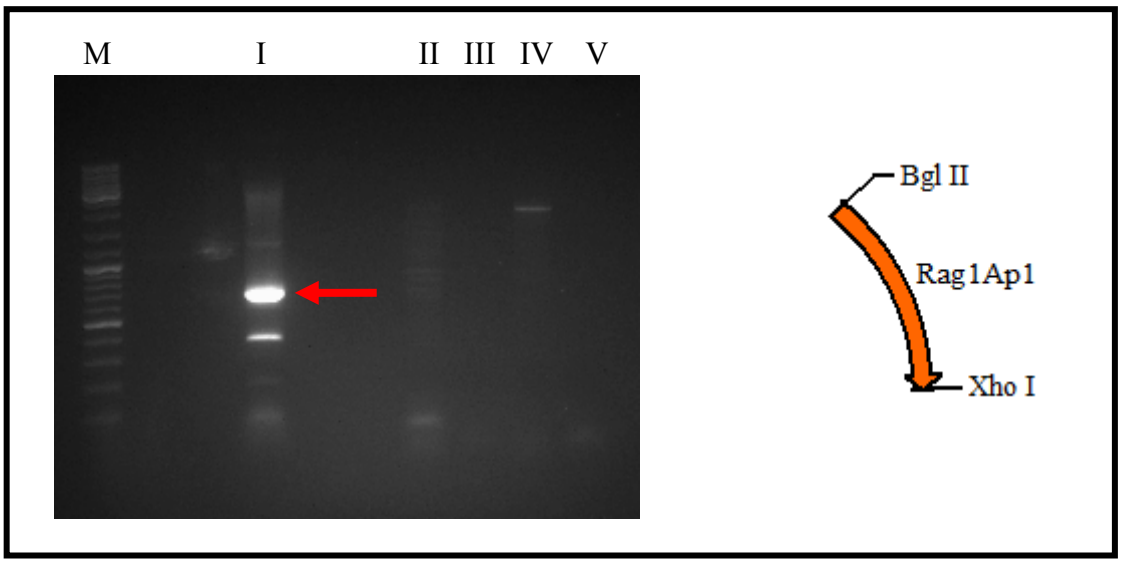

Figure E.1 PCR amplification of Rag1Ap1. Rag1Ap1 cDNA was amplified without a stop codon with a forward primer containing a Bgl II site and a reverse primer containing an XhoI. The agarose gel on the left shows the PCR product for Rag1Ap1 with the relevant controls. Lane M shows the DNA size marker, lane I shows PCR product, lane II shows the product of a PCR without template DNA, lane III shows the product of a PCR without forward primer, lane IV shows the product of a PCR without reverse primer and lane V shows the product of a PCR without *Pfu* polymerase. PCR amplification of the Rag1Ap1 cDNA without a stop codon is expected to generate a band of 700 bp shown with a red arrow. Schematic representation of Rag1Ap1 PCR product with restriction sites introduced by primers is shown on the right.

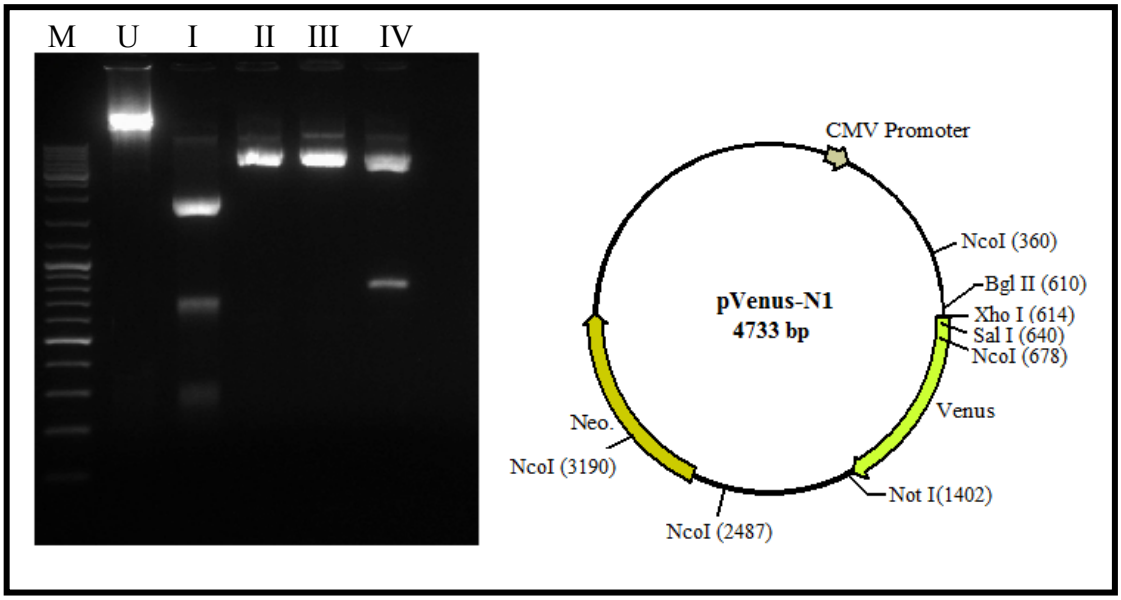

Figure E.2 Diagnostic digests of the pVenus-N1 plasmid. The agarose gel on the left shows the diagnostic digests of pVenus-N1 with NcoI and SalI – NotI. Lane M shows the DNA size marker, lane U shows the undigested pVenus-N1, lane I shows NcoI digested pVenus-N, lane II shows SalI digested pVenus-N1, lane III shows NotI digested pVenus-N1 and lane IV shows SalI – NotI digested pVenus-N1. The map of pVenus-N1, shown on the right, indicates that NcoI digestion should generate four bands of 317, 703, 1809 and 1904 bp, SalI digestion and NotI digestion should linearize pVenus-N1 and SalI – NotI double digestion should generate two bands of 762 and 3971 bp.

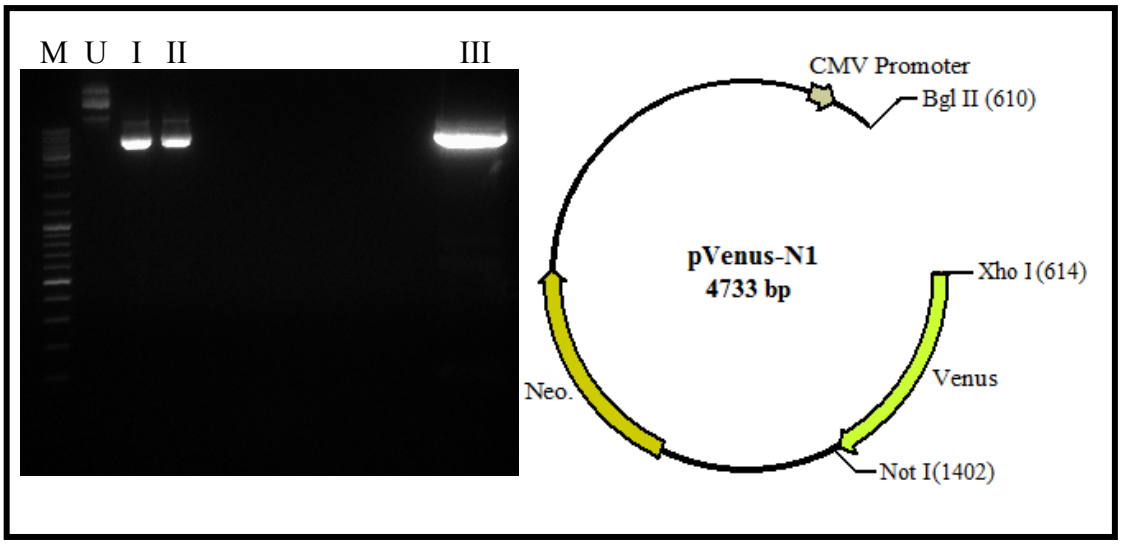

Figure E.3 Digestion of the pVenus-N1 plasmid with Bgl II – XhoI. The agarose gel on the left shows the double digestion of pVenus-N1 with Bgl II – XhoI. Lane M shows the DNA size marker, lane U shows the undigested pVenus-N1, lane I shows Bgl II digested pVenus-N1, lane II shows XhoI digested pVenus-N1 and lane III shows Bgl II – XhoI digested pVenus-N1. Schematic representation of Bgl II – XhoI double digested pVenus-N1 plasmid is shown on the right.

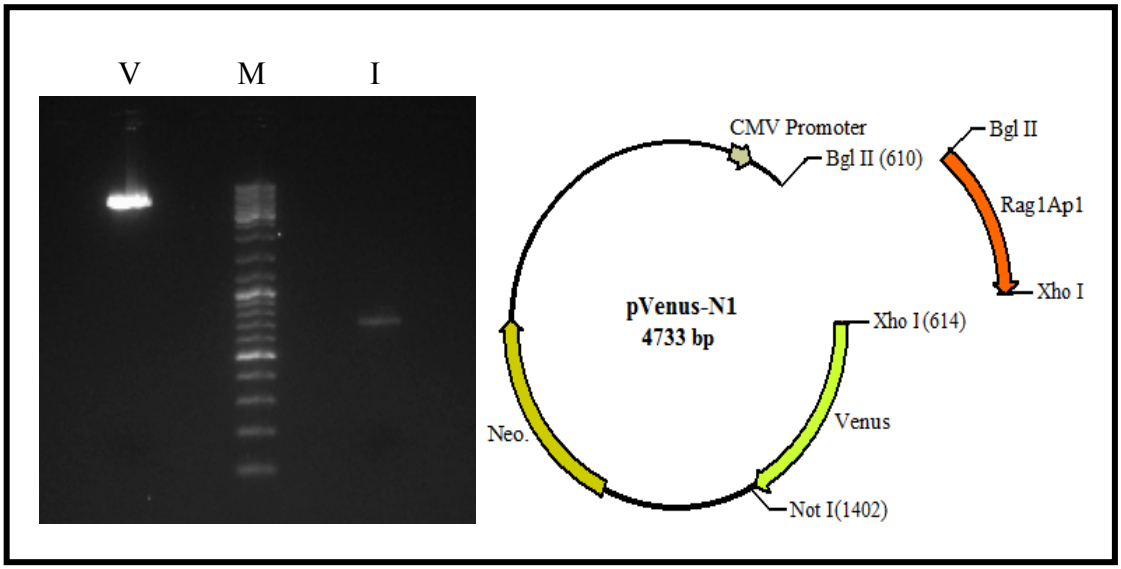

Figure E.4 Comparison the DNA fragments containing the purified Rag1Ap1 insert, and digested pVenus-N1 vector before ligation. The agarose gel on the left shows the comparison of vector (pVenus-N1) and insert (Rag1Ap1) before ligation. Lane V shows digested pVenus-N1, lane I shows Rag1Ap1 and lane M shows the DNA size marker. Schematic representation of comparison of pVenus-N1 and Rag1Ap1 before ligation is shown on the right.

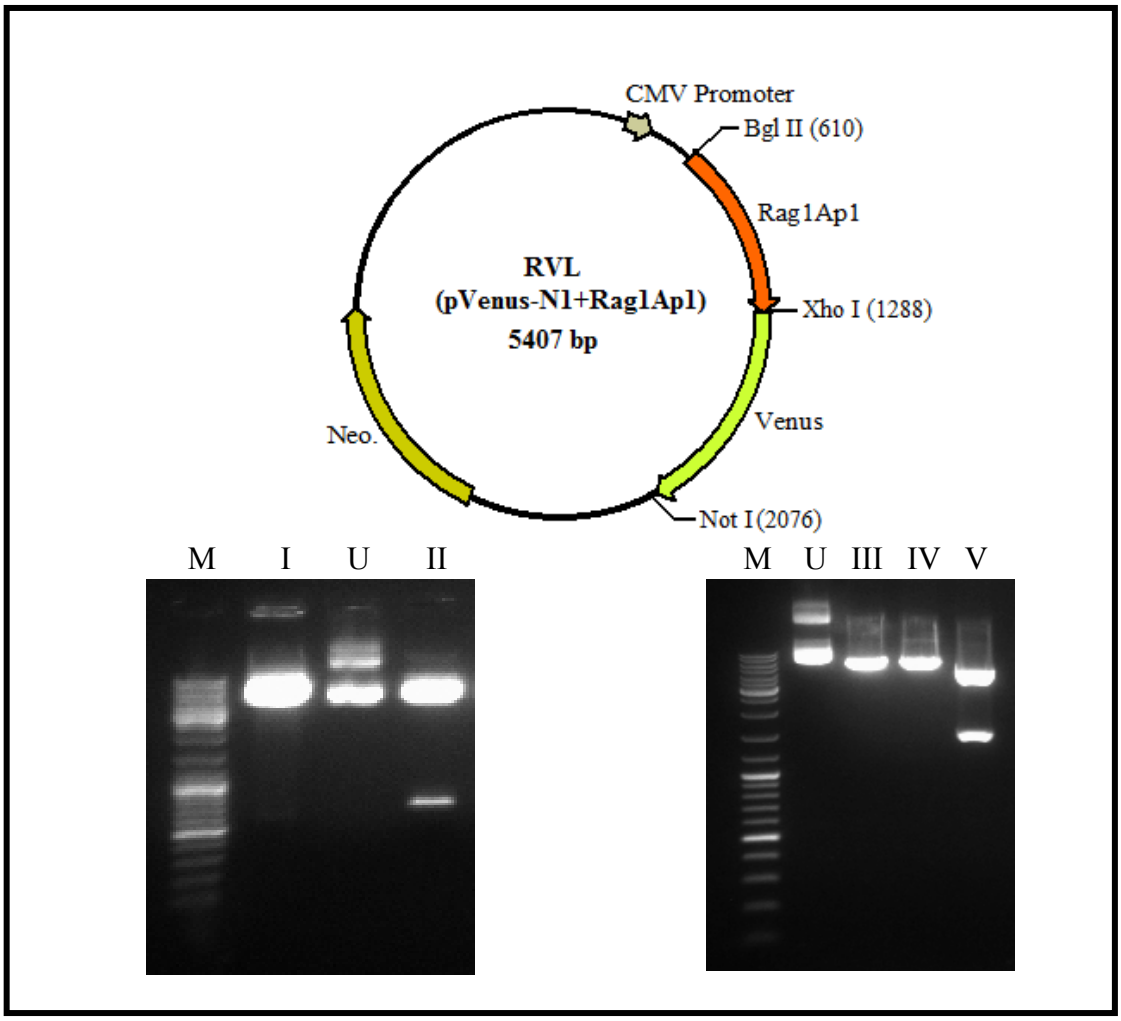

Figure E.5 Confirmation digests of the RVL (pVenus-N1+Rag1Ap1) plasmid. The agarose gel on the left shows the confirmation digest of RVL with Bgl II – XhoI whereas the agarose gel on the right shows the confirmation digests of RVL with Bgl II, NotI and Bgl II – NotI. Lane M shows the DNA size marker, lane U shows the undigested RVL, lane I shows Bgl II – XhoI digested pVenus-N1, lane II shows Bgl II – XhoI digested RVL, lane III shows Bgl II digested RVL, lane IV shows NotI digested RVL and lane V shows Bgl II – NotI digested RVL. The map of RVL, shown on the top, indicates that Bgl II – XhoI digestion of RVL should generate two bands of 678 and 4729 bp, whereas Bgl II – XhoI digestion of pVenus-N1 should generate two bands of 4 and 4729 bp. Bgl II digestion and NotI digestion of RVL should linearize RVL and Bgl II – NotI double digestion should generate two bands of 1466 and 3941 bp.

APPENDIX F: Confirmation Digests of TCR, Rag1Ap1 and CD3 delta Expression Plasmids

In section 4.3 we analyzed the interaction between CD3δ and Rag1Ap1 in the presence and absence of a fully assembled TCR. In order to express HA-Rag1Ap1 and CD3δ-Myc proteins, we co-transfected the pHA-Mex+Rag1Ap1 and pcDNA3.1Myc-CD3delta plasmids (shown in figures F.1 and F.2) into HEK293T cells. For this analysis, in order to make HEK293T cells express TCR on their cell surface, we used the pMIGIITCRab and pMIGIITCRdgez plasmids (shown in figures F.3 and F.4). This appendix details the confirmation of the plasmids used in these expreriments.

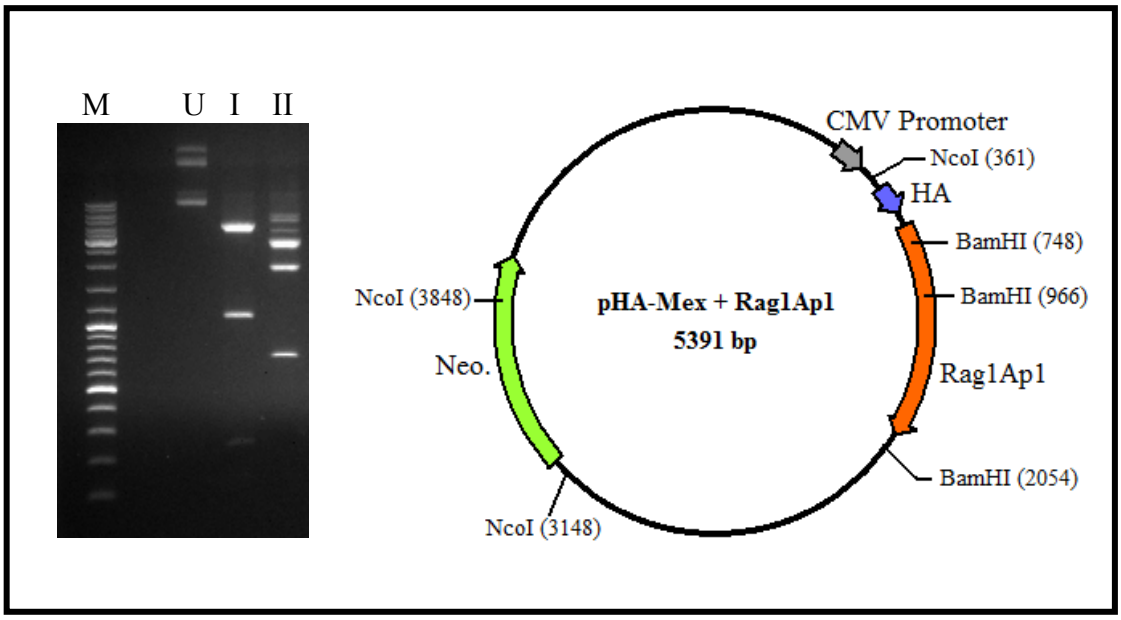

Figure F.1 Diagnostic digests of the pHA-Mex+RagAp1 plasmid. The agarose gel on the left shows the diagnostic digests of pHA-Mex+Rag1Ap1 with BamHI and NcoI. Lane M shows the DNA size marker, lane U shows the undigested pHA-Mex+Rag1Ap1, lane I shows BamHI digested pHA-Mex+Rag1Ap1 and lane II shows NcoI digested pHA-Mex+Rag1Ap1. The map of pHA-Mex+Rag1Ap1, shown on the right, indicates that BamHI digestion should generate three bands of 218, 1088 and 4085 bp and NcoI digestion should generate three bands of 700, 1904 and 2787 bp.

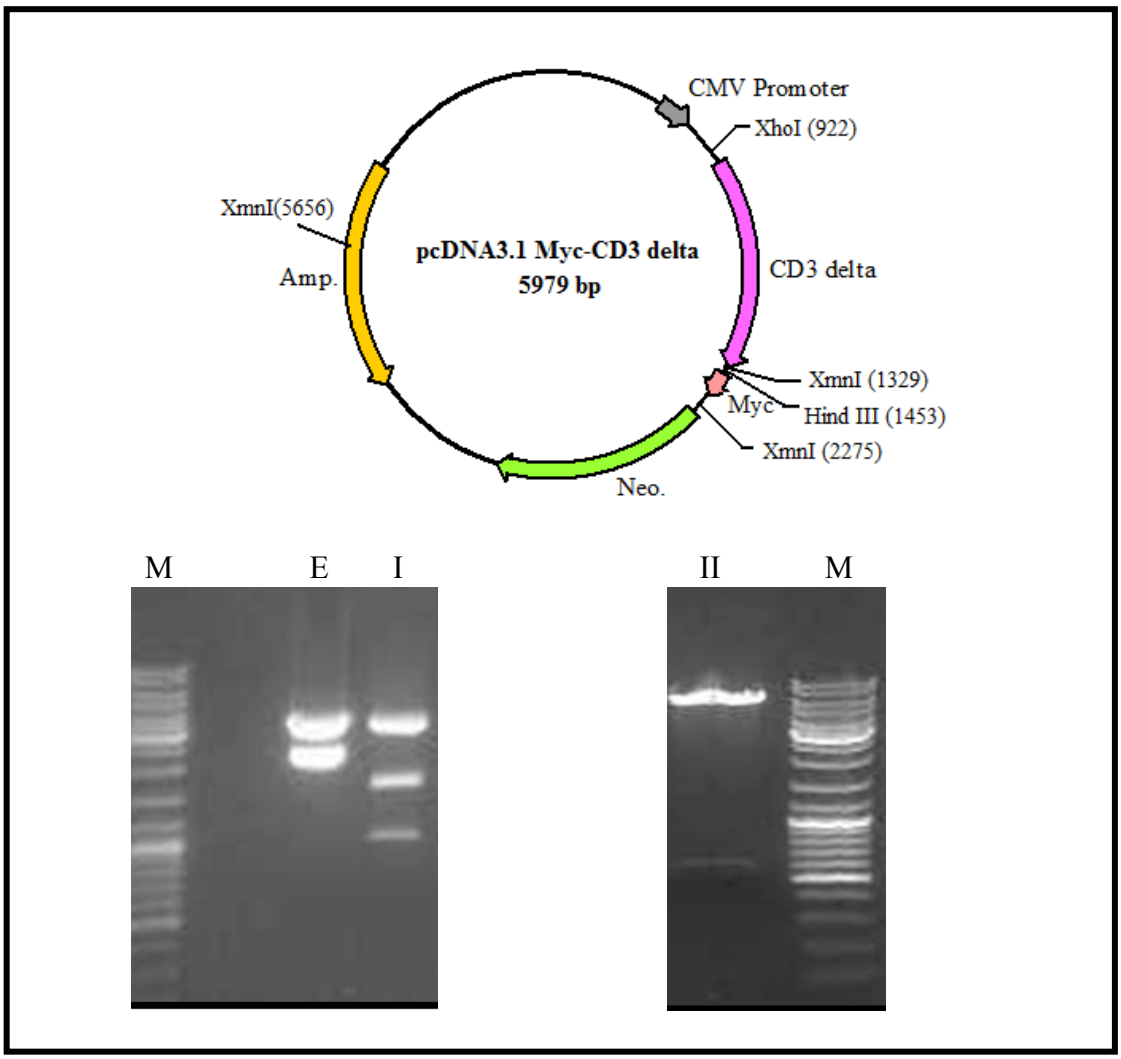

Figure F.2 Diagnostic digests of the pcDNA3.1Myc-CD3delta plasmid. The agarose gel on the left shows the diagnostic digest of pcDNA3.1Myc-CD3delta with XmnI wheras the agarose gel on the right shows the diagnostic digest of pcDNA3.1Myc-CD3delta with XhoI – HindIII. Lane M shows the DNA size marker, lane U shows the undigested pcDNA3.1Myc-CD3delta, lane E shows XmnI digested pcDNA3.1Myc, lane I shows XmnI digested pcDNA3.1Myc-CD3delta and lane II shows XhoI – HindIII double digested pcDNA3.1Myc-CD3delta. The map of pcDNA3.1Myc-CD3delta, shown on the top, indicates that XmnI digestion of pcDNA3.1Myc-CD3delta should generate three bands of 946, 1652 and 3381 bp whereas XmnI digestion of pcDNA3.1Myc should generate 2120 and3400bp. XhoI – HindIII digestion of pcDNA3.1Myc-CD3delta should generate two bands of 525 and 5479 bp.

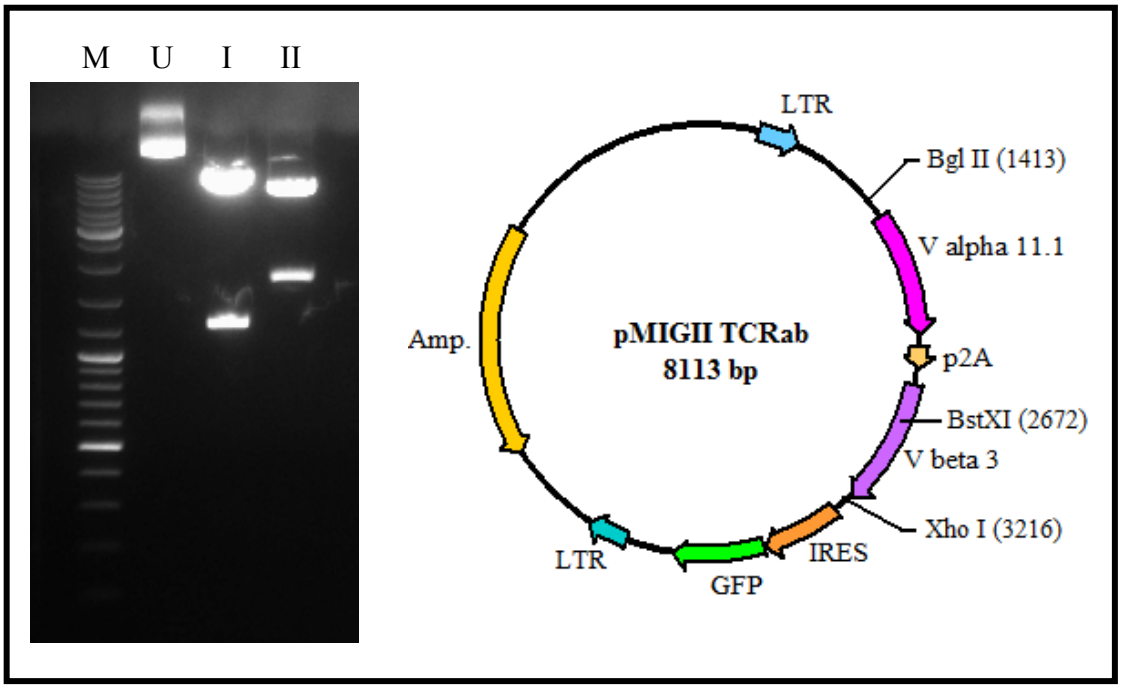

Figure F.3 Diagnostic digests of the pMIGIITCRab plasmid. The agarose gel on the left shows the diagnostic digest of pMIGIITCRab with Bgl II – BstXI and Bgl II – XhoI. Lane M shows the DNA size marker, lane U shows the undigested pMIGIITCRab, lane I shows Bgl II – BstXI double digested pMIGIITCRab and lane II shows Bgl II – XhoI double digested pMIGIITCRab. The map of pMIGIITCRab, shown on the right, indicates that Bgl II – BstXI double digestion of pMIGIITCRab should generate two bands of 1259 and 6854 bp and Bgl II – XhoI double digestion should generate two bands of 1803 and 6310 bp.

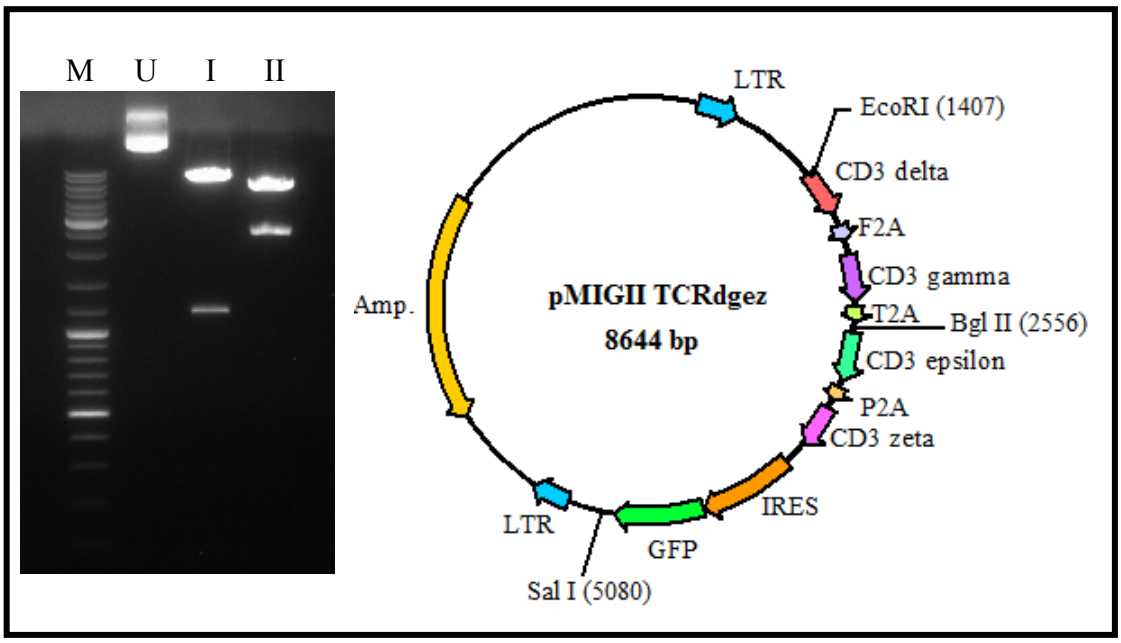

Figure F.4 Diagnostic digests of the pMIGIITCRdgez plasmid. The agarose gel on the left shows the diagnostic digest of pMIGIITCRdgez with EcoRI – Bgl II and Bgl II – SalI. Lane M shows the DNA size marker, lane U shows the undigested pMIGIITCRdgez, lane I shows EcoRI – Bgl II double digested pMIGIITCRdgez and lane II show Bgl II – SalI double digested pMIGIITCRdgez. The map of pMIGIITCRdgez, shown on the right, indicates that EcoRI – Bgl II double digestion of pMIGIITCRdgez should generate two bands of 1149 and 7495 bp and Bgl II – SalI double digestion should generate two bands of 2524 and 6120 bp.

APPENDIX G: FACS Analysis of TCR Expression Levels on HEK293T Cells Transfected with pMIGIITCRab, pMIGIITCRdgez, HA-Rag1Ap1 and CD3delta-Myc Expression Plasmids.

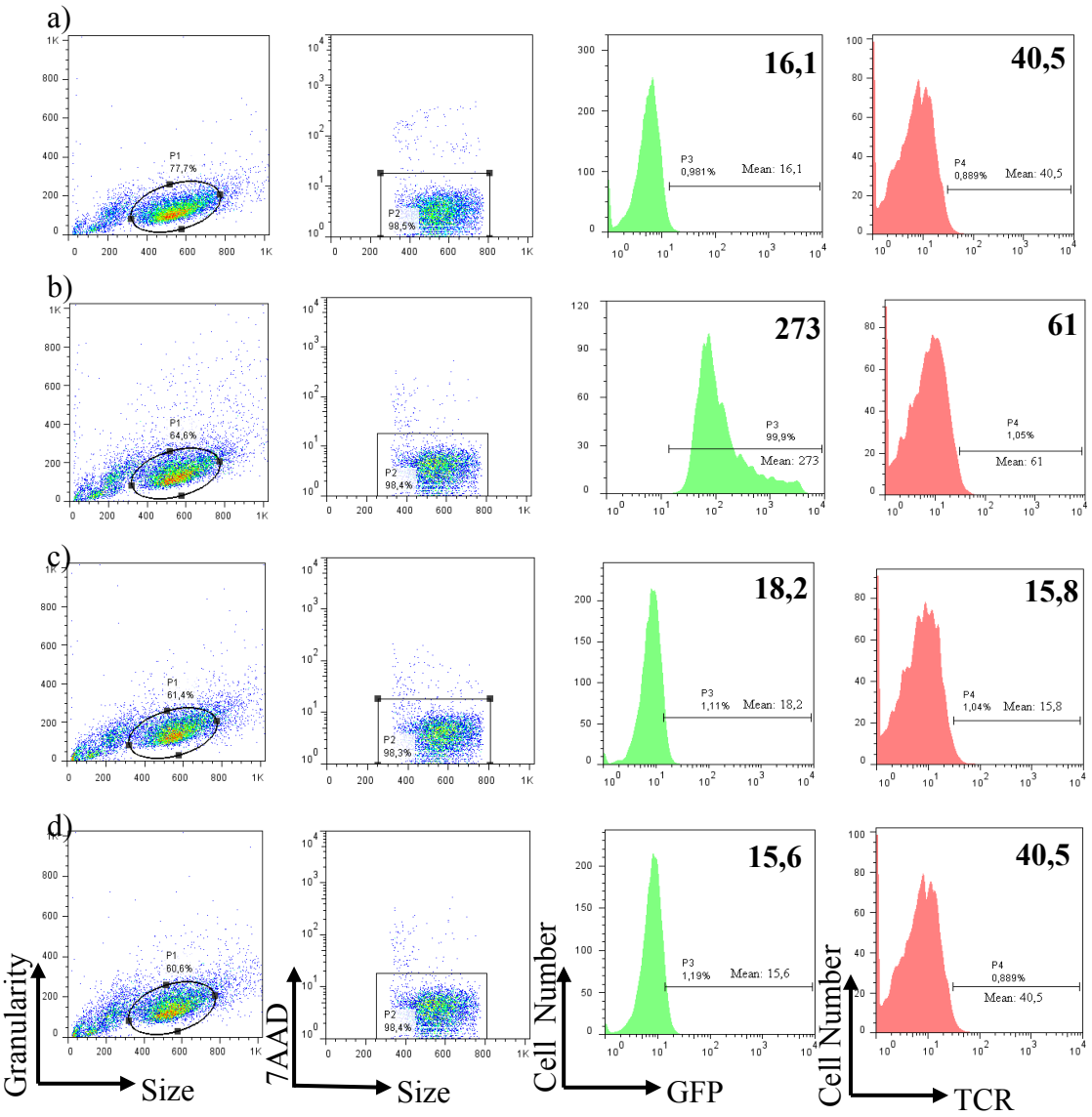

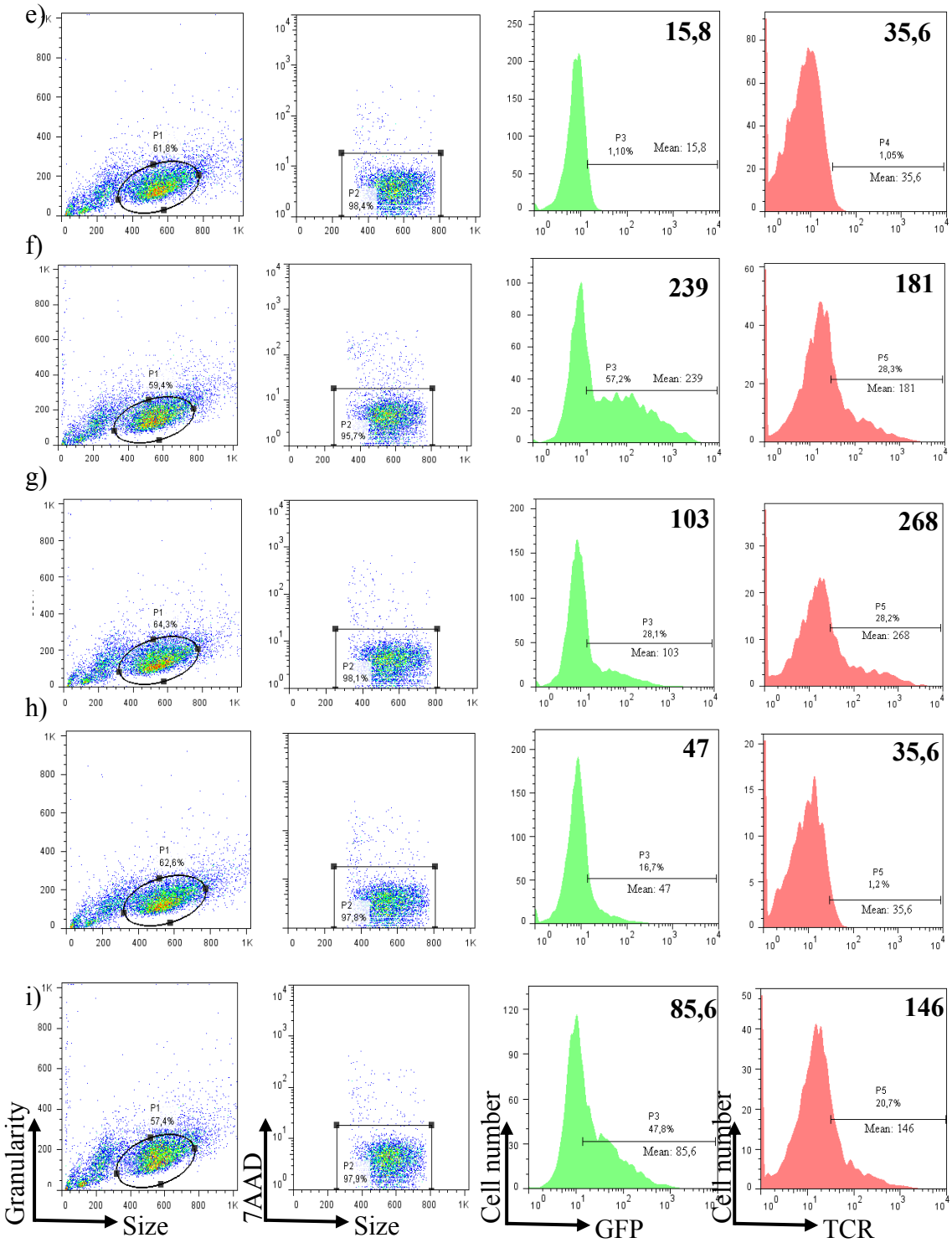

Figure G.1 FACS analysis of TCR expression on the surface of transfected HEK293T cells. The first column shows side scatter vs forward scatter dot plots, the second column shows 7AAD vs forward scatter dot plots, the third column shows histograms of GFP expression and the fourth column shows histograms of TCR expression.

Figure G.1 cont.. a) untransfected HEK293T Cells, b) pcDNAGFP transfected HEK293T cells c) pcDNA3.1CD3δMyc plasmid transfected HEK293T cells d) pHA-Mex+Rag1Ap1 plasmid transfected HEK293T cells e) pcDNA3.1CD3δMyc and pHA-Mex+Rag1Ap1 transfected HEK293T cells f) pcDNA3.1CD3δMyc, pMIGIITCRab and pMIGIITCRdgez transfected HEK293T cells g) pHA-Mex+Rag1Ap1, pMIGIITCRab and pMIGIITCRdgez transfected HEK293T cells h) pcDNA3.1CD3δ-Myc, pHA-Mex+Rag1Ap1 and pMIGIITCRdgez transfected HEK293T cells i) pcDNA3.1CD3δ-Myc, pHA-Mex+Rag1Ap1, pMIGIITCRab and pMIGIITCRdgez transfected HEK293T cells. Forward scatter, shows the size of the cells and side scatter shows the granularity of the cells. The analysis was restricted to live cells falling into the P1 and P2 gates shown in the granularity vs size and 7AAD vs size dot plots, respectively. The P3 gate shows the GFP positive cells and the P5 gate shows TCR positive cells. The analysis of TCR expression was restricted to the P3 (GFP+) population which correspond to transfected cells. TCR expression was detected with biotinylated H57 anti-TCR antibodies followed by Alexa647 labelled streptavidin. The bold numbers inside the graphs indicate the mean fluorescence intensity of the cells in the gates. The percentage of the cells falling into each gate is indicated under the label for each gate.

APPENDIX H: FACS Analysis of Rag1Ap1 Overexpression in VL3-3M2 Cells

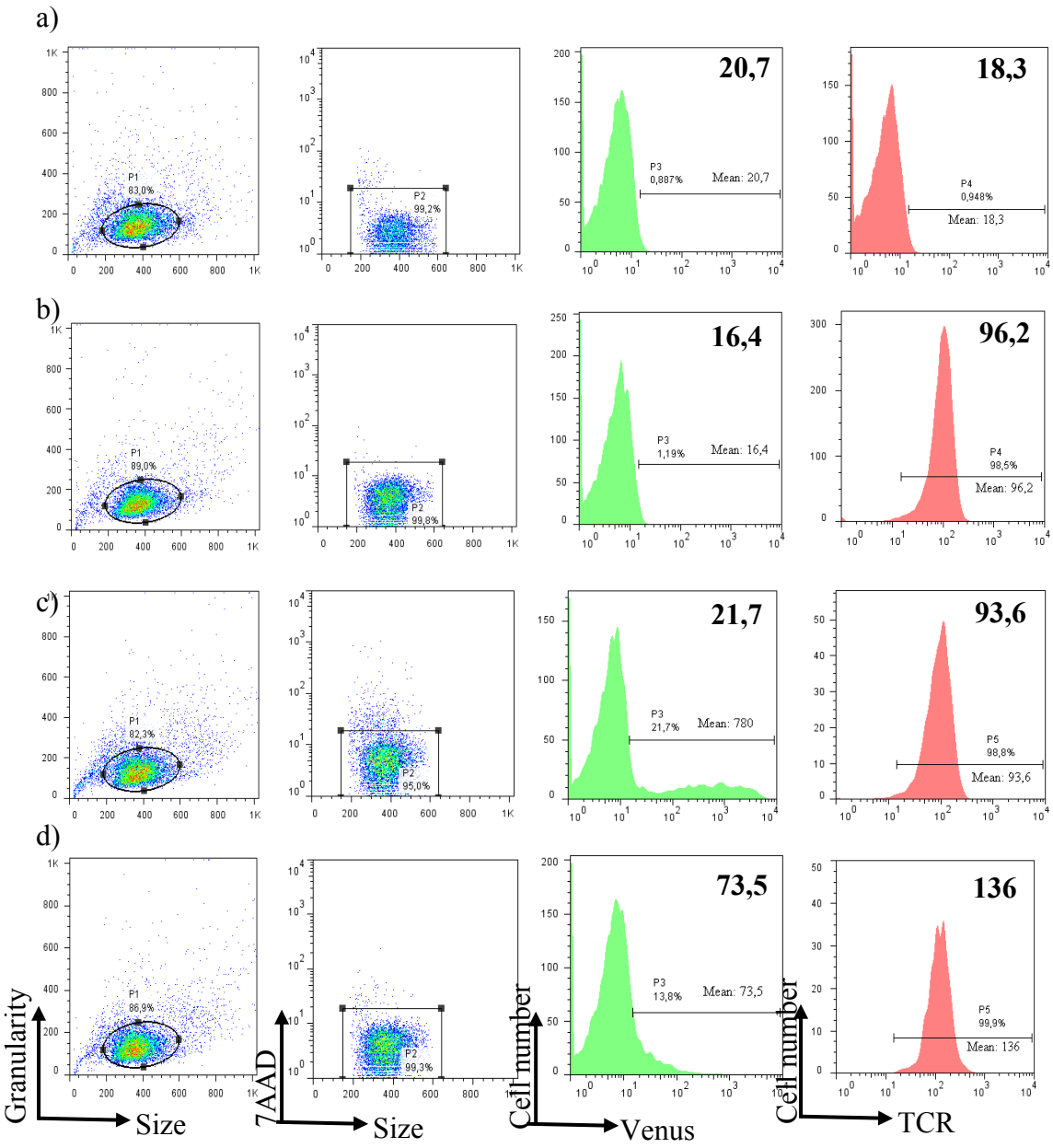

Figure H.1 FACS analysis of TCR expression on the surface of transfected VL3-3M2 cells. The first column shows side scatter vs forward scatter dot plots, the second column shows 7AAD vs forward scatter dot plots, the third column shows histograms of Venus expression and the fourth column shows histograms of TCR expression of a) Untransfected and unstained VL3-3M2 Cells b) Untransfected VL3-3M2 cells

Figure H.1 cont.. c) pVenus-N1 transfected VL3-3M2 cells d) RVL (pVenus-N1+Rag1Ap1) transfected VL3-3M2 cells. Forward scatter, shows the size of the cells and side scatter, shows the granularity of the cells. The analysis was restricted to live cells falling into the P1 and P2 gates shown in the granularity vs size and 7AAD vs size dot plots, respectively. The P3 gate shows the Venus positive cells and the P5 gate shows TCR positive cells. The analysis of TCR expression was restricted to the P3 (GFP+) population which correspond to transfected cells. TCR expression was detected with biotinylated H57 anti-TCR antibodies followed by Alexa647 labelled streptavidin. The bold numbers inside the graphs indicate the mean fluorescence intensity of the cells in the gates. The percentage of the cells falling into each gate is indicated under the label for each gate.

APPENDIX I: Construction of shRNAmir Plasmids Against Rag1Ap1

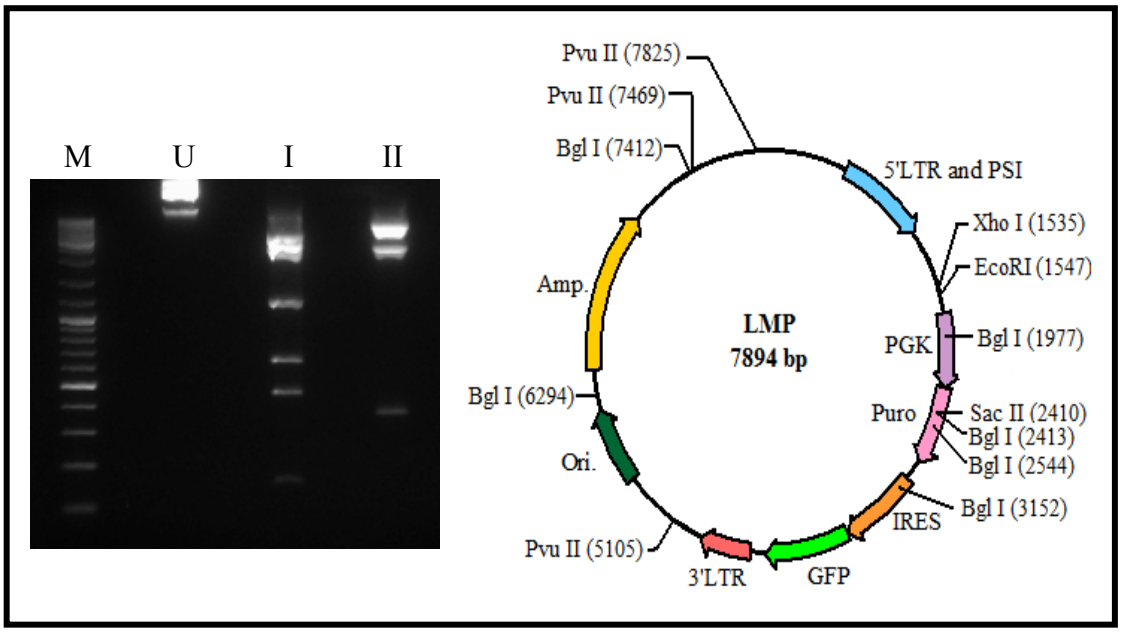

Figure I.1 Diagnostic digests of MSCV-LMP. The agarose gel on the left shows the diagnostic digests of LMP with Bgl I and PvuII. Lane M shows the DNA size marker, lane U shows the undigested LMP, lane I shows Bgl I digested LMP and lane II shows PvuII digested LMP. The map of LMP, shown on the right, indicates that Bgl I digestion should generate six bands of 131, 436, 608, 1118, 2459 and 3142 bp and PvuII digestion should generate three bands of 356, 2364 and 5174 bp.

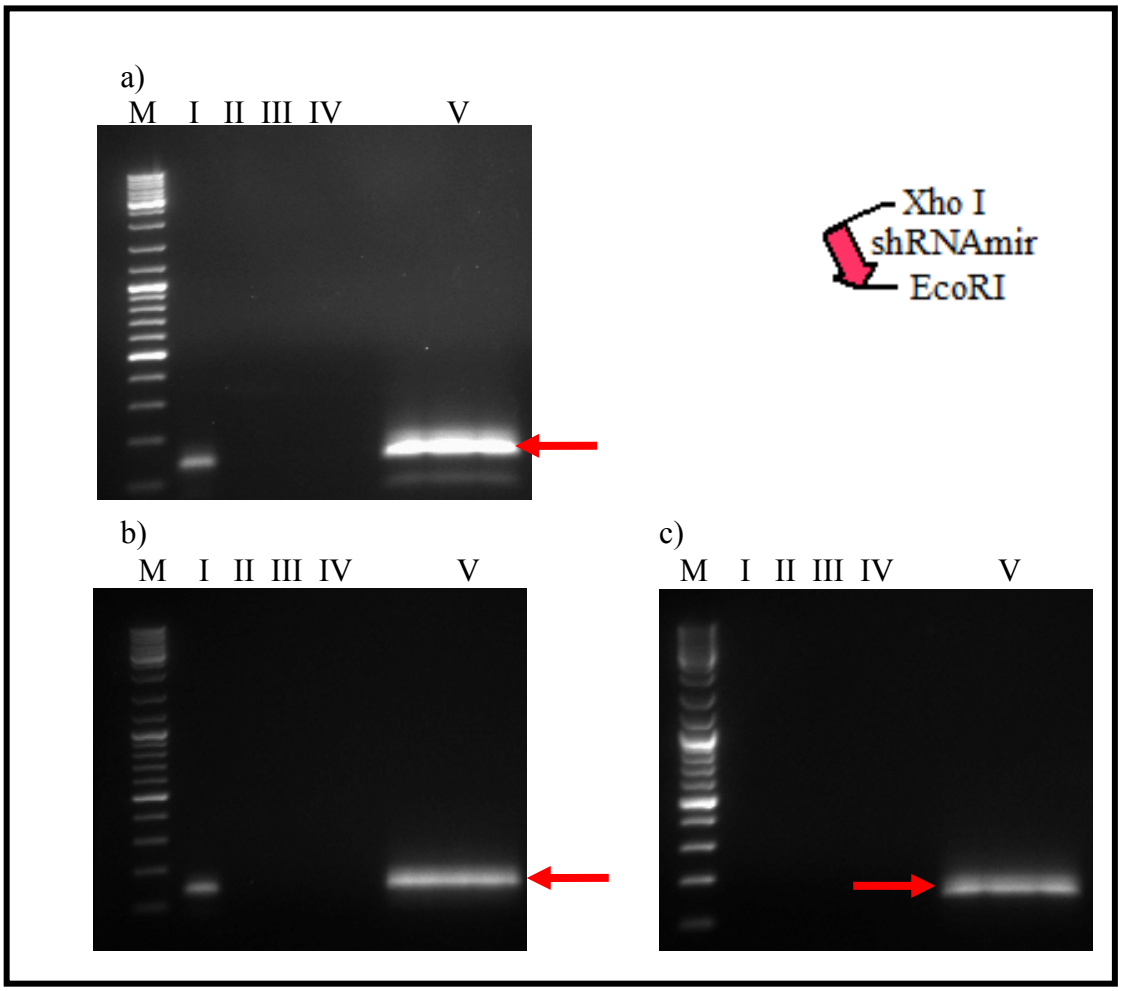

Figure I.2 PCR for shRNAmir inserts. The sequences to produce shRNAmir against Rag1Ap1 are amplified by a forward primer introducing XhoI to the beginning of the sequence and a reverse primer introducing EcoRI to the end of sequence. The agarose gels the PCR products for shRNAmirs against Rag1Ap1 with controls. Lane M shows the DNA size marker, lane I shows PCR without template DNA, lane II shows the PCR without forward primer, lane III shows PCR without reverse primer, lane IV shows PCR without Pfu and lane V shows PCR product. PCR amplification for shRNAmir against Rag1Ap1 is expected to generate a band of 135 bp shown with the red arrows. Schematic representation of the PCR product for shRNAmir with restriction sites introduced by primers is shown on the top right.

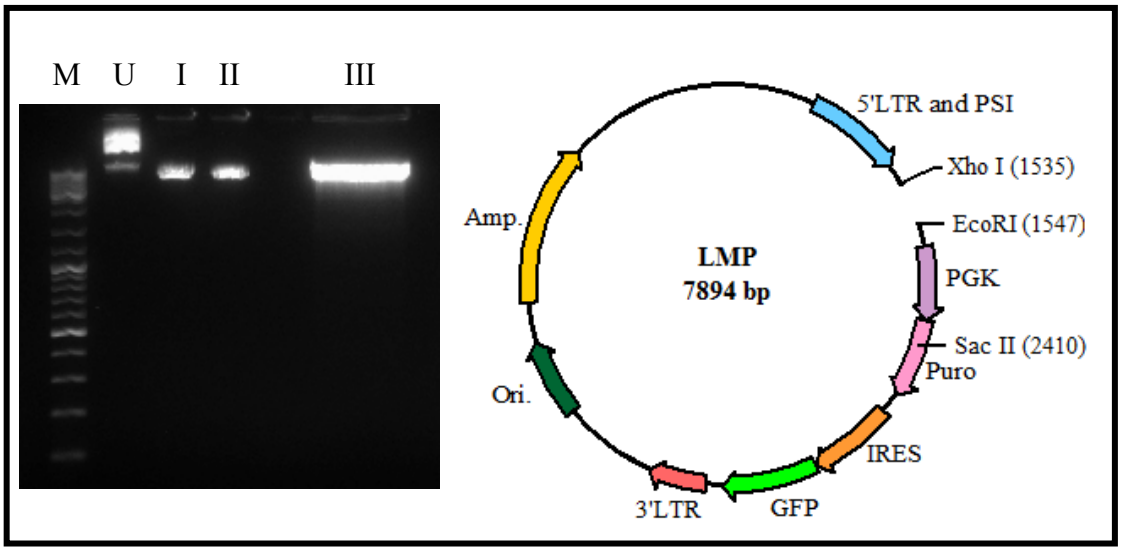

Figure I.3 EcoRI – XhoI double digestion of MSCV-LMP. The agarose gel on the left shows the double digestion of LMP with EcoRI – XhoI. Lane M shows the DNA size marker, lane U shows the undigested LMP, lane I shows EcoRI digested LMP, lane II shows XhoI digested LMP and lane III shows EcoRI – XhoI digested LMP. Schematic representation of EcoRI – XhoI double digested LMP plasmid is shown on the right.

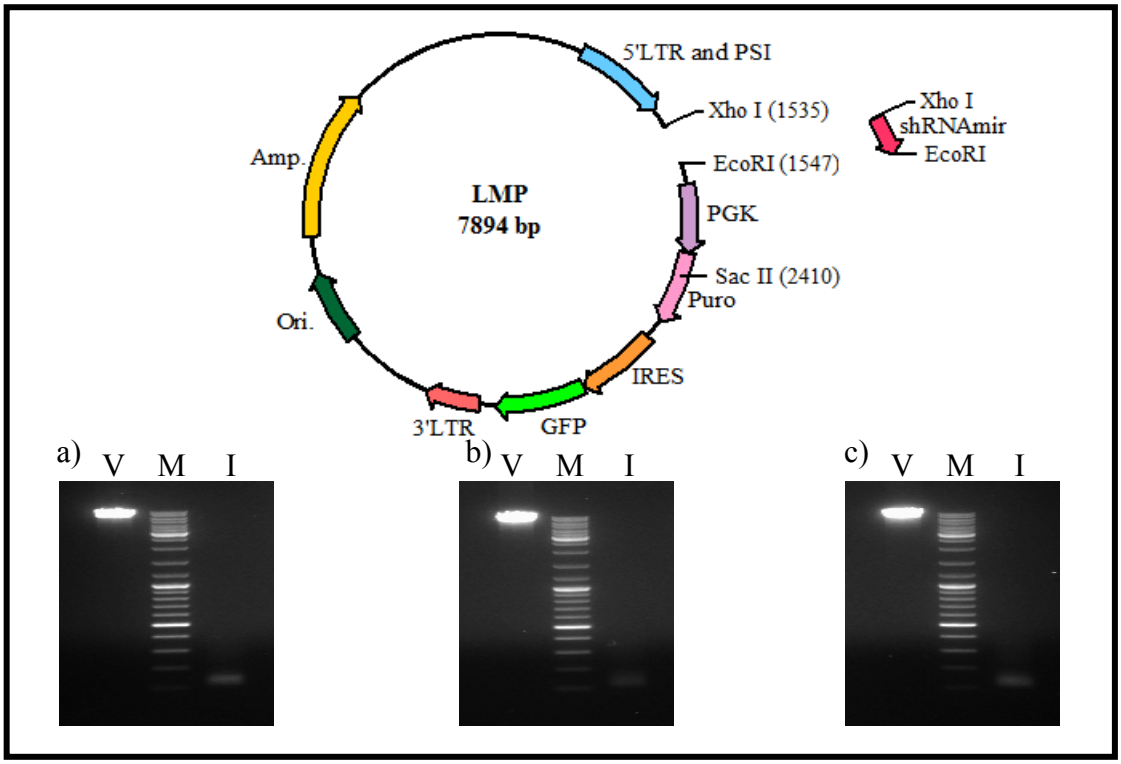

Figure I.4 Comparison of inserts and vector before ligation. Purified inserts, and digested vector, LMP before ligation. The agarose gels show the comparison of vector (LMP) and inserts (shRNAmir) before ligation. Lane V shows digested LMP, lane I shows inserts and lane M shows the DNA size marker. Schematic representation of comparison of vector and inserts before ligation is shown on the top.

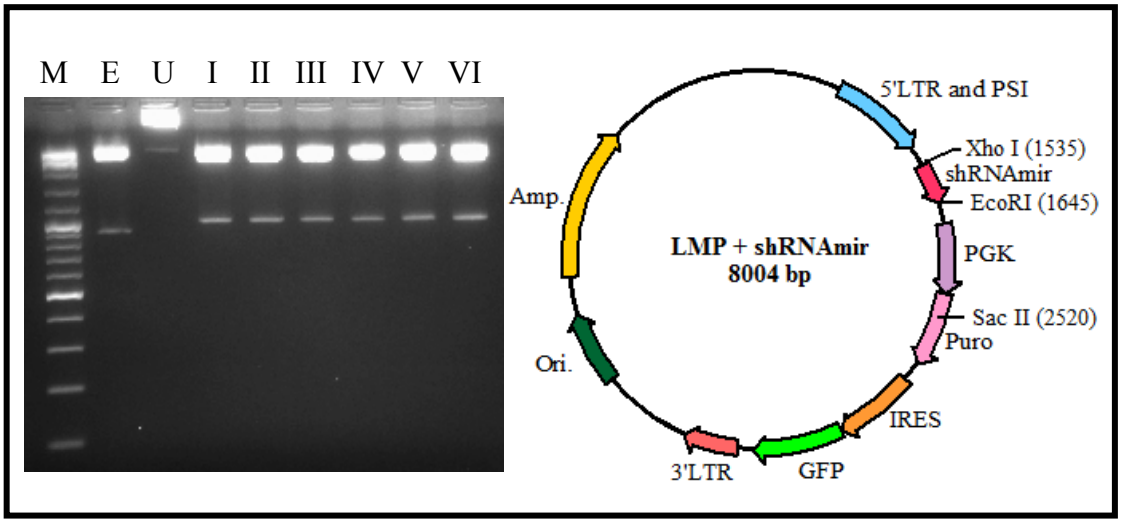

Figure I.5 Confirmation digests of LMP+shRNAmir plasmids. The agarose gel on the left shows the confirmation digest of LMP+shRNAmir plasmids with XhoI – SacII. Lane M shows the DNA size marker,lane E shows XhoI – SacII double digested LMP, lane U shows the undigested shRNAmirplasmid 1/4, lane I shows XhoI – SacII double digested shRNAmir plasmid 1/4, lane II shows XhoI – SacII double digested shRNAmir plasmid 1/8, lane III shows XhoI – SacII double digested shRNAmir plasmid 2/2, lane IV shows XhoI – SacII double digested shRNAmir plasmid 2/7 and lane V shows XhoI – SacII digested shRNAmir plasmid 3/2 and lane VI shows XhoI – SacII double digested shRNAmir plasmid 3/8. The map of shRNAmir plasmids, shown on the right, indicates that XhoI – SacII doulbe digestions of shRNAmir plasmids should generate two bands of 985 and 7019 bp.

APPENDIX J: FACS Analysis Of Rag1Ap1 Silencing In VL3-3M2 Cells

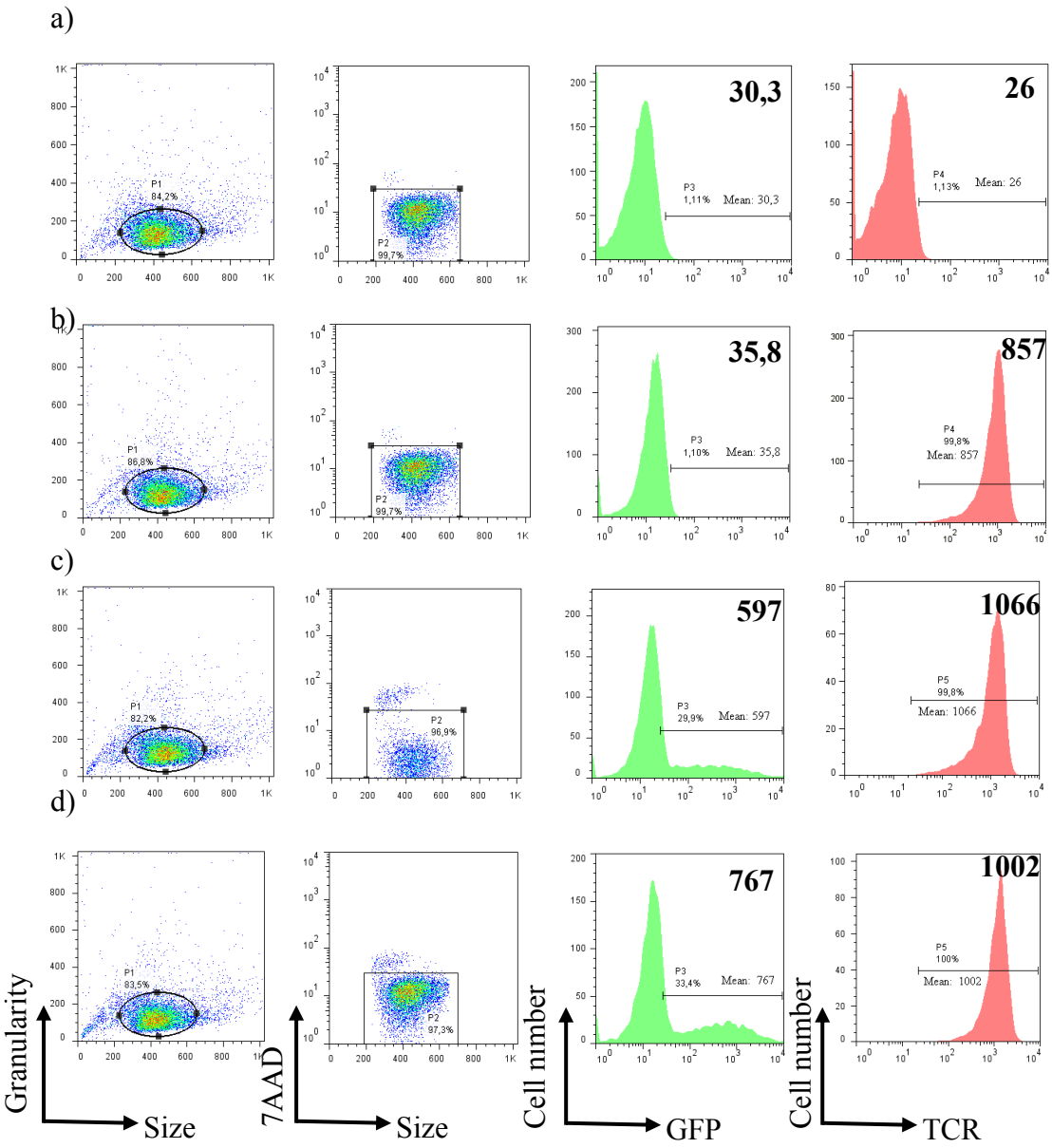

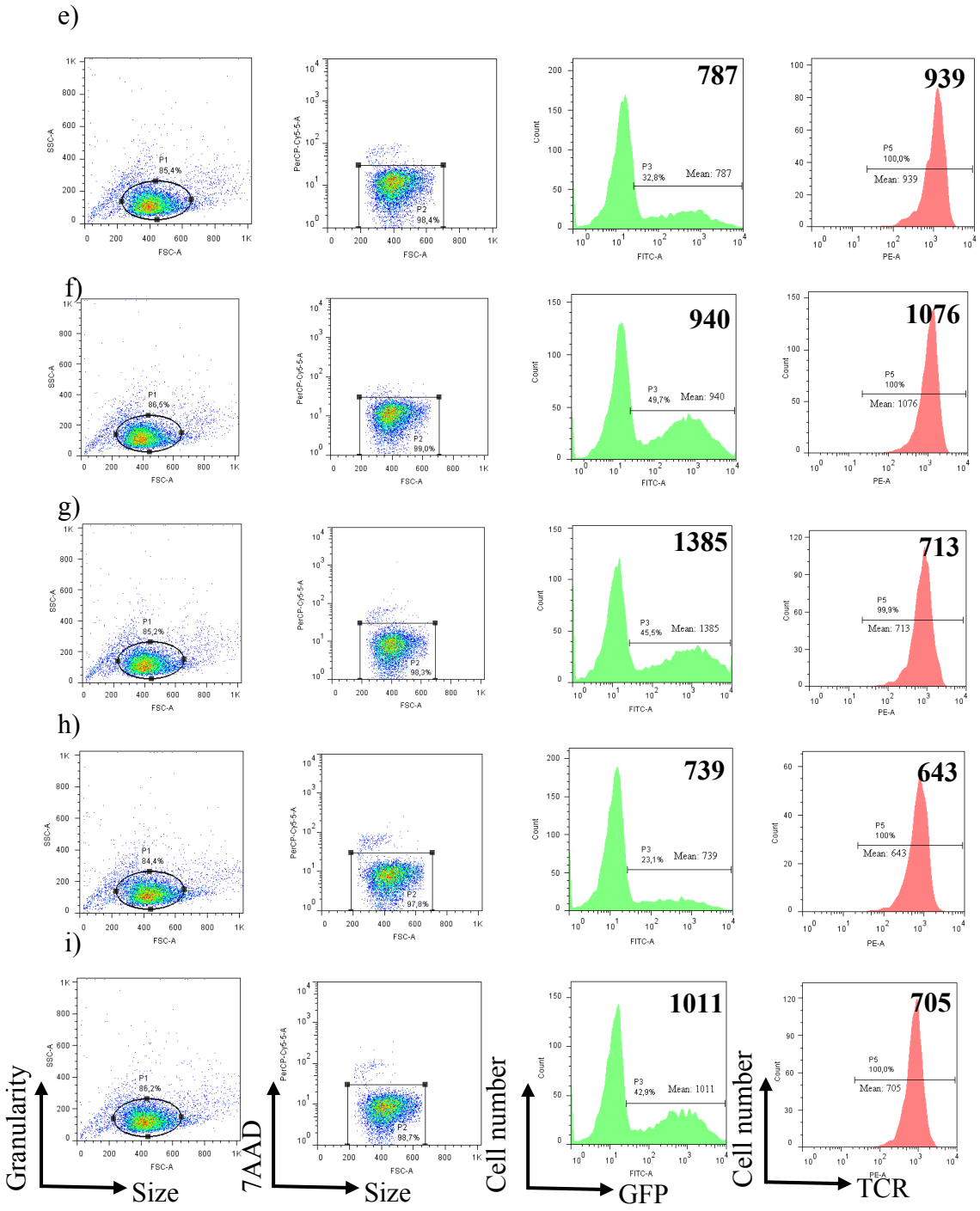

Figure J.1 FACS analysis of TCR expression on the surface of shRNAmir plasmids transfected VL3-3M2 cells. The first column shows side scatter vs forward scatter dot plots, the second column shows 7AAD vs forward scatter dot plots, the third column shows histograms of Venus expression and the fourth column shows histograms of TCR expression of a) Untransfected and unstained VL3-3M2 cells b) Untransfected VL3-3M2 cells c) LMP transfected VL3-3M2 cells d) shRNAmir 1/4 plasmid transfected VL3-3M2 cells e) shRNAmir1/8 plasmid transfected VL3-3M2 cells f) shRNAmir 2/2 plasmid transfected VL3-3M2 cells h) shRNAmir 2/7 plasmid transfected VL3-3M2 cells i) shRNAmir3/2 plasmid transfected VL3-3M2 cells j) shRNAmir3/8 plasmid transfected VL3-3M2 cells. Forward scatter, shows the size of the cells and side scatter,

Figure J.1 cont.. shows the granularity of the cells. The analysis was restricted to live cells falling into the P1 and P2 gates shown in the granularity vs size and 7AAD vs size dot plots, respectively. The P3 gate shows the Venus positive cells and the P5 gate shows TCR positive cells. The analysis of TCR expression was restricted to the P3 (GFP+) population which correspond to transfected cells. TCR expression was detected with biotinylated H57 anti-TCR antibodies followed by Alexa647 labelled streptavidin. The bold numbers inside the graphs indicate the mean fluorescence intensity of the cells in the gates. The percentage of the cells falling into each gate is indicated under the label for each gate.